QUANTUM MECHANICAL STUDY OF ADSORPTION ON a-FERRIC OXIDE (111) SURFACE

BY

UZAIRU, ADAMU
B. Sc. (lions) CHEMISTRY (A.B.U.)

A THESIS SUBMITTED TO THE POSTGRADUATE SCHOOL, AHMADU BELLO UNIVERSITY, ZARIA
IN PARTIAL FULFILMENT OF THE REQUIREMENT FOR THE DEGREE OF DOCTOR OF PHILOSOPHY (Ph.D.) CHEMISTRY

DEPARTMENT OF CHEMISTRY
FACULTY OF SCIENCE
AHMADU BELLO UNIVERSITY, ZARIA - NIGERIA

AUGUST, 1997.

DECLARATION

I declare that this thesis has been written by me. It is a record of my own research and has never been presented in any previous application for a higher degree.

All sources of information are specifically acknowledged by means of references.

UZAIRU, ADAMU

August, 1997.

CERTIFICATION

This thesis entitled: "QUANTUM MECHANICAL STUDY OF ADSORPTION ON α-FERRIC OXIDE (111) SURFACE" by UZAIRU ADAMU meets the regulations governing the award of the degree of Doctor of Philosophy (Ph.D.) of Ahmadu Bello University, and is approved for its contribution to knowledge and literary presentation.

Dr. G.E.S. Harrison Chairman, Supervisory Committee	17/9/97 **Date**
Prof. S.A. Thomas Member, Supervisory Committee	20.2.98 **Date**
External Examiner	20 August 1997 **Date**
Dr. J.O. Amupitan Head, Department of Chemistry	20.2.98 **Date**
Dean, Post-Graduate School	13/11/98 **Date**

ACKNOWLEDGMENTS

I wish to sincerely thank my supervisor Dr. G.F.S. Harrison for supervising this work and also for his patience, material input, untiring efforts and, thorough and constructive criticisms which made this work a reality. I also wish to thank Prof. S.A Thomas for co-supervising the work.

I extend my gratitude to Prof. S.B. Ojo of the Department of Physics and to Dr. G.I. Balogun of the Centre for Energy Research and Training for providing me with versions of FORTRAN 77 compiler for the computations. My heartiest thanks to Prof. S.B. Elegba, Director Centre for Energy Research and Training; Dr. Oyedokun, former Head, Department of Electrical Engineering; the Iya Abubakar Computer Centre, A.B.U. and NEARLS, A.B.U, Zaria for allowing me the use of their "computing facilities". Once more, I am very grateful to Dr. G.F.S. Harrison who introduced me to all the people and bodies mentioned above.

I am highly indebted to my parents for their moral and financial support, and for showing me the road to school.

My sincere regards to my friends, well wishers and colleagues most especially my wife and children for their endurance during the research.

UZAIRU, ADAMU

August, 1997.

DEDICATION

This thesis is dedicated to my late grandparents (especially BAPPA INUSA and BABA IYANIYO), my parents UZAIRU and HAUWA MOHAMMED and for the everlasting memory of my aunt ALTINE.

ABSTRACT

An attempt has been made to study the energetics of physisorptive and chemisorptive adsorption of H^{1}, OH^{-} and NH_3 on the (111) surface of a-Fe_20_3. The physisorption energies of H^{4}, 0H and NH-, were computed as -6.6173 x 10" , -2.5775 and -2.2766 KJ/mol respectively. Whereas the chemisorption of H^{+} ion was found to be in the range of -41 to -42 KJ/mol those of OH^{-} and $NH_{(}$ fell in the ranges of -62 to -67 KJ/mol and -44 to -50 KJ/mol respectively. Furthermore, the results show that, most of H^{1} binding is by the surface oxygens. In the case of OH^{-} and NH_3 chemisorptions, the binding energies obtained suggest that the two adsorbates chemisorb through o-interactions only, while π-interactions lead to physisorption.

TABLE OF CONTENTS

	Page
Title	i
Declaration	ii
Certification	iii
Acknowledgments	iv
Dedication	v
Abstract	vi
Table of Contents	vii
List of Tables	x
List of Figures	xii

CHAPTER ONE

INTRODUCTION

1.0 Iron (III) Oxide, α-Fe_2O_3	1
1.1 The Electrical and Magnetic Properties of α-Fe_2O_3	3
1.2 The Electronic Structure of α-Fe_2O_3	5
1.3 The Surface Electronic Structure of α-Fe_2O_3	15
1.4 Solid Surface and Adsorption	18
1.5 Adsorption and Catalysis by α-Fe_2O_3	24
1.6 Quantum Models for Adsorption on α-Fe_2O_3	28

CHAPTER TWO

REVIEW OF LITERATURE	32
2.1 The Extended Hückel Theory (EHT)	32
2.2 Semi-empirical Techniques	34
2.3 Simple Hückel Molecular Orbital (HMO) Theory	34
2.4 The Extended Hückel Theory (EHT)	42
2.4.1 Determination of the EHT Parameters, α_k and β_{kl}	43

CHAPTER THREE

3 RESEARCH METHODS I: QUANTUM CHEMISORPTION METHODS 49

3.0 A Self-Consistent Field Molecular Orbital Extended Hückel Theory (SCF-MO EHT Method) 49

3.1.0 A Self-Consistent Field Molecular Orbital Spin-Restricted Extended Hückel Theory: SCF-MO EHT-SR Method 50

3.1.1 Matrix Elements of the SCF-MO Spin-Restricted Method 59

3.2.0 A Self-Consistent Field Molecular Orbital Spin-Polarized Extended Hückel Theory: SCF-MO EHT-SP Method 71

3.2.1 Matrix Elements of the SCF-MO Spin-Polarized Method 80

3.3 OPTIMIZATION OF NUMERICAL VALUES FOR THE MATRIX ELEMENTS 85

3.4 Determination of $\sigma_{BOND}{}^{a-b}$ and its Physical Significance 90

CHAPTER FOUR

4. RESEARCH METHODS II: QUANTUM ADSORPTION METHODS 107

4.1.0 PHYSISORPTION OF H^+ ION BY FeO_5A^{n-7} PHYSISORPTIVE INTERACTION MODEL 107

4.1.1 $U(r_j)$ in the Symmetry Group of FeO_5H^{6-} Cluster 113

4.1.2 The Physisorption Energy of H^+ ion by FeO_5H^{6-} Model 117

4.2.0 The Physisorption of NH_3 and OH- by FeO_5A^{n-7} Physisorption Interaction Model 120

4.2.1 $U_u(r_j)$ in the Symmetry Group of FeO_5A^{n-7} System 132

4.2.2 The Dipole Physisorption Energy by the FeO_5A^{n-7} Model 135

4.3.0 The Chemisorption of NH_3 by $FeO_5NH_3{}^{7-}$ Model 136

4.3.1 Chemisorption Energy of NH_3 by the $FeO_5NH_3{}^{7-}$ Model 138

CHAPTER FIVE

5. RESULTS AND DISCUSSION I: ENERGY LEVELS OF THE ADSORBENT - ADSORBATE SYSTEMS 141

5.0 The Electronic Structure of the FeO_6A^{n-6} and FeO_5A^{n-7} Adsorbent - Adsorbate Systems 141

5.1 Results for FeO_6H^{8-} Cluster 141

5.2 Results for FeO_6OH^{10-} Cluster 150

5.3 Results for $FeO_6NH_3^{9-}$ Cluster 159

5.4 Results for FeO_5A^{n-7} Type Clusters 165

CHAPTER SIX

6. RESULTS AND DISCUSSION II: ADSORPTION ENERGIES OF H^+, OH^- AND NH_3 ADSORBATES ON THE (111) FACE OF α-Fe_2O_3 173

6.1 Physisorption Energies of H^+, OH^- and NH_3 on the (111) Surface of α-Fe_2O_3 173

6.2 Chemisorption Energies of H^+, OH^- and NH_3 on the (111) Surface of α-Fe_2O_3 176

6.2.1 The Chemisorption Energies of H^+, OH^- and NH_3 from FeO_5A^{n-7} Cluster Model 177

6.2.2 The Chemisorption Energies of H^+, OH^- and NH_3 from FeO_6A^{n-9} Cluster Model 178

6.3 CONCLUSION 184

REFERENCES 185

LIST OF TABLES

Table	Heading	Page
2.0	Approximate Formulas for β_{kl} Parameter	44
3.0	The Basis Set for FeO_6^{9-}, H^+,OH^- and NH_3 Systems	94
3.1	O2p -Nonbonding Orbital of the FeO_6^{9-} System	95
3.2	The Basis Set Used for FeO_5^{7-} and OH^- in FeO_5OH^{8-} System	95
3.3	The Basis Set Used for FeO_5^{7-} and H^+ in FeO_5H^{6-}	95
3.4	The Orbitals of the Various Irreducible Representations	95
3.5	The Possible Molecular Orbitals Combination in FeO_6A^{n-9} Cluster Adsorbent - Adsorbate Systems	101
5.1	Results for the FeO_6H^{8-} System: Orbital Energies and Other Quantities, σ- Interaction	142
5.2	Results for the FeO_6H^{8-} System: Orbital Energies and Other Quantities - O2p σ-Nonbonding Interaction with H^+ Adsorbate	144
5.3	Results for the FeO_6OH^{10-} System: Orbital Energies and Other Quantities, σ-Interactions	151
5.4	Results for the FeO_6OH^{10-} System: Orbital Energies and Other Quantities,π-Interactions	157
5.5	Results for the $FeO_6NH_3^{9-}$ System: Orbital Energies and Other Quantities,σ-Interactions	159
5.6	Results for the $FeO_6NH_3^{9-}$ System: Orbital Energies and Other Quantities, π-Interactions	164
6.1	Physisorption Energies of H^+, OH^- and NH_3 on the (111)Surface of α-Fe_2O_3	173
6.2	Chemisorption Energies and Equilibrium Bond Distances of H^+, OH- and NH_3 on (111) Face of	

	α-Fe_2O_3 Simulated by the FeO_5A^{n-7} Cluster Model	177
6.3	Chemisorption Energies and Equilibrium Bond Distances of H^+, OH^- and NH_3 from FeO_6A^{n-9} Cluster Model	178
6.4	The Chemisorption Energy of H^+ ion, Bonding by the Surface Oxygen Only, Simulated by FeO_6H^{8-} O2p Nonbonding Orbital	178
6.5	Chemisorption Energies and Equilibrium Bond Distances of OH^- and NH_3 Absorbates from FeO_6A^{n-9} Cluster Model	179
6.6	Comparison of Chemisorption Energies of the Adsorbates on α-Fe_2O_3 (111) Surface as Obtained by EHT and SCF - MO EHT - SP Methods	180
6.7	Comparison of Chemisorption Energies from FeO_5A^{n-7} Chemisorption Model with Experiment	182
6.8	Chemisorption Energies by SCF - MO EHT - SP Method from FeO_6A^{n-9} Chemisorption Model Compared with Experiment	182
6.9	Chemisorption Energies by EHT Method from FeO_6A^{n-9} Chemisorption Model Compared with Experiment	183

LIST OF FIGURES

Figure	Heading	Page
	Chapter One	
1.	The Arrangement of Atoms in the Units of Structure of Hematite	2
2.	Spin Arrangements of Successive Fe^{3+} Cations in the Units of α-Fe_2O_3 Structure along the [111] Axis	4
3.	Sketch of Energy Band Structure as a Function of Inverse Parameter for an Iron Group Transition Metal Oxide	6
4.	Valence Molecular Orbital Diagram of FeO_6^{9-} Cluster by SCF - Xα Spin Polarized Calculation	12
5.	The Valence Region x-ray Photoelectron Spectrum of α-Fe_2O_3	14
6.	A Diagram Illustrating Adsorption of a Gas Molecule by a Surface	19
	Chapter Two	
2.0	Scale Relative to an Electron at infinity	43
	Chapter Three	
3.0	The σ- and π-Bond in FeO_6A^{n-9} Cluster	98
3.1	Spheroidal Coordinate System	100
3.2	Bonding Scheme for the FeO_6OH^{10-} Cluster in which only σ-Bonding is Operative	103
3.3	Bonding Scheme for the FeO_6OH^{10-} Cluster in which only π-Bonding is Operative	103
3.4	Bonding Scheme for the $FeO_6NH_3^{9-}$ Cluster in which only σ-Bonding is Operative	104
3.5	Bonding Scheme for the $FeO_6NH_3^{9-}$ Cluster in which only π-Bonding is Operative	104
3.6	Bonding Scheme for the FeO_6H^{8-} Cluster	105
3.7	Bonding Scheme for the FeO_6H^{8-} Cluster in which only O2p	

LIST OF FIGURES

Figure	Heading	Page
	Chapter One	
1.	The Arrangement of Atoms in the Units of Structure of Hematite	2
2.	Spin Arrangements of Successive Fe^{3+} Cations in the Units of α-Fe_2O_3 Structure along the [111] Axis	4
3.	Sketch of Energy Band Structure as a Function of Inverse Parameter for an Iron Group Transition Metal Oxide	6
4.	Valence Molecular Orbital Diagram of FeO_6^{9-} Cluster by SCF - Xα Spin Polarized Calculation	12
5.	The Valence Region x-ray Photoelectron Spectrum of α-Fe_2O_3	14
6.	A Diagram Illustrating Adsorption of a Gas Molecule by a Surface	19
	Chapter Two	
2.0	Scale Relative to an Electron at infinity	43
	Chapter Three	
3.0	The σ- and π-Bond in FeO_6A^{n-9} Cluster	98
3.1	Spheroidal Coordinate System	100
3.2	Bonding Scheme for the FeO_6OH^{10-} Cluster in which only σ-Bonding is Operative	103
3.3	Bonding Scheme for the FeO_6OH^{10-} Cluster in which only π-Bonding is Operative	103
3.4	Bonding Scheme for the $FeO_6NH_3^{9-}$ Cluster in which only σ-Bonding is Operative	104
3.5	Bonding Scheme for the $FeO_6NH_3^{9-}$ Cluster in which only π-Bonding is Operative	104
3.6	Bonding Scheme for the FeO_6H^{8-} Cluster	105
3.7	Bonding Scheme for the FeO_6H^{8-} Cluster in which only O2p	

σ-Nonbonding is Operative 105

Chapter Four

4.1.0 The Physisorption of H^+ ion by FeO_5H^{6-} Model 108

4.1.1 The Symmetry Elements of the FeO_5H^{6-} Cluster 113

4.2.0 The Physisorption of a Dipole by FeO_5A^{n-7} Model 121

4.2.1 The Symmetry Group of FeO_5A^{n-7} System 132

4.3.0 The Chemisorption of NH_3 by $FeO_5NH_3^{7-}$ Model 137

Chapter Five

5.1 The Energy Levels of the Adsorbent - Adsorbate System of FeO_6H^{8-} Cluster,Calculated by SCF - MO EHT - SP 145

5.2 The Energy Levels of the Adsorbent - Adsorbate System of FeO_6H^{8-} Cluster, Calculated by EHT 146

5.3 The Energy Levels of the Adsorbent - Adsorbate System of FeO_6H^{8-} Cluster: (H^+ ion Chemisorption by the Oxygens), Calculated by EHT 147

5.4 The Energy Levels of the Adsorbent - Adsorbate System of FeO_6H^{8-} Cluster:(H^+ ion Chemisorption by the Oxygens), Calculated by SCF - MO EHT-SR 148

5.5 The Energy Levels of the Adsorbent - Adsorbate System of FeO_6OH^{10-} Cluster: (OH- ion,σ-Bonding), Calculated by EHT 152

5.6 The Energy Levels of the Adsorbent - Adsorbate System of FeO_6OH^{10-} Cluster: (OH- ion, σ-Bonding), Calculated by SCF - MO EHT - SP 153

5.7 The Energy Levels of the Adsorbent - Adsorbate System of FeO_6OH^{10-} Cluster: (OH- ion π-Bonding), Calculated by EHT 154

5.8 The Energy Levels of the Adsorbent - Adsorbate System of FeO_6OH^{10-} Cluster: (OH- ion π-Bonding), Calculated by SCF - MO EHT - SP 155

5.9 The Energy Levels of the Adsorbent - Adsorbate System of $FeO_6NH_3^{9-}$ Cluster: (NH_3 σ-Bonding), Calculated by EHT 160

5.10 The Energy Levels of the Adsorbent - Adsorbate System of $FeO_6NH_3^{9-}$ Cluster: (NH_3 σ-Bonding), Calculated by SCF - MO EHT- SP 161

5.11 The Energy Levels of the Adsorbent - Adsorbate System of $FeO_6NH_3^{9-}$ Cluster: (NH_3 π-Bonding), Calculated by EHT 162

5.12 The Energy Levels of the Adsorbent - Adsorbate System of $FeO_6NH_3^{9-}$ Cluster: (NH_3 π-Bonding), Calculated by SCF - MO EHT - SP 163

5.13 The MO Diagram of the FeO_5H^{6-} Adsorbent - Adsorbate Cluster: Calculated by EHT 167

5.14 The MO Diagram of the FeO_5OH^{8-} Adsorbent - Adsorbate Cluster: Calculated by EHT 168

5.15 The Potential Energy Curve for NH_3 Chemisorption 169

5.16 The Potential Energy Curve for H^+ Physisorption 170

5.17 The Potential Energy Curve for OH^- Physisorption 171

5.18 The Potential Energy Curve for NH_3 Physisorption 172

CHAPTER ONE

INTRODUCTION

1.0 Iron (III) Oxide, α-Fe_2O_3

Iron (III) oxide belongs to the class of oxides of the first row transition metals with the general formula M_2O_3:

Sc	Ti	V	Cr	Mn	Fe	Co	Ni	Cu	Zn
Sc_2O_3	(Ti_2O_3)	V_2O_3	Cr_2O_3	Mn_2O_3	Fe_2O_3	Co_2O_3	(Ni_2O_3)	Cu_2O_3	-

The oxides in parentheses are very unstable but that of Ti is, in addition, nonstoichiometric and metallic. Zn_2O_3 does not exist (Phillips and Williams,1965). The crystals of all the compounds consist primarily of O^{2-} anions in close-packed arrangement and partially ionized metallic M^{3+} cations that occupy octahedral holes.

As for α-iron(III) oxide, the constituents are Fe^{3+} and O^{2-} ions as expected. This oxide has the corundum structure which belongs to the trigonal crystal system (Slater, 1975). The unit cell (as determined by Pauling and Hendricks, 1925) is a rhombohedron generated by three primitive vectors (of equal lengths, a = b = c = 5.414Å) that make equal angles with one another, these being $\alpha = \beta = \gamma = 55^\circ 17'$. This unit cell is shown in Figure 1.

Looking down along the [111]-axis one sees an equilateral triangular network of O^{2-} anions, in O_3 planes. Following the topmost O_3 plane is a plane of single Fe^{3+} cation, then another O_3 plane rotated by 180°. Thus the Fe^{3+} cation is located on the [111]-axis and at the mid-point between the O_3 planes giving a perfect octahedron of FeO_6^{9-} cluster (Bragg et al., 1965).

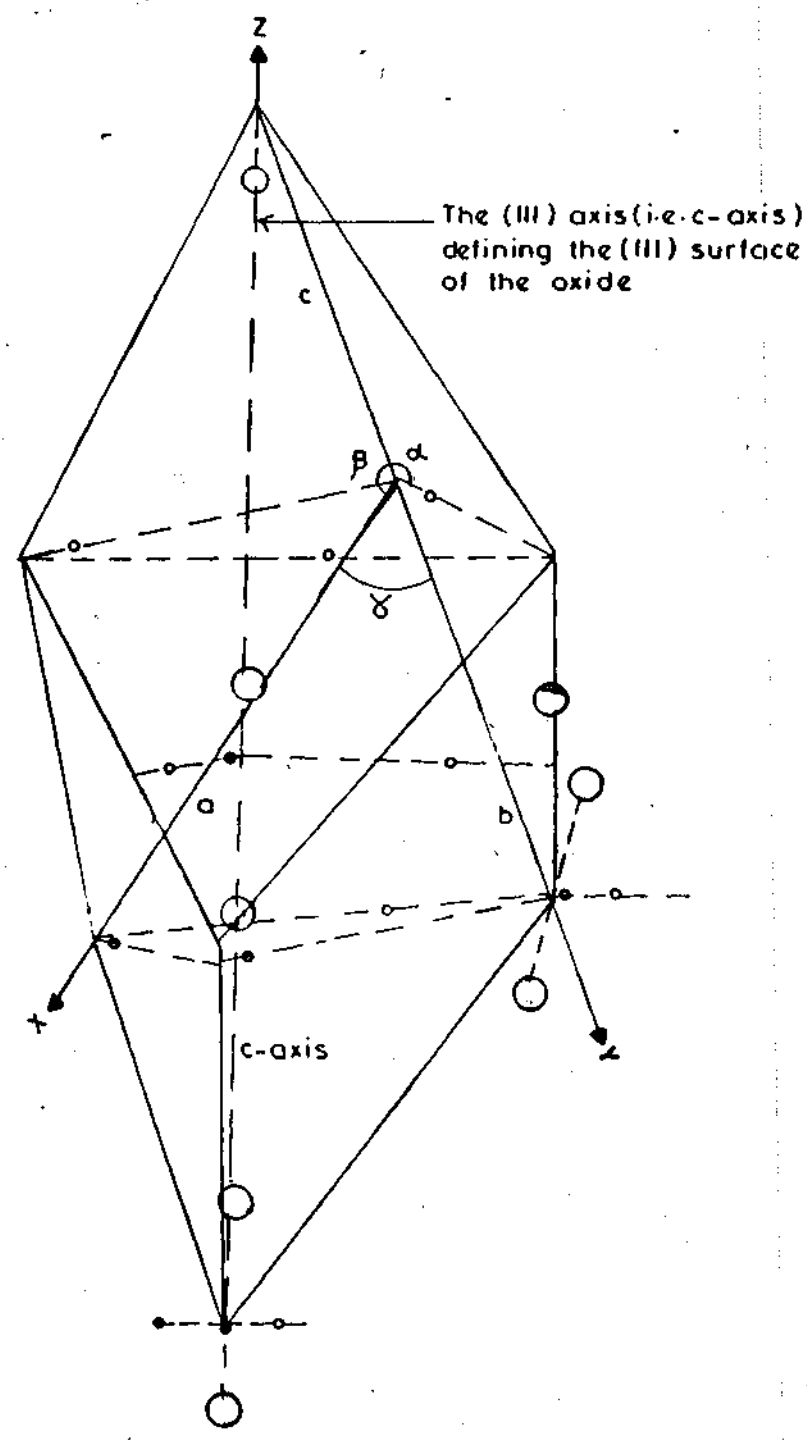


Figure 1: The Arrangement of Atoms in the Units of Structure of Hematite; Small Circles Represents Oxygen Atoms, Large Circles Atoms of Iron

Another feature of the arrangement of atoms in the unit cell is the location of ferric ions (Fe^{3+}) in octahedral holes created by close-packed neighbouring O^{2-} anions giving FeO_6^{9-} as the basic polyatomic or polyhedral unit of the oxide. Other forms of iron (III) oxide exist. They are designted as β-, γ-, and δ-Fe_2O_3 and all but one have crystal structures different from α-Fe_2O_3. These other structures are also ferromagnetic in constrast to α-Fe_2O_3 which antiferromagnetic (Remy, 1956; and Adler, 1968).

1.1 The Electrical and Magnetic Properties of α- Fe_2O_3

The electrical conductivity behaviour of α-Fe_2O_3 is apparently complicated because of the ease of obtaining either p-type or n-type hematite. There is conductivity anisotropic, the measured conductivity value being several orders of magnitude smaller parallel to the [111]-axis than it is in the basal plane (Adler, 1968). Furthermore its temperature dependence is such that in the region around the Néel temperature (T_N) a conductivity maximum has been reported.

α-Ferric oxide is an antiferromagnetic material with a very high T_N of 960K (Adler, 1968) and has two temperature regions of magnetic ordering. The spins are aligned parallel in each basal plane, with alternate planes coupled antiferromagnetically. However, the spin alignment is temperature dependent: in the first temperature region, i.e. between 260K and T_N, the spins are nearly perpendicular to the [111]-axis; in the second temperaure region, i.e. below 260K, they are parallel to the [111]-axis. These arrangements are shown in figure 2.

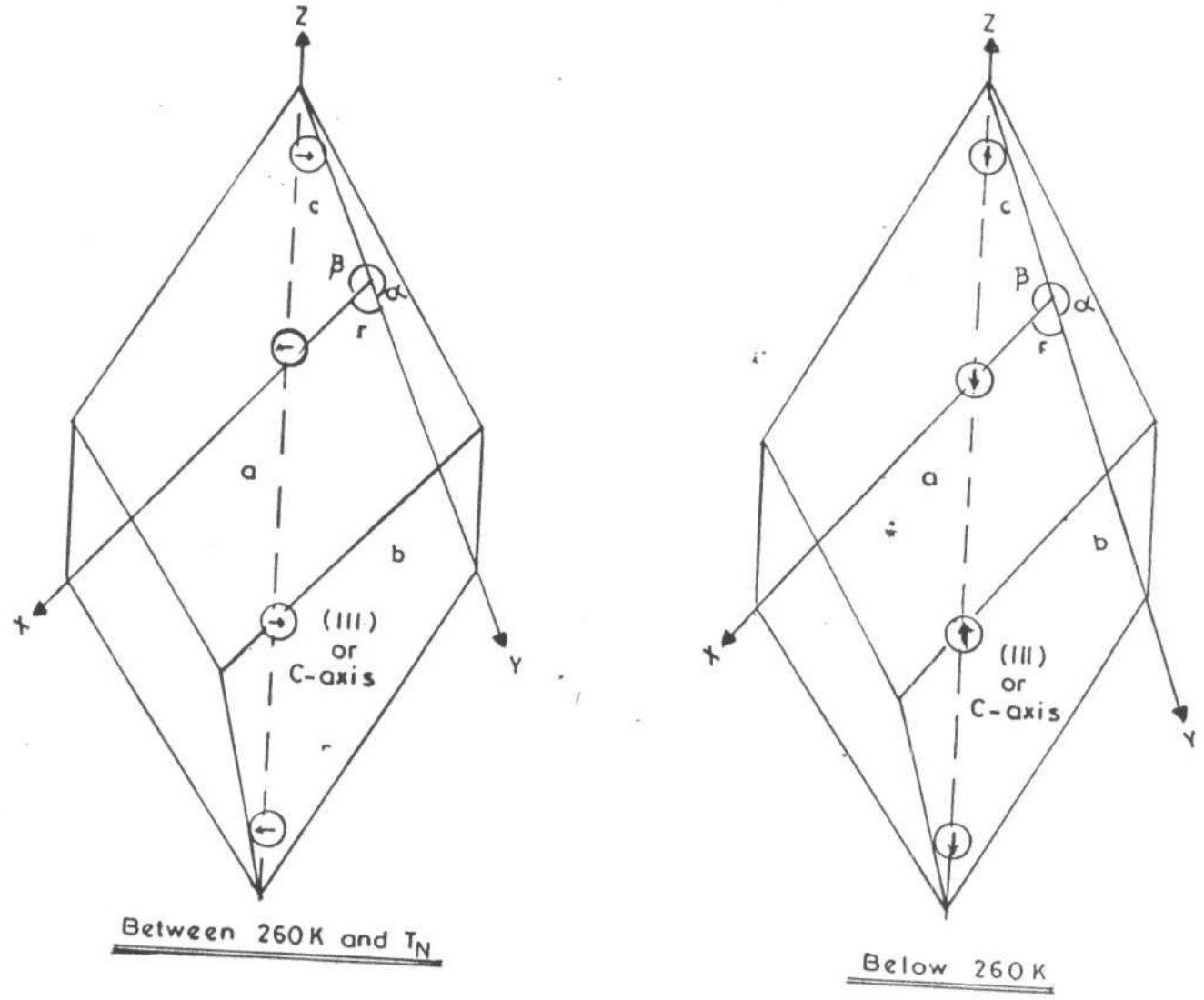


Figure 2: Spin Arrangements of Successive Fe^{3+} Cations in the Units of $\alpha - Fe_2O_3$ Structure Along the (III) - Axis

In the former antiferromagnetic region, there is a weak parasitic ferromagnetism (Adler, 1968), which has been attributed to slight canting of the spins in the basal plane. This canting of the spins leads to the appropriate magnetic symmetry for the observed effect.

1.2 The Electronic Structure of α-Fe_2O_3

The energy band structure of the iron group transition metal oxides has been calculated by the band theory (Adler, 1968). According to these calculations, the energy band structure of the oxides consists mainly of 2p, 3d and 4s bands as shown in figure 3.

The band lowest lying in energy arises primarily from the 2p orbitals on the O^{2-} anions and is completely filled at zero temperature. Above the O^{2-}-2p band is the partially filled 3d band arising from the 3d orbitals of the cations. Above the partially filled 3d band comes the 4s band primarily from the 4s orbitals of the cations and well separated from the 3d band. The 4s band is completely empty at zero temperature. The Fermi level lies within the 3d band and can be split by crystalline field. The wave functions for these bands are simply Bloch waves, and since the valence band (the 3d band) is partially filled, the band theory predicts that the iron group transition metal oxides are metallic.

Although band theory calculations predict that the iron group transition metal oxides should be metallic, they are, infact, highly insulating, Ti_2O_3 being the only exception. A simple explanation of the failure of band theory to account for the low

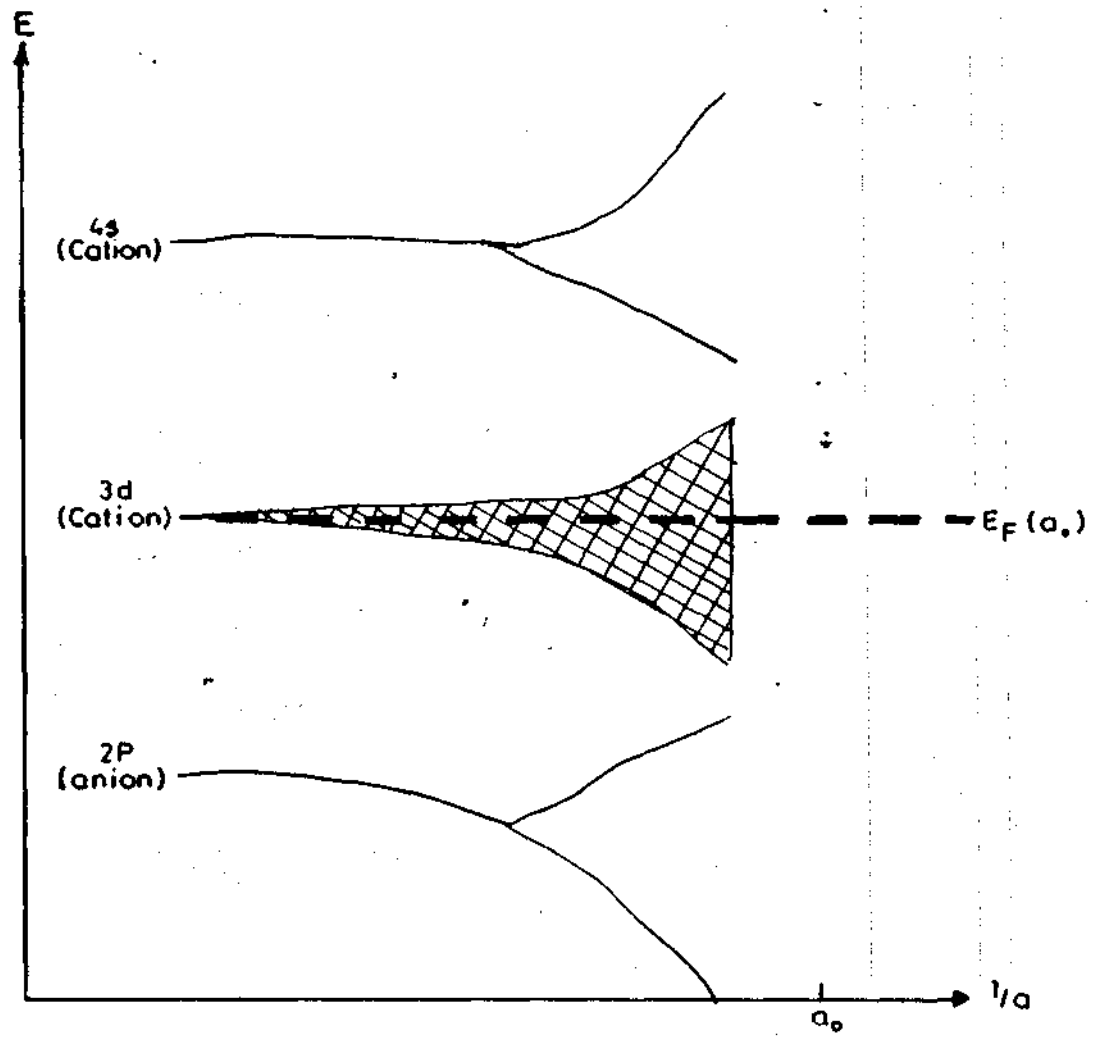


Figure 3: Sketch of Energy Band Structure as a Function of Inverse Lattice Parameter for an Iron Group Transition Metal Oxide

electrical conductivity of these oxides would seem to lie in concluding categorically that d bands, at least in these oxides, are too narrow to support metallic conductivity, and also, since no s or p bands are present in the vicinity of the Fermi level these materials must be nonconductors. However, the likely reason is the assuption, in band theory for the iron group transition metal oxides, that electrons are delocalised in the solid and that correlation effects from electron - electron interactions are not important (that is neglected).

One can, therefore, improve on the results of the band theory by introducing techniques that include the electronic correlations in a localized electron model, with all electrons localized on their particular ion or cluster of ions. It is possible to perform a quantitative localized MO calculation of a few ions of the oxides that form a "cluster" which would yield the correct electrical properties. This is the so-called cluster model of electronic structure of solids.

The electronic structure of α-Fe_2O_3 has been calculated using the quantum cluster model (Tossel and Vaughan, 1973). The calculation was undertaken by a localized SCF-Xα spin-polarized MO variant of the cluster model (Johnson, 1973; Slater and Johnson, 1972). It may be helpful here to give some highlights on the spin-polarized MO calculation so that its advantage over the familiar nonspin-polarized MO calculation could be seen. Consider a determinantal function, formed from $u_{1\uparrow}$, $u_{2\uparrow}$,...,$u_{M\uparrow}$ spin up MOs and $u_{1\downarrow}, u_{2\downarrow}, \ldots, u_{N\downarrow}$ spin down MOs with $M \neq N$ (Slater,1974).

$$\psi = 1/\sqrt{(M+N)!}\sum_R (-1)^R \bar{R}\, u_{1\uparrow}(1)u_{2\uparrow}(2).....u_{M\uparrow}(M)$$

x $u_{1\downarrow}(M+1)\ u_{2\downarrow}(M+2)$ ..... $u_{N\uparrow}(M+N)\}$ ..... (1-1)

and an electronic Hamil tonian.

$$H_{el} = \sum(i)\ (-\sum(A)\ \frac{Z_A}{r_{Ai}} - \frac{\nabla_i^2}{2}) + \sum(i,j,i<j) 1/r_{ij}$$

$$= \sum(i) f_i + \sum(i,j,i<j) g_{ij} .....(1-2)$$

The energy of such a determinantal function takes the well-known form using standard reduction procedure (Slater, 1974)

$$\langle EHFR\rangle = \sum(i\uparrow) n_{i\uparrow}\int u_{i\uparrow}^*(1)[f_1 + \sum(j\uparrow) n_{j\uparrow}\int u_{j\uparrow}^*(2)u_{j\uparrow}(2)g_{12}dv_2$$

$$+\sum(j\downarrow) n_{j\downarrow}\int u_{j\downarrow}^*(2)u_{j\downarrow}(2)g_{12}dv_2 - \sum(j\uparrow) n_{j\uparrow}\int \frac{u_{i\uparrow}^*(1)u_{j\uparrow}^*(2)g_{12}u_{j\uparrow}(1)u_{i\uparrow}(2)dv_2}{u_{i\uparrow}^*(1)u_{i\uparrow}(1)}$$

$$x]u_{i\uparrow}(1)dv_1 + \sum(i\downarrow) n_{i\downarrow}\int u_{i\downarrow}^*(1)[f_1 + \sum(j\uparrow) n_{j\uparrow}\int u_{j\uparrow}^*(2)u_{j\uparrow}(2)g_{12}dv_2 + \sum(j\downarrow)$$

$$x n_{j\downarrow}\int u_{j\downarrow}^*(2)u_{j\downarrow}(2)g_{12}dv_2 - \sum(j\downarrow) n_{j\downarrow}\int \frac{u_{i\downarrow}^*(1)u_{j\downarrow}^*(2)g_{12}u_{j\downarrow}(1)u_{i\downarrow}(2)dv_2}{u_{i\downarrow}^*(1)u_{i\downarrow}(1)}]u_{i\downarrow}(1)$$

xdv_1 ..... (1-3)

where integrations include summation over spin.

The next step to derive the Hartree - Fock - Roothaan

equations is to vary the occupied spin orbitals, $u_{i\uparrow}$ and $u_{i\downarrow}$, while preserving their normalization and orthogonality to the other spin orbitals. The normalization and orthogonality is handled by the method of undetermined multipliers, namely

$$\delta(\langle EHFR\rangle - \sum (i\uparrow)\epsilon_{i\uparrow} n_{i\uparrow} \int u^*_{i\uparrow}(1) u_{i\uparrow}(1) dv_1 - \sum (i\downarrow)\epsilon_{i\downarrow} n_{i\downarrow} \int u^*_{i\downarrow}(1) u_{i\downarrow}(1) dv_1)$$

$$= \sum (i\uparrow) n_{i\uparrow} \int \delta u^*_{i\uparrow}(1) [f_1 + \sum (j\uparrow) n_{j\uparrow} \int u^*_{j\uparrow}(2) u_{j\uparrow}(2) g_{12} dv_2 + \sum (j\downarrow) n_{j\downarrow} \int u^*_{j\downarrow}(2) u_{j\downarrow}(2) g_{12} dv_2 - \sum (j\uparrow) n_{j\uparrow} \int \frac{u^*_{i\uparrow}(1) u^*_{j\uparrow}(2) g_{12} u_{j\uparrow}(1) u_{i\uparrow}(2) dv_2}{u^*_{i\uparrow}(1) u_{i\uparrow}(1)} - \epsilon_{i\uparrow}] u_{i\uparrow}(1) dv_1$$

$$+ \text{complex conjugate}$$

$$+ \sum (i\downarrow) n_{i\downarrow} \int \delta u^*_{i\downarrow}(1) [f_1 + \sum (j\uparrow) n_{j\uparrow} \int u^*_{j\uparrow}(2) u_{j\uparrow}(2) g_{12} dv_2$$

$$+ \sum (j\downarrow) n_{j\downarrow} \int u^*_{j\downarrow}(2) u_{j\downarrow}(2) g_{12} dv_2 - \sum (j\downarrow) n_{j\downarrow} \int \frac{u^*_{i\downarrow}(2) u^*_{j\downarrow}(2) g_{12} u_{j\downarrow}(1) u_{i\downarrow}(2) dv_2}{u_{i\downarrow}{}^*(1) u_{i\downarrow}(1)}$$

$$- \epsilon_{i\downarrow}] u_{i\downarrow}(1) dv_1 + \textit{complex conjugate} = 0 \quad \ldots\ldots\ldots (1\text{-}4)$$

The undetermined multipliers are $-\epsilon_{i\uparrow}$ and $-\epsilon_{i\downarrow}$. Equation (1-4) cannot be satisfied for arbitrary variations $\delta u_{i\uparrow}{}^*(1)$ and $\delta u_{i\downarrow}{}^*(1)$ unless the quantities multiplying them in (1-4) vanish (which also applies to $\delta u_{i\uparrow}$ (1) and $\delta u_{i\downarrow}$ (1) in the complex conjugate terms). Consequently, this leads to separate Hartree - Fock - Roothaan

equations for spin up and spin down orbitals

$$[f_1+\sum(j\uparrow)n_{j\uparrow}\int u_{j\uparrow}^*(2)u_{j\uparrow}(2)g_{12}dv_2+\sum(j\downarrow)n_{j\downarrow}\int u_{j\downarrow}^*(2)u_{j\downarrow}(2)g_{12}dv_2$$

$$+V_{XHFRi\uparrow}(1)]u_{i\uparrow}(1) = \epsilon_{i\uparrow}u_{i\uparrow}(1)\ldots\ldots\ldots\ldots\ldots(1\text{-}5)$$

where

$$V_{XHFRi\uparrow}(1)\equiv-\sum(j\uparrow)n_{j\uparrow}\int u_{i\uparrow}^*(1)u_{j\uparrow}^*(2)g_{12}u_{j\uparrow}(1)u_{i\uparrow}(2)dv_2/u_{i\uparrow}^*(1)u_{i\uparrow}(1)$$

$$\ldots\ldots\ldots\ldots\ldots(1\text{-}6)$$

and

$$[f_1+\sum(j\uparrow)n_{j\uparrow}\int u_{j\uparrow}^*(2)u_{j\uparrow}(2)g_{12}dv_2+\sum(j\downarrow)n_{j\downarrow}\int u_{j\downarrow}^*(2)u_{j\downarrow}(2)g_{12}dv_2$$

$$+V_{XHFRi\downarrow}(1)]u_{i\downarrow}=\epsilon_{i\downarrow}u_{i\downarrow}(1)\ldots\ldots\ldots\ldots(1\text{-}7)$$

where also for the spin down

$$V_{XHFRi\downarrow}(1)\equiv-\sum(j\downarrow)n_{j\downarrow}\int\frac{u_{i\downarrow}^*(1)u_{j\downarrow}^*(2)g_{12}u_{j\downarrow}(1)u_{i\downarrow}(2)dv_2}{u_{i\downarrow}(1)u_{i\downarrow}(1)}$$

Thus for a nonfilled shell of electrons, such as in FeO_6^{9-} cluster, it is an unwarranted assumption to postulate equal numbers of electrons with spin up and spin down and consequently equal exchanges for both spins. This for FeO_6^{9-} system with $\Sigma(i\uparrow)n_{i\uparrow} \neq \Sigma(i\downarrow)n_{i\downarrow}$ would lead to different potentials, since from (1-6) and (1-8) there will be unequal exchanges

$$V_{XHFRi\uparrow}(1) \neq V_{XHFRi\downarrow}(1),$$

hence different eigenvalues,

$$\epsilon_{i\uparrow} \neq \epsilon_{i\downarrow},$$

and different MOs ($u_{i\uparrow}$ and $u_{i\downarrow}$) for spin up and spin down, therefore to a spin polarized calculation.

For crystals, the equations (1-5) and (1-7) have proved in most cases to be unmanageable. The problematic terms are the exchange correlation terms, $V_{XHFRi\uparrow}(1)$ and $V_{XHFRi\downarrow}(1)$. The simplifications of these terms (Slater, 1974) were proposed with the hope that they might make the calculations more practical. The terms were replaced by a weighted mean as

$$[V_{XHFRi\uparrow}(1)]_{av} = V_{X\alpha\uparrow}(1)$$

$$= -6\alpha\left[\frac{3}{4\pi}\Sigma(i\uparrow)n_{i\uparrow}u_{i\uparrow}^{*}(1)u_{i\uparrow}(1)\right]^{1/3} \ldots\ldots\ldots (1\text{-}9)$$

with a similar expression for spin down, where α is taken to be an adjustable parameter. This leads to

$$[f_1+\sum(j\uparrow)n_{j\uparrow}\int u_{j\uparrow}^{*}(2)u_{j\uparrow}(2)g_{12}dv_2+\sum(j\downarrow)n_{j\downarrow}\int u_{j\downarrow}^{*}(2)u_{j\downarrow}(2)g_{12}dv_2$$

$$+V_{X\alpha\uparrow}(1)]u_{i\uparrow}(1)=\epsilon_{i\uparrow X\alpha}u_{i\uparrow}(1)\ldots\ldots\ldots\ldots\ldots(1\text{-}10)$$

one - electron equations with similar expression for spin down. Calculations are carried out to self-consistency, thus SCF-Xα spin polarized MO model.

The localized SCF-Xα spin polarized model for α-Fe_2O_3 is the FeO_6^{9-} cluster (Tossel and Vaughan, 1974), a Fe^{3+} cation surrounded by six O^{2-} anions. This cluster was used as model for the hematite mineral and the calculations were used to elucidate the nature of the mineral's electronic structure. The justification for choosing

FeO_6^{9-} cluster is that it is the basic building block of the hematite mineral (with its electrons localized within it in MOs).

The isolated FeO_6^{9-} cluster is an open shell system with crystal field electronic configuration of $(2t_{2g})^3$ $(3e_g)^2$ and ground electronic state of $^6A_{1g}$ (Tossel and Vaughan, 1974). The SCF-Xα MO spin polarized calculated (Tossel and Vaughan, 1974) orbital energies of the FeO_6^{9-} cluster valence are sketched in figure 4. The highest filled molecular orbital of the FeO_6^{9-} cluster is predicted to be the $3e_g\uparrow$ (mainly Fe3d and O2p) with orbital energy

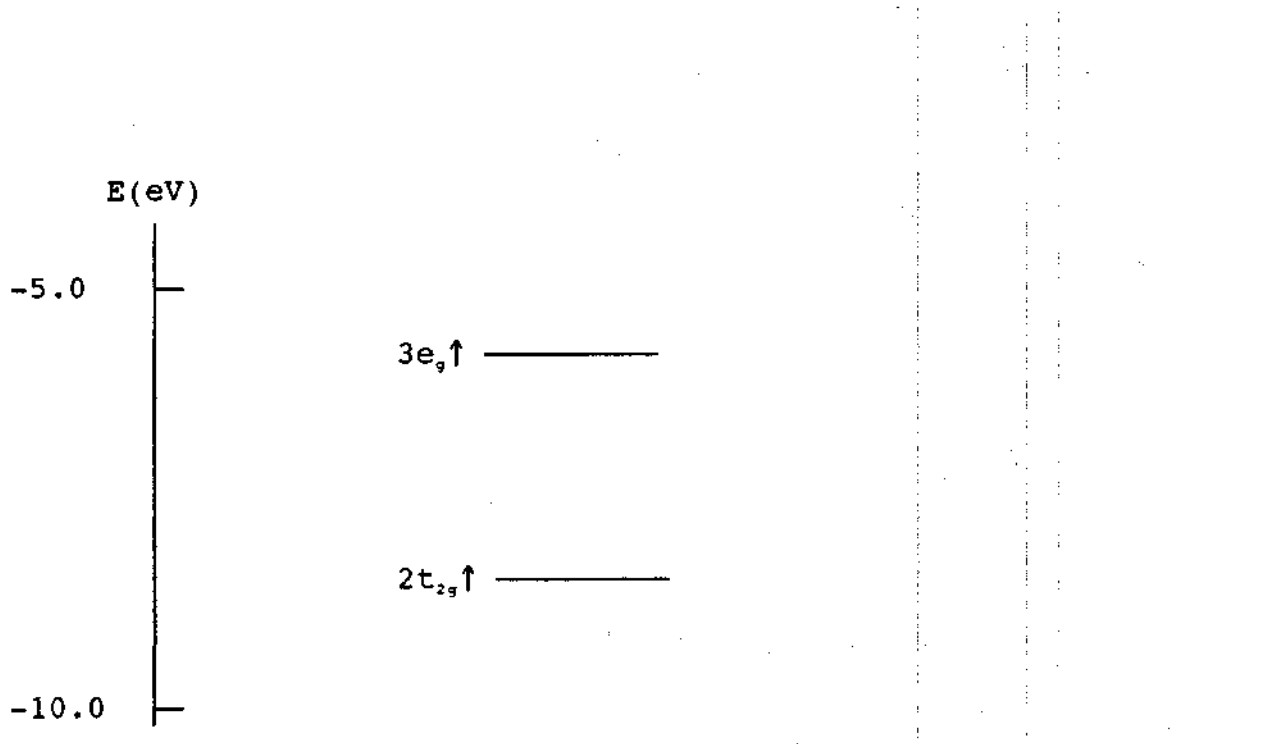


FIGURE 4: **Valence Molecular Orbital Diagram of FeO_6^{9-} Cluster by the SCF-Xα MO Spin Polarized Calculation.**

of between -5 and -6 eV. It is separated from the lower $2t_{2g}\uparrow$ (also Fe3d and O2p) by the $1t_{1g}\uparrow$ and $6t_{1u}\uparrow$ orbitals which are essentially O2p nonbonding orbitals. The $1t_{2u}\uparrow$ orbital is slightly below $2t_{2g}$.

The $2t_{2g}\uparrow$ --→ $3e_g\uparrow$ crystal field splitting was calculated as 2.7 eV. Furthermore, the corresponding spin down 02p nonbonding orbitals ($1t_{2u}\downarrow$, $6t_{1u}\downarrow$ and $1t_{1g}\downarrow$) lie slightly higher than their spin up counterparts ($1t_{2u}\uparrow$, $6t_{1u}\uparrow$ and $1t_{1g}\uparrow$). About 3 - 4eV below the 02p nonbonding levels come $2e_g$, $1t_{2g}$, $6a_{1g}$ and $5t_{1u}$ group of Fe-O bonding orbitals (Fe 3d, 4s, 4p and 02p in character) and below them, about 24eV from the zero level, lie a group of primarily 02s nonbonding orbitals ($1e_g$, $4t_{1u}$ and $5a_{1g}$). The empty antibonding levels, $7a_{1g}$ and $7t_{1u}$, are located about 9eV above the highest filled orbital, $3e_g\uparrow$. They are the conduction levels of the α-Fe_2O_3 solid, and because of this rather very wide gap between them and the valence levels ($2t_{2g}\uparrow$ and $3e_g\uparrow$), the oxide will exhibit insulating rather than metallic electrical properties than metallic.

In summary, the energy levels of the FeO_6^{9-} cluster consist of five distinct groups. The completely full molecular orbitals at zero temperature are the 02s ($1e_g$, $4t_{1u}$ and $5a_{1g}$) nonbonding levels, the Fe-O ($2e_g$, $1t_{2g}$, $4t_{1u}$ and $5t_{1u}$) bonding levels and the 02p ($1t_{2u}$, $6t_{1u}$ and $1t_{1g}$) nonbonding levels. The $2t_{2g}\uparrow$ and $3e_g\uparrow$ levels are the highest occupied or valence energy levels. They are the crystal field levels, half-filled and separated by about 2.7 eV. The Fermi level is the highest occupied $3e_g\uparrow$ level. The $7a_{1g}$ and $7t_{1u}$ are very far above the Fermi level (about 9eV) and are completely empty at zero temperature.

The position and energies of the various orbital sets of the α-Fe_2O_3 solid have been experimentally measured by the X-ray photo electron spectroscopy and also by X-ray emission spectroscopy

(Tossel and Vaughan, 1973 and 1974). The X-ray spectra gave FeK, FeL and OK peaks. From the optical spectra (Tossel and Vaughan, 1973) of the α-Fe_2O_3, the exact positions of all the spin up and spin down sets of orbitals have been determined. The calculated optical transitions for FeO_6^{9-} cluster agreed very well with the experimentally measured (Tossel and Vaughan, 1973) optical transitions of α-Fe_2O_3.

A result of even greater importance, for our purpose, is the *valence* region X-ray photoelectron spectrum of α-Fe_2O_3. Only the $2t_{2g}\uparrow$ and $3e_g\uparrow$ levels appeared in the spectrum (Tossel and Vaughan, 1974; and Koshcheev and cherkashin, 1980) and the crystal field splitting was the prominent feature (see figure 5). The $2t_{2g}\uparrow$ --→ $3e_g\uparrow$ separation was measured as 1.9eV. The Fermi and top of the core levels were located at -5.9 and -10.5 eV respectively.

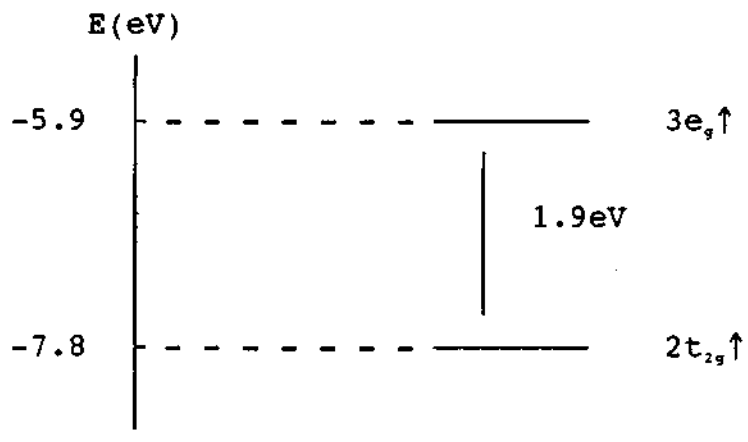


FIGURE 5: The Valence Region X-ray Photoelectron Spectrum of α-Fe_2O_3

1.3 The Surface Electronic Structure of α-Fe_2O_3:

Real solids have surfaces. Quantum mechanics shows that because of the fact that periodicity is broken at the surface localized electronic energy levels, called surface states, will arise at the surface. From a theoretical point of view states localized at the surface arise because surface atoms have quite different characteristics from the normal bulk atoms. There are basically two extremes of surface states. The first type are the Tamm states, which arise on ionic solids in which the surface atoms have electron affinity different from bulk atoms and so electrons on the surface atoms occupy states of energy different from bulk electrons. The other are the Shockley states which arise particularly on covalent solids where the electrons on the incompletely coordinated surface atoms are in orbitals directed toward the surface ("dangling bonds") and so occupy states of different energy from the bulk electrons. More generally, localized surface state energy levels can arise from many causes. Impurities at the surface, or adsorbates, or even ions nearby in solution that are close enough to exchange electrons with the bands of the solid will give rise to localized surface energy levels. Because surface electronic energy levels are of central importance in adsorption processes, the surface electronic structure of α-Fe_2O_3 must be presented.

The techniques employed in calculating electronic structure of surfaces are similar to those used in the study of bulk systems. First of all, the surface considered is assumed to be planar. The

normal to the surface defines the "z" axis. The definition of the surface plane is somewhat arbitrary, but is usually chosen to pass through the atomic nuclei of the outer most layer (Joseph, 1991). Actually, it is better to speak of a surface region, comprising the few outer atomic layers in which the electronic structure and possibly lattice are altered in comparison with that of the bulk, rather than of a sharp surface plane. As in the bulk problem, there are also two distinct models for calculating electronic structure of surfaces: The band and cluster models.

In the band theory of surface electronic structure, it is usually assumed that (Joseph, 1991) the surface region is periodic in directions parallel to the surface and Bloch's theorem applies with respect to displacements in the surface. In this way, Bloch wave functions are constructed, and Schrödinger equation solved yielding surface energy bands $\epsilon_s^n(k_{11})$ which depend on a two-dimensional surface wave vector k_{11} and band index n. However, it is usually more convenient, from a calculational point of view, to work in a slab (or film) geometry (Appelbaum and Hamann, 1980) rather than in the semi-infinite geometry. So one considers a moderate number of atomic planes and applies techniques that are closely related to those used in bulk band structure calculation. In a method based on localized functions, one can divide the slab into cells that repeat with two dimensional translation vector $R_\mu//$, and a set of atoms located at displacements d_j with respect to local origin (Joseph, 1991). The trial Bloch functions are constructed as linear combination of atomic like functions. The

Hamiltonian matrix elements H_{ij} are treated as parameters. Solution of the secular problem yields surface energy bands. To date, no such calculation has been reported on the surface electronic structure of α-Fe_2O_3. Even if there were, owing to electron localization in this solid, band theory is very likely to fail as it did in the bulk problem.

In the cluster approach to surface electronic structure, few or a cluster of surface atoms or ions are used as model to represent the semi-infinite surface based on the division of the surface into component polyatomic clusters. The electronic structure of the surface cluster is calculated by an appropriate quantum method yielding energy levels and orbitals. The problem then reduces to finding an appropriate cluster to represent the surface.

In the case of α-Fe_2O_3, (taking a few outer atomic layers of the (111) surface with the z axis perpendicular to it) we could have a topmost layer of O_3 planes, beneath which is a layer of Fe planes, then another layer of O_3 planes rotated by 180° and so on with each Fe^{3+} cation surrounded by six O^{2-} anions in a perfect octahedral arrangement (Cotton, 1972). Thus the basic polyatomic component of α-Fe_2O_3 (111) surface is the FeO_6^{9-} cluster, several of which join together, as blocks, to form the (111) surface. The FeO_6^{9-} cluster can then be used as a model for the α-Fe_2O_3 (111) surface.

An experimental method can also be used to determine the polyatomic component of a solid surface; it is the ESCA surface

spectral and semi-quantitative surface state analysis. Using this experimental method, the surface oxidation state and coordination type of the Fe atoms in α-Fe_2O_3 surface was determined (Hirokawa and Masaoku, 1979) as Fe^{3+} and octahedral coordination respectively. This confirms FeO_6^{9-} cluster as the basic polyatomic component and a model for α-Fe_2O_3 (111) surface. Fortunately, both the theoretical and experimental electronic structure (Tossel and Vaughan, 1974; Hirokawa and Masaoku, 1979) of FeO_6^{9-} cluster are known and thence the electronic structure of α-Fe_2O_3 (111) surface.

1.4 Solid Surfaces and Adsorption

Because periodicity is broken at the surface of a solid, the fields of force around each surface atom/molecule/ion will reach out into the space beyond the sharp surface plane. Consider such a solid surface in contact with a gas. These surface fields of force, which are external to the gas, can therefore interact with the molecules of the gas. This interaction may be strong enough on some of the gas molecules that they become attracted (by the fields of force) from the gas phase to the surface which results in the gas molecule loosing its 3 translational degrees of freedom to become attached (or bonded) to the surface as shown in figure 6. This process of attachment is termed adsorption. The forces of attraction involved in adsorption are of two main kinds, physical and chemical, and they lead to physisorption and chemisorption respectively.Adsorption is therefore a surface reaction and sometimes requires activation called activation energy of

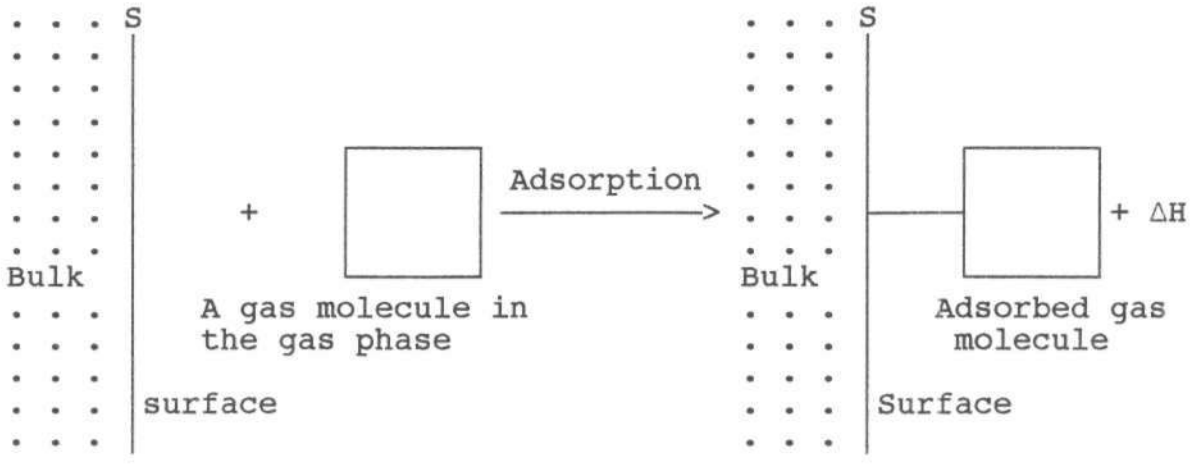


FIGURE 6: A Diagram Illustrating Adsorption of a Gas Molecule by a Surface.

adsorption, E_A. However, physisorption is a non-activated process - fast at all temperatures even very low ones (Gregg, 1961).

A model that is used to interpret adsorption processes is the adsorption isotherm. The most well-known isotherm is the Langmuir's isotherm. In the Langmuir's formalism, it is assumed that (i) the adsorbed entities (gas molecules or adsorbates) are attached to the surface of the adsorbent at "definite localized" sites; (ii) each site can accommodate "one" and only "one adsorbed" entity; and (iii) the energy of the adsorbed entity is the same at all sites on the surface, and is independent of the presence or absence of other adsorbed entities at neighbouring sites. In this way, Langmuir visualized the dynamic equilibrium between the adsorbate molecule in the gas phase at a pressure p, and the adsorbed entities in the surface layer, the fraction of sites covered being θ. Accordingly, the number of molecules inpinging on the adsorbent surface per unit area in unit time is proportional to the pressure. The rate of

adsorption is, therefore, proportional to $p(1 - \theta)$, and the rate of desorption is proportional to θ only. At equilibrium these two rates are equal, so that

$$k_1 p(1 - \theta) = k_{-1}\theta \quad \ldots\ldots\ldots\ldots\ldots\ldots\ldots \quad (1 - 11)$$

where k_1 and k_{-1} are the rate constants for adsorption and desorption respectively. Thence

$$\theta/(1-\theta) = (k_1/k_{-1})p$$

$$= bp \quad \ldots\ldots\ldots\ldots\ldots\ldots\ldots\ldots\ldots\ldots \quad (1 - 12)$$

$$\text{or } \theta = bp/(1+bp) \quad \ldots\ldots\ldots\ldots\ldots\ldots\ldots\ldots \quad (1 - 13)$$

θ is usually referred to as the fraction of the monolayer covered at an equilibrium pressure p. It is expressed as $\theta = v/V_m$, where v is the volume of gas adsorbed and V_m is the volume required to cover the adsorbent surface with a monolayer of the adsorbate. Equation (1 - 13) is called the Langmuir's equation. It is applicable to both physisorption and chemisorption. The physical meaning of the constant b is more understandbale from the full kinetic derivation (Thomas and Thomas, 1967) of equation (1 - 13). It has the implication of determining the energy of the adsorption.

Langmuir's isotherm leads to localized (i.e. cluster) adsorption model and numerous adsorption systems conform to it. However, deviation from the Langmuir's isotherm can occur if surface heterogeneity is severe because, then, surface sites may not be uniform. Other isotherms than Langmuir's (that are applicable to both physisorption and chemisorption) exist. They are the Henry's, Freundlich's and Slygin - Frumkin's isotherms. The

first two isotherms are the limiting forms of the Langmuir's isotherm. There is another isotherm called BET's isotherm which is only applicable to multilayer adsorption (physisorption).

The adsorption of a gas molecule by the surface, as illustrated in figure 6, is accompanied by an energy change, ΔH. This energy change that occurs during the adsorption process is called adsorption energy and can be defined as the total work done by the surface fields of force in attracting the gas molecule from the gas phase to the surface. These forces, as already mentioned, are of two kinds: physical or chemical, leading to physisorption or chemisorption.

The forces bringing about physisorption are those associated with permanent dipole moments in the adsorbed molecule, polarization within the adsorbed molecule etc. If F is the electric field at a site on the surface of a solid, in the Langmuir's formalism, a physisorbing molecule with a permanent dipole moment μ will have a potential energy $U_e(r)$ given by (Thomas and Thomas, 1967)

$$U_e(r) = - F \mu \quad \ldots\ldots\ldots\ldots\ldots\ldots\ldots\ldots \quad (1 - 14)$$

where F is the value of the field at the point, where the centre of the dipole is located, distance r from the surface site. If the physisorbing molecule has no permanent dipole moment, as is the case in non-polar molecules, the potential energy will depend on the polarizability α of the molecule, and is given by

$$U_e(r) = \frac{-F^2\alpha}{2} \quad \ldots\ldots\ldots\ldots\ldots\ldots\ldots\ldots (1\text{-}15)$$

If H_{site}° is the Hamiltonian for the free site on the surface, then the Hamiltonian for the site after physisorbing the gas molecule with permanent dipole moment μ is given by

$$H_{site} = H_{site}^{\circ} + U_{s}(r) \quad \ldots\ldots\ldots\ldots\ldots\ldots \quad (1 - 16)$$

Usually the magnitude of the matrix element of $U_{s}(r)$ is far smaller than that of H_{site}°, so it is regarded as a perturbation to the ground state of the surface site. This perturbation energy, which is the physisorption energy, is given by (first order perturbation)

$$\Delta H = \langle \Psi_{site}^{\circ} \mid U_{s}(r) \mid \Psi_{site}^{\circ} \rangle \quad \ldots\ldots\ldots\ldots \quad (1 - 17)$$

where Ψ_{site}° is the ground state function of the site at the surface where the adsorption takes place.

Chemical forces bringing about chemisorption arise when complete or partial transfer of electrons takes place between the surface site and the chemisorbing molecule. In essence chemical compound is formed, but is confined to a layer one molecule thick at the surface. One can therefore associate such a localized surface molecule with molecular orbitals given by

$$\Psi_{SM},k = \Sigma(i)C_{ki}^{site}\phi_{i}^{site} + \Sigma(j)C_{kj}^{ad}\phi_{j}^{ad} \quad \ldots\ldots\ldots \quad (1\text{-}18)$$

where $\Sigma(i)$ and $\Sigma(j)$ indicate summation over the valence orbitals of the site at the surface and the adsorbate (ϕ_{i}^{site} and ϕ_{j}^{ad}) respectively. The total wavefunction of the (surface site - adsorbate system) surface molecule can be written as a normalized Slater determinant

$$\Psi_{SM}\ (1,2,\ ....,\ L,\ L+1,\ L+2,\ ....,\ L+N)$$

$$= 1/\sqrt{(L+N)!}\sum_{R}(-1)^{R}R\psi^{\alpha}_{SM,1}(1)\alpha(1)....\psi^{\alpha}_{SM,L}(L)\alpha(L)\psi^{\beta}_{SM,1}(l+1)\beta(l+1)$$

$$x...\psi_{SM,N}{}^{\beta}(L+N)\beta(L+N) \qquad .....(1\text{-}19)$$

where the ψ_{SM}'s are given by equation (1-18).

Next is the definition of the surface molecule total Hamiltonian, H_{SM} (containing all possible electrostatic interactions and kinetic energies of electrons)

$$H_{SM} = \sum_{i}(-\sum_{A}\frac{Z_A}{r_{Ai}} - \frac{\nabla_i^2}{2}) + \sum_{i<}\sum_{j}1/r_{ij} + \sum_{A<}\sum_{B}\frac{Z_AZ_B}{R_{AB}}...(1\text{-}20)$$

where Σ_i and Σ_A indicate summation over the valence electrons and nuclei of the surface site and adsorbate respectively. By solving the Schrödinger equation of the surface molecule system, and

$$H_{SM}\Psi_{SM}(1,2,...,L+N) = E_{SM}\Psi_{SM}(1,2,...,L+N) \qquad .....(1\text{-}21)$$

and

$$E_{SM} = \int\Psi_{SM}(1,2,..,L+N)H_{SM}\Psi^{*}_{SM}(1,2,..,L+N)d\tau/\int\Psi^{2}_{SM}d\tau..(1\text{-}22)$$

the binding of the adsorbed bond, chemisorption energy, can be obtained. It is given by

$$\Delta H = E_{SM} - E_{site} - E_{adsorbate} \qquad ..... \quad (1\text{-}23)$$

where E_{SM}, E_{site} and $E_{adsorbate}$ are the total energies of the surface molecule (surface site - adsorbate), surface site and adsorbate systems respectively.

Experimentally, adsorption energy is measured in two different ways each useful in its own context. The first is called the "differential" adsorption energy (Bikerman, 1958) and is measured as the amount of heats dq_1, dq_2, dq_3, ..., given out when the adsorbent surface already charged with x mole of the gas is allowed to take up dx_1, dx_2, dx_3, ...additional amounts of the adsorbate. It is therefore expressed in terms of joules per mole of adsorbate. The second is the integral adsorption energy and is simply the adsorption energy of an adsorbate on a solid surface (Bikerman, 1958). It is measured as the total amount of heat, ΔH, which is given out when 1 mole of an outgassed solid takes up x mole of a gas or vapour; it is therefore expressed in terms of joules per mole of adsorbent, for the adsorption of x mole of adsorbate. The adsorption energy can also be calculated from the differential adsorption energy measurements (Bikerman, 1958)

$$\Delta H = \frac{1}{x}\int_o^x dqdx \qquad \text{.....(1-24)}$$

1.5 Adsorption and Catalysis by α-Fe_2O_3

α-Fe_2O_3 has for long been of great technological importance because of its catalytic behaviour (Jean and Benard, 1962; Salmoiraghi, 1931; Diaconescu and Pantea, 1957; and Jiri and Jaros, 1963). Adsorption and catalysis by this oxide has often been

attributed to the presence of active surface sites. These surface sites are envisioned to interact with adsorbing or reactant molecules/atoms/ions to form surface complex either as a final state in adsorption or as an intermediate state in catalysis. One may, therefore, not be surprised about the amount of experimental effort that has been made on the study of adsorption on this surface and on testing and developing it as a catalyst (alone and in combination with other oxides).

The most important catalysis of α-Fe_2O_3 may broadly speaking be classified into alkylation (Moley, 1979; Yukel'son and Raevskaya, 1970) - dealkylation (Jean and Bernard, 1962; Jaromir, 1960), hydration (Pralus et al., 1970) - dehydration (Haskel and Charles, 1953; Hands and Walker 1948), hydrogenation (Ryonosuke, 1931; Komori, 1941) - dehydrogenation (Warren and Wilson, 1960; Ballard et al., 1956; and Tomassi and Bulawa, 1959), amination (Yoshiro and Ishikura, 1971; Bel'chev, 1958) and oxidation (Bielanshi et al., 1956; Grzelczylc et al., 1955; and Usines de Mille, 1949) processes. Others are hydrolysis (Kagan and Ya, 1933), decarboxylation (Zoltan et al., 1948), synthesis (Hirochi et al., 1953; Virginia and Chales 1952; Kirillov, 1956) and decompositions (Salmoiraghi, 1931; Kamarov and Chernikova, 1962) etc. processes. The ability of α-Fe_2O_3 to catalyse such wide range of chemical reactions may be understood if we consider the experimental measurements of adsorptions on its surface. We shall review only those cases of adsorptions that are relevant to our research, the above catalytic processes and to the properties of the oxide when

immersed in aqueous solution.

Adsorption of H^+ or OH^- ions by α-Fe_2O_3, which is preceded by their abstractions, is the most critical stage in many of its catalysed reactions (eg hydration - dehydration catalysis) and the most important factor in determining its surface character when immersed in aqueous solution (Morrison, 1978). This tendency was detected by Elwira and Proszynska (1963) from their studies of H^+ and OH^- adsorption on the surface of α-Fe_2O_3. The adsorption was studied by a pH method in the range of pH 4 to 10. They observed that at low pH, adsorption of H^+ ions is the greatest and decreases as pH increases until at last adsorption ceases. At still higher pH, adsorption of OH^- ions begins and was found to increase with increasing pH. More informative studies on the adsorption of these ions was that reported by Berube et al (1967). These workers studied, quantitatively, the time dependent abstraction of H^+ and OH^- ions from solution by crystalline α-Fe_2O_3. A pH drift analysis, which they conducted, revealed that H^+ ions were abstracted from H_2O multilayers (ie. physisorbed H_2O layers on the surface) to adsorb on the ferric oxide surface. The migration of the H^+ ions through the H_2O multilayers to the surface, where they finally become adsorbed, yielded a diffusion coefficient of $\approx 10^{-21}$ cm^2/sec. The result of this experiment not only showed that ferric oxide surface adsorbs H^+ and OH^- ions but that it may abstract them from compounds other than H_2O containing H-atoms or OH^- groups when physisorbed on its surface (perhaps more readily when activation energy of adsorption is supplied). Unfortunately, experimental or theoretical

data on either H^+ or OH^- adsorption energies on ferric oxide surface are not yet available.

Adsorption of NH_3 by α-Fe_2O_3 surface is no doubt important in its amination catalysis (Yoshiro and Ishikura, 1971; Bel'cher, 1958) and probably the catalytic link in its NH_3 conversion to HNO_3 acid (Jiri and Jaros, 1963). Thus, the investigation of NH_3 adsorption on this oxide, in the gas or liquid phase, is also important and many reports (on experimental detection) have appeared in the literature. For example, Edwin (1962) detected NH_3 to adsorb on α-Fe_2O_3 from the gas phase. The same author (Edwin and Blyholder, 1962) in another report detected a very important phenomenon on the adsorption of NH_3 (aq) on this oxide. In that experiment, it was observed that H_2O chemisorbs on Ferric oxide by dissociating to form surface OH^- and H^+ ions whereas NH_3 chemisorbs without dissociating. Furthermore, NH_4^+ ion forms only when physisorbed H_2O and NH_3 were present and not when only NH_3 and surface OH^- groups from chemisorbed water were present. In another report (Cremer and Grunner, 1951) also, NH_3 molecules were detected to considerably adsorb on α-Fe_2O_3 over a very wide range of NH_3 (aq) concentrations.

Other class of substances, such as alcohols and carboxylic acids (Koshurrikov, 1948), were also found to adsorb on the oxide even at low temperature of 20°c. For intance, humic and fulvic acids (Evans and Russel, 1959) were detected to adsorb on the oxide from their suspension as component of a soil organic matter and the adsorption was observed to increase with decreasing pH.

Also, alkali and alkaline earth metal cations were reported to adsorb (Maidanovskaya et al., 1955) on the oxide from aqueous solution of their chlorides.

It should be mentioned that for this oxide, experimental data on adsorption energies is scarce. Not withstanding the scarcity of such data on α-Fe_2O_3, other iron-group transition metal oxides have been explored. Even then, adsorption energy data for those oxides with M_2O_3 general formula are limited to O_2, CO, CO_2 and CO/O_2 adsorbates as most workers were interested on oxides with MO general formula.

1.6 Quantum Models for Adsorption on α-Fe_2O_3

Since adsorption of H^+, OH^- and NH_3 is the most critical stage in many of α-Fe_2O_3 catalysed reactions and the most important factor determining its surface character when immersed in aqueous solution (Morrison, 1978), then the knowledge of the general nature and extent of the energy changes that accompanies their adsorptions will be of great value to the chemist. This apart from enabling us to draw acceptable conclusions from experimental measurements, calculation of their adsorption energies will play an important role in the assessment and prediction of the type of bonding involved in a particular adsorbed link in its (for example, hydration-dehydration, hydrolysis, amination etc) catalysis. Some how, to date, there has not been any report on the quantum mechanical studies of H^+, OH^- and NH_3 adsorption on α-Fe_2O_3 that would furnish this information.

Because of the importance of such information we undertook to study, quantum mechanically, the adsorption of the H^+, OH^- and NH_3 adsorbates on α-Fe_2O_3 and calculate their adsorption energies. Since the physical phenomenon of adsorption is of very short range (typically of the order of one internuclear separation), we have simulated the adsorption by a cluster representation of the surface. The paramount reason for this choice, as we saw in sections 1.3 and 1.4, is the failure of the semi-infinite band theory in this solid (Adler, 1968) and the success afforded by the cluster model in accounting for the correct properties of the solid (Tossel and Vaughan, 1973 and 1974). Furthermore, only long-range phenomenon, like electrical conductivity, are better studied using the techniques of band theory; studies related to the formation and breaking of chemical bonds, like adsorption, are far more amenable to the approach of cluster method (Kunz, 1980), since the long-range order in the plane of the surface are absent (the traditional solid state techniques using translational periodicity being of little use).

Following the discussions of sections 1.3 and 1.4 (dealing with bulk and surface electronic structure of α-Fe_2O_3), FeO_6^{9-} cluster is used as a model to represent (111) surface of ferric oxide. This cluster is fully saturated and FeO_5^{7-} cluster is added as model to simulate this surface with an oxygen vacancy. Thus we have

(i) FeO_6A^{n-9}

(ii) FeO_5A^{n-7}

as cluster adsorption models - where A^{n} represents an adsorbing specie, n being the net charge on the adsorbate - to simulate the adsorption of H^{+}, OH^{-} and NH_3 on the ferric oxide (111) face. Because the adsorption of these adsorbates can occur through physisorption or chemisorption and physisorption may precede chemisorption, the adsorption are studied by both cluster physisorption and chemisorption models.

Since H^{+} is a bare proton, and OH^{-} and NH_3 have permanent dipole moment, μ, 1.66 and 1.47D respectively, they can physisorb on the (111) face of this oxide according to equation (1-16) with corresponding physisorption energy given by (1-17). The consequences of the situation are better dealt with by the crystal field theory and forms the basis of our cluster physisorption model for the adsorption of H^{+}, OH^{-} and NH_3 adsorbates. However, we have attempted to modify the familiar crystal field theory by allowing the adsorbate to come from infinity so as to find a distance of maximum binding to the surface. Furthermore, a dipole treatment is developed by us in the course of this research.

On the other hand, chemisorption of H^{+}, OH^{-} and NH_3 involves the rearrangement of the electrons of these adsorbates and the surface with consequential formation of chemical bonds. Using this approach, the chemisorption of H^{+} and OH^{-} in the context of FeO_5A^{n-7} cluster is studied by ligand field theory extended Hückel method, whereas the chemisorption of NH_3 by the same cluster is studied by an electron pair bond pseudo-diatomic model. The chemisorption of all the three adsorbates by FeO_6A^{n-9} cluster are studied by the

familiar extended Hückel theory and the self-consistent field molecular orbital extended Hückel (spin restricted and spin polarized versions) theories - SCF MO EHT methods.

It is hoped that these adsorption models will provide us with the information about the nature, energetics and equlibrium distances of the H^+, OH^- and NH_3 adsorption on the (111) face of α-Fe_2O_3.

CHAPTER TWO

REVIEW OF LITERATURE

2.0 The Extended Hückel Theory (EHT)

The starting point of any electronic structure calculation for molecules, clusters, condensed matter and in adsorption etc. is the provision of an approximate or exact (analytical or numerical) solution to the Schrödinger equation for the system of several particles (such as electrons) subjected to a potential V

$$H_{op}\,\Psi = E\,\Psi \qquad \text{.....(2-1)}$$

where the Hamiltonian operator H_{op} is

$$H_{op} = -\sum_i \frac{\nabla_i^2}{2} + V(\text{----}r_i\text{----}) \qquad \text{.....(2-2)}$$

In (2-2), ∇_i^2 is the Laplacian operator for the ith particle. The wavefunction Ψ, which is understood to depend on the position vectors r_i of all the particles, describes the state of the system: Ψ is the probability amplitude, while $\Psi\cdot\Psi\ d\tau_1\ d\tau_2\ \ldots\ d\tau_N$, where $d\tau_1$ is the volume element of electron 1, represents the probability distribution function for the N particles. For bound states, it is common to normalize the probability to unity:

$$\int \Psi^*\Psi\ d\tau_1 d\tau_2 \ldots\ldots\ldots d\tau_N = 1 \qquad \text{.....(2-3)}$$

In the study of the electronic structure of molecules etc., one is concerned with that particular Schrödinger equation which deals with the movement of the electrons, and more precisely that equation for the movement of nuclei and electrons in the field of fixed nuclei. In the Born-Oppenheimer approximation, the Schrödinger equation (2-1) yields an electronic wave-function Ψ and an electronic energy E. The Hamiltonian operator is then

$$H_{op} = -\sum_i \left(\sum_A \frac{Z_A}{r_{Ai}} + \frac{\nabla_i^2}{2}\right) + \sum_i \sum_{j<} 1/r_{ij} \quad \ldots\ldots\ldots (2\text{-}4)$$

where the successive terms represent operators for the nuclear-electronic attraction, electron kinetic energy, and repulsion between electrons. Unfortunately, for systems with more than two electrons, the solution of (2-1) is mathematically impossible for this Hamiltonian unless one makes rather drastic assumptions. This impracticality is the reason for the various approximate electronic theories; there are generally two major divisions of approximate theories with various degrees of chemical or physical intuition, approximations and levels of sophistication. They are:

1. The *ab initio* or first principles methods; and
2. The semi-empirical methods.

All that need to be said about the ab initio methods here is that all integrals are evaluated and no parameters are introduced in the computations. On the other hand, because of the enormity of computational effort required by the ab initio methods and the

poor accuracy afforded by them for certain properties or larger molecules of interest, the semiempirical theories are built by the use of all available experimental data which are both simple to implement computationally and accurate enough for the molecular systems of interest. Therefore the semiempirical theories are generated from chemical intiutions. The diversity of the chemical intuition of various researchers has led to a vast array of different semiempirical schemes, each with its own peculiarities and parameters.

2.2 **Semiempirical Techniques**:

Semiempirical techniques may be seen to fall into two groups:

1. The LCAO MO methods; and
2. The SCF MO methods.

The extended Hückel theory (EHT) belongs to the LCAO MO group and is an extension of the simple Hückel molecular orbital (HMO) theory. Since the extended Hückel theory is an extension of the simple Hückel molecular orbital theory, it will be of great value to review some of the essential points of the HMO method.

2.3 **The Simple Hückel Molecular Orbital (HMO) Theory**:

Simple Hückel molecular orbital theory is the starting point of the LCAO Mo methods. In this theory, the assumption is made that the solution Ψ in equation (2-1) be a simple one-electron molecular orbital product (Gerald, 1977).

$$\Psi(1,2,\ldots,N) = \psi_1(1)\psi_2(2)\ldots\ldots\psi_N(N)\ldots\ldots\ldots\ldots(2\text{-}5)$$

where the ψ's are the one-electron molecular orbitals and 1 represents the coordinates of electron 1 etc. Furthermore, certain modifications of the Hamiltonian operator are made to ensure that the corresponding Schrödinger equation does admit a solution of this form. Thus the Hückel theory makes the crucial approximation of rewriting the Hamiltonian (2-2) in the form of a sum of one-electron terms:

$$H_{op} = -\sum_i \frac{\nabla_i^2}{2} + V(\ldots\ldots r_i\ldots\ldots\ldots) \approx \sum_i \left(-\frac{\nabla_i^2}{2} + v_i\right)$$

$$= \Sigma\ H_{eff}\ (i) \ldots\ldots\ldots\ldots\ldots\ldots\ (2\text{-}6)$$

In other words, it makes the crude assumption that the potential of an electron is a function v of its coordinates alone and independent of the positions of the other electrons; therefore v represents the field of nuclei and some average effect of all the other electrons. Or, v represents some average (in some way) of potential of an electron in the molecule. The potential v and the corresponding effective Hamiltonian H_{eff} are not defined any explicitly; they will be determined by their matrix elements, which will be related to empirical quantities. More fundamentally, no justification is provided for replacing the true Hamiltonian (2-4) with one and two-electron operators by the simpler one body form (2-6). Assuming (2-5) and (2-6), the Schrödinger equation becomes

$$[H_{eff}(1) + H_{eff}(2) + \ldots\ldots + H_{eff}(N)]\psi_1(1)\psi_2(2)\ldots\ldots\ldots\psi_N(N)$$

$$= E\psi_1(1)\psi_2(2)\ldots\ldots\ldots\psi_N(N)\ldots\ldots\ldots\ldots\ldots(2\text{-}7)$$

Multiplying through equation (2-7) by

$$\int\psi_1^*(1)\psi_2^*(2)\ldots\ldots\psi_N^*(N)d\tau_1 d\tau_2\ldots\ldots d\tau_N,$$

we have

$$[\int\psi_1^*(1)H_{eff}(1)\psi_1(1)d\tau_1\int\psi_2^*(2)\psi_2(2)d\tau_2\ldots\ldots\int\psi_N^*(N)\psi_N(N)d\tau_N$$

$$+\int\psi_2^*(2)H_{eff}(2)\psi_2(2)d\tau_2\int\psi_1^*(1)\psi_1(1)d\tau_1\int\psi_3^*(3)\psi_3(3)d\tau_3\ldots\ldots$$

$$\int\psi_N^*(N)\psi_N(N)d\tau_N\ldots\ldots+\int\psi_N^*(N)H_{eff}(N)\psi_N(N)d\tau_N$$

$$x\int\psi_1^*(1)\psi_1(1)d\tau_1\ldots\ldots\int\psi_{N-1}^*(N\text{-}1)\psi_{N-1}(N\text{-}1)d\tau_{N-1}$$

$$=E\int\psi_1^*(1)\psi_1(1)d\tau_1\ldots\int\psi_N^*(N)\psi_N(N)d\tau_N\ldots\ldots(2\text{-}8a)$$

From equation (2-3), it follows that

$$\int\psi_1^*(1)\psi_1(1)d\tau_1.....\int\psi_N^*(N)\psi_N(N)d\tau_N=\int\Psi^*\Psi d\tau_1...d\tau_N = 1$$

which implies that the individual one-electron molecular orbitals must satisfy the normalization condition:

$$\int\psi_p^*(p)\psi_p(p)d\tau_p=1 \quad p=1,2,3,....,N \quad .....(2\text{-}8b)$$

By using (2 - 8b) in (2 - 8a), we obtain

$$[\int\psi_1^*(1)H_{eff}(1)\psi_1(1)d\tau_1+\int\psi_2^*(2)H_{eff}(2)\psi_2(2)d\tau_2+.....$$

$$.....+\int\psi_N^*(N)H_{eff}(N)\psi_N(N)d\tau_N]$$

$$= \sum_p\int\psi_p^*(p)H_{eff}(p)\psi_p(p)d\tau_p \quad p = 1,2, ...,N$$

$$= E \quad ..... \quad (2\text{-}8c)$$

The sum $\Sigma(p)\int\psi_p^*(p)H_{eff}\psi_p(p)d\psi d\tau_p$ contains independent terms which, according to quantum mechanics, can individually be written as

$$\int\psi_p^*(p)H_{eff}(p)\psi_p(p)d\tau_p = \epsilon_p \quad p = 1,2,...,N \quad ...(2\text{-}8d)$$

or in other words, equation (2-8c) becomes

$$\sum_p \epsilon_p = E \qquad p = 1,2, \ldots,N \quad \ldots.(2\text{-}9)$$

From equation (2-8d), the molecular orbitals $\{\Psi_p;\ p = 1, 2, \ldots N\}$ are the eigenfunctions of the Hamiltonian operator H_{eff} inth (real) energies $\{E_p;\ p = 1,2, \ldots, N\}$ that satisfy the Schrödinger equations

$$H_{eff}\,\psi_p = \epsilon_p \psi_p \quad p = 1,2,\ldots,N \ldots(2\text{-}10)$$

And the total energy is simply the sum of the (filled) orbital energies given by equation (2-9).

The molecular orbitals are expanded as linear combination of independent functions $\phi_1, \phi_2, \ldots\ldots, \phi_N$ with undetermined coefficients $\{C_{pk}\ ;\ p = 1,2, \ldots N\ ;\ k = 1,2, \ldots, N\}$. In other words the pth molecular orbital is written as

$$\psi_p = \sum_k C_{pk}\phi_k \quad k = 1,2,\ldots\ldots,N \quad \ldots\ldots(2\text{-}11)$$

where ϕ_k is an atomic orbital. Apart from noting the atomic centre (which they are located) and symmetry, the orbitals $\{\phi_k\}$ are unspecified - they are not given any precise analytical form. They are therefore termed "chemical orbitals". Equation (2-11) constitutes the linear combination of atomic orbitals (LCAO) approximation. Therefore, the Hückel theory is founded upon mathematically vaguely defined orbitals and an unspecified

effective Hamiltonian.

From equation (2-10), the trial orbital energies in equation are given by (expectation values):

$$\epsilon_p = \int \psi_p^* H_{eff} \psi_p d\tau_p \,/ \int \psi_p^2 d\tau_p \quad p = 1,2,....,N \quad ..... \quad (2\text{-}12)$$

If we introduce the symbols

$$H_{kl} = \int \phi_k^* H_{eff} \phi_l d\tau \text{ and } S_{kl} = \int \phi_k^* \phi_l d\tau$$

then the expression for ϵ_p expectation value becomes, putting equation (2-11) into (2-12),

$$\epsilon_p = \sum_k \sum_l C_{pk}^* C_{pl} H_{kl} / \sum_k \sum_l C_{pk}^* C_{pl} S_{kl} \ldots . (2\text{-}12a)$$

or

$$\epsilon_p \sum_k \sum_l C_{pk}^* C_{pl} S_{kl} = \sum_k \sum_l C_{pk}^* C_{pl} H_{kl} \ldots . (2\text{-}12b)$$

To find the values of C_{p1}^*, C_{p2}^*, ... C_{pk}^* which give the lowest value for ϵ_p and therefore the best approximation to the energy, we differentiate equation (2-12b) with respect to each C_{pk}^* ($k = 1,2, ..., N$):

$$\frac{\partial \epsilon_p}{\partial C_{pk}^*} \sum_k \sum_l C_{pk}^* C_{pl} S_{kl} + \epsilon_p \sum_l C_{pl} S_{kl} = \sum_l C_{pl} H_{kl} \ldots (2\text{-}12c)$$

The condition for the lowest value of the energy or minimum is that

$$\partial\epsilon_p/\partial C_{pk}^{*} = 0 \quad for \quad each \quad k \quad index \ldots\ldots (2\text{-}12d)$$

which reduces equation (2-12c) to

$$\epsilon_p \sum_l C_{pl} S_{kl} = \sum_l C_{pl} H_{kl} \; or \; \sum_l C_{pl}(H_{kl} - \epsilon_p S_{kl}) = 0 \ldots (2\text{-}13)$$

where the S_{kl}'s are overlap integrals.

In order to solve the equations in (2-13), certain approximation were made:

(i) (For hydrocarbons) H_{kk} is a constant for all indentical orbitals regardless of their position in the molecule. It is called α_k (or simply α)

$$\alpha_k = \int \phi_k^{*} H_{eff} \phi_k d_\tau \quad \ldots\ldots\ldots\ldots\ldots\ldots \quad (2\text{-}14)$$

and is negative. It represents the effective energy of a bound electron in orbital ϕ_k, and is normally called the Coulomb integral. The Hückel theory regards it as an empirical parameter.

(ii) That H_{kl} ($k \neq l$) is zero unless ϕ_k and ϕ_l are centred on bonded atoms.

(iii) That for bonded atoms, H_{kl} is written β_{kl} and is assumed a constant (β for carbon - carbon bonds) for all similar bonds, that is independent of the environment of orbitals ϕ_k and ϕ_l:

$$\beta_{kl} = \int \phi_k \, H_{eff} \, \phi_l d\tau \quad (k,l \text{ bonded atoms}) \ldots (2\text{-}15)$$

The constant ß is also an empirical quantity, to be determined by comparison with experiment. It is commonly called resonance or bond integral, and is a negative quantity.

(iv) That atomic overlap can be neglected:

$$S_{kl} = \delta_{kl} \ldots\ldots\ldots\ldots\ldots\ldots\ldots\ldots (2\text{-}16)$$

(δ_{kl}, Kronecker symbol)

Under these conditions the secular equations take the simple form

$$(\alpha_p - \epsilon_\beta) C_{pt} + \sum_5 \beta_{ts} C_{ps} = 0 \quad t = 1,2,\ldots,N \ldots\ldots (2\text{-}17)$$

(For hydrocarbon systems, $ß_{ts}$ is simply ß) and the orbital energies, which are the solution of (2-17), normally take the general form

$$\epsilon_p = \alpha + n_p \beta \ldots\ldots\ldots\ldots (2\text{-}18)$$

where n_p is a real number that is found by solving the characteristic polynomial that arises from expanding the determinant of (2-17) through the usual $(\alpha - \epsilon)/ß$ manupulation. Since ß is negative, a molecular orbital is said to be bonding if the coefficient n_p of ß is positive and antibonding if this coefficient is negative. It is said to be nonbonding if the coefficient n_p is zero.

Hence, given numerical values of α_p and β_{pt}, the energies ϵ_p and the expansion coefficients C_{pt} of equation (2-17) may be evaluated despite the ignorance in $\{ \phi_p \}$ and $H_{eff}(p)$. The $\{\alpha_p, \beta_{pt}\}$ are then the parameters of the Hückel theory that are numerically determined by requiring that the predictions of Hückel agree with experiment. Thus Hückel theory contains the implicit assumption that there exist a $H_{eff}(p)$ of sufficient accuracy that its use with a minimum basis set is worth comparing with experiment.

2.4 The Extended Hückel Theory (EHT)

This method was principally developed by Hoffmann (Hoffmann, 1963) in 1963. In the extended Hückel theory, the secular determinant is set up as in Hückel theory, but all off-diagonal elements are retained (i.e. no assumptions are made about any of these being zero). Thus each matrix element is of the form $[H_{kl} - \epsilon S_{kl}]$, where k = l or not. Further still, all overlap integrals S_{kl} are calculated between all pairs of orbitals ϕ_k and ϕ_l on all pairs of atoms, not just nearest neighbours. Thus no integrals S_{kl} are assumed to be zero, although some infact may turn out to be zero.

The fact that the overlap matrix $\{S_{kl}\}$ is to be calculated means that the mathematically analytical form for the chemical basis $\{\phi_k\}$ has to be known. However, H_{eff} remains undefined explicitly but will be determined by the numerical values of their matrix elements. Thus the parameters that embody the extended Hückel theory (EHT) are

$$\{\alpha_k, \beta_{kl}, S_{kl}\} \quad \ldots\ldots\ldots\ldots\ldots\ldots\ldots\ldots \quad (2\text{-}19)$$

While the overlap integrals { S_{kl} } are calculated from the analytical form of the basis set $\{\phi_k\}$ chosen, the α_k and β_{kl} parameters are optimized from experimental data. Furthermore, EHT allows one to handle σ-systems and problems of conformations where as HMO is restricted, more or less, to π - systems.

2.4.1 Determination of the EHT Parameters, α_k and β_{kl}

Coulomb integrals α_k for all normally occupied orbitals are taken to be equal to the approximate ionization potentials (IP) or electron affinities (EA) for vacant orbitals

$$\alpha_k = \langle \phi_k \mid H_{eff} \mid \phi_k \rangle$$
$$= H_{kk}$$
$$= - IP_k \quad \ldots\ldots\ldots\ldots\ldots\ldots\ldots\ldots\ldots\ldots \quad (2\text{-}20)$$

The assumption here is that the energies of electrons in isolated atomic orbitals, which correspond to the term H_{kk} in the calculations, can be approximated on a scale relative to an electron at infinity by using suitable ionization potentials and electron affinities.

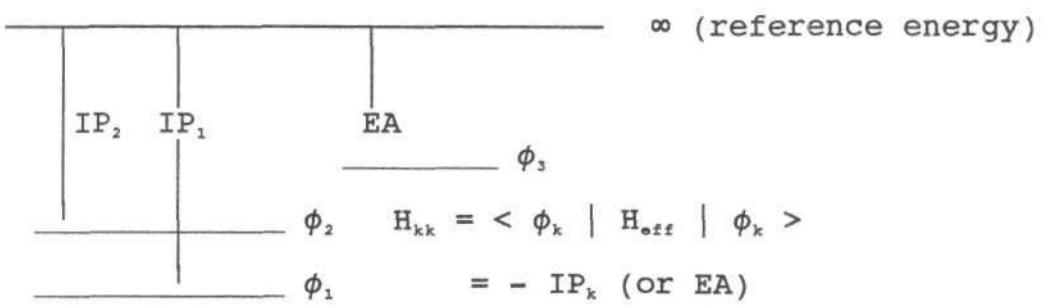


Figure 2.0: Scale Relative to an Electron at Infinity

Once one decides not to neglect the off-diagonal matrix elements, including overlap integrals, in the secular determinant, one is faced with the problem of estimating the bond integrals $ß_{kl}$ which are distance dependent. But since the relation of S_{kl} to distance is familiar, a similar relation of $ß_{kl}$ to distance is more easily computed if $ß_{kl}$ is related to S_{kl} and this has led to various formulas for optimizing the bond integral $ß_{kl}$ by relating it to the overlap integral S_{kl}. Therefore, we shall present a table of such formulas, and names of their originators:

Table 2.0: Approximate Formulas For $ß_{kl}$ Parameters

Bond Integral Formula	Author(s)	Year
$ß_{kl} = - S_{kl} (IP_k + IP_l)/2$	Mulliken (Doggett and Mckendrick,1968)	1949
$ß_{kl} = - KS_{kl} (IP_k + IP_l)/2$	Wolfberg-Helmholz	1952
$ß_{kl} = - S_{kl} (\lambda_1 IP_k + \lambda_2 IP_l)$	Löwdin (Per-OLov)	1953
$ß_{kl} = - A_T S_{kl} I_{kl}$	Mulliken	1955
$ß_{kl} = - (\lambda_1 \Sigma_k' IP_k S_{kl} + \lambda_2 \Sigma_l' IP_l S_{l,k})$	Löwdin (Doggett and Mckendrick,1968)	1956
$ß_{kl} = - K''(IP_k\ IP_l)^{½}$	Baullhausen and Gray	1962
$ß_{kl} = K' S_{kl}$	Hoffmann	1963
$ß_{kl} = - S_{kl} (IP_k + IP_l)ß' + ß''/R_{kl}$	Dewar and Baird	1963
$ß_{kl} = - S_{kl} (IP_k + IP_l)/2 - S_{kl} (EA_k + EA_l)/2$	Van-Catledge	1971

The adjustable constants K, K', K", ß' and ß" are emprical parameters while λ_1 and λ_2, also adjustable parameters, are chosen to satisfy $\lambda_1 + \lambda_2 = 1$.

On the above basis, the complete secular determinant is then solved to obtain eigenvalues and coefficients (or eigenvectors). Solution of the secular problem requires the use of a matrix diagonalization procedure.

The extended Hückel theory (EHT), like the HMO theory, assumes the existence of the Hamiltonian (2-2) in the form of a sum of one electron terms H_{eff} (p) in equation (2-6). These effective Hamiltonian H_{eff} are not defined any more explicitly by the theory. Consequently, one is not certain of exactly what one is doing - where does quantum mechanics begin and end, and parameter fitting takes over. Furthermore, no justification is provided for replacing the true Hamiltonian (electronic),

$$-\sum_{P}\left(\sum_{A}\frac{Z_A}{rAP}+\frac{\nabla_P^2}{2}\right)+\sum_{p<}\sum_{t}1/r_{pt},$$

with one - and two - electron operators by the simpler one-body form,

$$\sum_{p}\left(-\frac{\nabla_p^2}{2}+V_p\right)=\sum_{p}H_{eff}(p)$$

except that it "works".

Since the Hamiltonian in (2-6) is assumed to be a sum of effective one-electron terms $H_{eff}(p)$, electronic repulsions are being treated implicitly in both the HMO and EHT theories (i.e. LCAO MO methods). To take into account electronic repulsions explicitly as do the ab initio methods, the second group of semi-empirical theories (Gerald, 1977), the SCF-MO semiempirical methods, emerged in the 1960s. The purpose was to develop a simple procedure that takes into account electronic repulsions explicitly, if not completely, at least in some average form which allows all the electrons to find a distribution of lowest energy while subject to each others' repulsion.

To take into account Coulomb and exchange electronic correlations, the SCF-MO semiempirical methods use the true Hamiltonian (2-4) which contains the two - electron terms $\Sigma(p)\Sigma(t)1/r_{pt}$, a solution for Ψ in equation (2-1) is assumed to be a normalized Slater determinant

$$\Psi\ (1,2,\ .....\ ,L,L+1,\ ....,\ L+M)\ =\ 1/\sqrt{(L+M)!}\ \sum_R (-1)^R\ \bar{R}$$

$$x\ \psi_1^{\alpha}(1)\alpha(1)...\psi_L^{\alpha}(L)\alpha(L)\psi_1^{\beta}(L+1)\beta(L+1)....\psi_M^{\beta}(L+M))\beta(L+M)\ ...\ (2\text{-}21)$$

not a simple product as represented by equation (2-5) and used by the HMO and EHT methods. The ψ's are one-electron molecular orbitals that satisfy the Hartree - Fock - Roothaan equations,

$$F_{op}\psi_p\ =\ \epsilon_p\psi_p \quad p = 1,2,\ ...N,\ \ ....\ (2\text{-}22)$$

F_{op} being the Hartree - Fock - Roothaan operator (Gerald, 1977). Like the HMO and EHT methods, the molecular orbitals are expanded as linear combination of atomic orbitals. Depending on the approximation concerning the $\phi_k(1)\phi_l(1)$ overlap charge density, the SCF - MO semiempirical methods may be categorized into three main groups. The approximations to the overlap charge density and SCF - MO methods emanating therefrom, are as follows:

(a) The zero differential overlap approximation (ZDO). This approximation led to the CNDO theories (Pople and Segal, 1966).

(b) The modified intermediate neglect of differential overlap (MINDO) theories (Pople et al., 1967).

(c) The Partial Neglect of Diatomic Differential Overlap (PNDDO) approximation. The PNDDO methods (Klopman, 1964) emanated from this approximation.

The differential overlap (DO) approximations are intended to reduce the number of electron repulsion integrals. What one has to ask is whether they are able to do this on a sound mathematical or physical basis, i.e. whether one can find the conditions under which these are good approximations? One can also ask if the rigour (Mathematical) sought by use of full spin-free Hamiltonian and antisymmetrized wavefunction is not lost through these approximations?

It may be possible to develop the EHT from the use of the true Hamiltonian (2-4), with one - and two- electron operators, the antisymmetrized wave function (2 - 21) and the Hartree - Fock -

Roothaan equations (2-22) without any differential overlap approximation. Part of this research is taken to be the development of such a theory, and since we have already developed it, it turned out to be, of course, self-consistent but has the general form of the familiar EHT method. Unlike the familiar EHT method, there are two separate versions of the theory depending on whether one is dealing with a closed or open shell system. We have called these versions:

(1) The self-consistent field molecular orbital spin restricted extended Hückel theory, SCF - MO EHT - SR; and

(2) The Self-Consistent field molecular orbital spin polarized extended Hückel theory, SCF - MO EHT - SP methods, for closed and open shell systems respectively.

(As already mentioned in chapter one, these two new SCF - MO EHT methods will be applied to the studies of H^+, OH^- and NH_3 chemisorptions on α-Fe_2O_3).

CHAPTER THREE

3. RESEARCH METHODS I: QUANTUM CHEMISORPTION METHODS

3.0 A Self-Consistent Field Molecular Orbital Extended Hiickel Theory (SCF - MO EHT Method):

To develop the self-consistent field molecular orbital extended Hückel theory, we define a total electronic Hamiltonian as the sum of all possible nuclear-electron and electron-electron eletrostatic interactions plus kinetic energy of electrons

$$H_{op} = -\sum_{i}\left(\sum_{A}\frac{Z_A}{r_{Ai}} + \frac{\nabla_i^2}{2}\right) + \sum_{i<j}\sum\frac{1}{r_{ij}} \qquad .....(3\text{-}1)$$

Writing the one-electron terms as a core Hamiltonian, we have

$$H(i) = -\sum_{2}\frac{Z_A}{r_{Ai}} - \frac{\nabla_i^2}{2} \qquad .....(3\text{-}2)$$

So that equation (3-1) can be written as

$$H_{op} = \sum_{i}H(i) + \sum_{i}\sum_{j}\frac{1}{r_{ij}} .....(3\text{-}3)$$

The wave function Ψ , which describes the state of the system, involves one-electron molecular orbitals and satistactory solution

must satisfy the Schrödinger equation

$$H_{op}\Psi = E\Psi \quad \text{and} \quad E = \int \Psi^* H_{op} \Psi d\tau / \int \Psi^2 d\tau \qquad .....(3\text{-}4)$$

where for bound state, the wave function Ψ must satisfy the normalization condition

$$\int \Psi^* \Psi d\tau_1 d\tau_2 ..... d\tau_n = 1 \qquad .....(3\text{-}5)$$

From equation (3-3), the total energy E can thus be written as

$$E = \int \Psi^* \left(\sum_i H(i) + \sum_{i<j} \sum \frac{1}{r_{ij}} \right) \Psi d\tau$$

$$= \int \Psi^* \sum_i H(i) \Psi d\tau + \int \Psi^* \sum_i \sum_{<j} \frac{1}{r_{ij}} \Psi d\tau \qquad .....(3\text{-}6)$$

In equation (3-6), the total energy is given as a sum of one-electron terms and electron-electron repulsions.

3.1.0 A Self-Consistent Field Molecular Orbital Spin Restricted Extended Hückel Theory: SCF - MO EHT-SR Method

This is for the closed shell system where each molecular orbital is doubly occupied and the wave function is usually under the form of a single Slater determinant

$$\Psi = \frac{1}{\sqrt{n!}} \sum_R (-1)^R \hat{R} \psi_p(1)\alpha(1)\psi_p(2)\beta(2) \ldots\ldots \psi_z(n-1)\alpha(n-1)\psi_z(n)\beta(n)$$

$$.....(3\text{-}7)$$

where $\hat{R}$ is the usual permutation operator, so the expectation

value E in equation (3 - 6) becomes

$$E = \frac{1}{n!}\int \sum_R (-1)^R \hat{R}\psi_p^*(1)\alpha(1)\psi_p^*(2)\beta^*(2) \ .... \ \psi_z^*(n-1)\alpha^*(n-1)\psi_z^*(n)\beta^*(n)$$

$$x \left\{ \sum_i H(i) + \sum_{i<j} \sum \frac{1}{r_{ij}} \right\}$$

$$x \sum_Q (-1)^Q \hat{Q}\psi_p(1)\alpha(1)\psi_p(2)\beta(2) \ ..... \ \psi_z(n-1)\alpha(n-1)\psi_z(n)\beta(n)$$

$$x \, d\tau_1 d\tau_2 .....d\tau_{n-1} d\tau_n \qquad .....(3\text{-}8)$$

Assuming the ψ 's are normalized and orthogonal to each other, we obtain (Gerald, 1977) after integrating out the spin part, the energy E in terms of the molecular orbitals only and may be written as

$$E = 2\sum_p H_{pp} + 2\sum_p \sum_q (J_{pq} - \frac{1}{2}K_{pq}) \qquad .....(3\text{-}9)$$

where

$$J_{pq} = \int \psi_p^*(i)\left(\int \psi_q^*(j)\psi_q(j)\frac{1}{r_{ij}}d\tau_j\right)\psi_p(i)d\tau_i$$

$$= \int \psi_p^*(i)J_q\psi_q(i)d\tau_i \qquad .....(3\text{-}10)$$

$$K_{pq} = \int \psi_p^*(i)\psi_q^*(j)\frac{1}{r_{ij}}\psi_q(i)\psi_p(j)d\tau_i d\tau_j$$

$$= \int \psi_p^*(i)\left(\int \frac{\psi_p^*(i)\psi_q^*(j)\frac{1}{r_{ij}}\psi_q(i)\psi_p(j)d\tau_j}{\psi_p^*(i)\psi_p(i)}\right)\psi_p(i)d\tau_i$$

$$= \int \psi_p^*(i)K_q\psi_p(i)d\tau_i \qquad .....(3\text{-}11)$$

(where the J_q and K_q are one-electron Coulomb and exchange operators) and

$$H_{pp} = \int \psi_p^*(i)H(i)\psi_p(i)d\tau_i \qquad .....(3\text{-}12)$$

Using equations (3-10), (3-11) and (3-12), the energy expression in (3-9) may be written as

$$E = 2\sum_{p}\int\psi_p^*(i)\quad\left\{H(i) + \sum_{q}(J_q - \frac{1}{2}K_q)\right\}\psi_p(i)d\tau_i \quad ...(3\text{-}13)$$

which can simply be written in terms of one-electron operators

$$E = 2\sum_{p}\int\psi_p^*(i)F_i\psi_p(i)d\tau_i \quad .....(3\text{-}14)$$

where the one-electron operator F_i, called the Hartree-Fock-Roothaan operator, is defined from equation (3-13) as

$$F_i = H(i) + \sum_{q}\left\{J_q - \frac{1}{2}K_q\right\}$$

The sum $\sum_{p}\int\psi_p^*(i)F_i\psi_p(i)d\tau_i$ contains independent terms which, according to quantum mechanics, can individually be written as

$$\int\psi_p^*(i)F_i\psi_p(i)d\tau_i = \varepsilon_p \qquad p = 1,2, ... \quad .....(3\text{-}15)$$

or in other words, equation (3-14) becomes

$$2\sum_{p}\epsilon_p = E \qquad p = 1,2, ...(\text{occupied MO}_s) \quad .....(3\text{-}16)$$

From equation (3-15), the molecular orbitals $\{\psi_p;\ p = 1,2,\ ...\}$ are the eigenfunctions of the one-electron Hartree-Fock-Roothaan operator F_i with (real) energies $\{\varepsilon_p;\ p = 1,2,\ ...\}$ that satisfy the Hartree-Fock-Roothaan equations

$$F_i\psi_p(i) = \varepsilon_p\psi_p(i) \qquad p = 1,2,\ ....\ \ .....(3\text{-}17)$$

And the total energy is simply the sum of the (filled) orbital energies given by equation (3-16).

The molecular orbitals are expanded as linear combination of independent functions, atomic orbitals, $\phi_1,\phi_2,\phi_3,\ ....\phi_k\ ....$ with undetermined coefficients $\{C_{kp};\ p = 1,2,\ ...;k = 1,2,\ ....\}$. In other words the pth molecular orbital is written as

$$\psi_p = \sum_p C_{pk}\phi_k \qquad k = 1,\ 2,....\ \ ....(3\text{-}18)$$

Using this expansion, J_q becomes

$$J_q = \int \psi_q^*(j)\psi_q(j)\frac{1}{r_{ij}}d\tau_j$$

$$= \int \sum_{p} C_{qm}^{*} \phi_{m}^{*}(j) \sum_{n} C_{qn} \phi_{n}(j) \frac{1}{r_{ij}} d\tau_j$$

$$= \int \sum_{m} \sum_{n} C_{qm}^{*} C_{qn} \int \phi_{m}^{*}(j) \phi_{n}(j) \frac{1}{r_{ij}} d\tau_j \qquad \text{.....(3-19)}$$

Similarly, K_q may be written as

$$K_q = \frac{\int \psi_p^{*}(i) \psi_q^{*}(j) \frac{1}{r_{ij}} d\psi_q(i) \psi_p(j) d\tau_j}{\psi_p^{*}(i) \psi_p(i)}$$

$$= \frac{\int \sum_{k} C_{pk}^{*} \phi_{k}^{*}(i) \sum_{m} C_{qm}^{*} \phi_{m}^{*}(j) \frac{1}{r_{ij}} \sum_{n} C_{qn} \phi_{n}(i) \sum_{l} C_{pl} \phi_{l}(j) d\tau_j}{\sum_{k} C_{pk}^{*} \phi_{k}^{*}(i) \sum_{l} C_{pl} \phi_{l}(i)}$$

$$= \sum_{m} \sum_{n} C_{qm}^{*} C_{qn} \int \frac{\phi_{k}^{*}(i) \phi_{m}^{*}(j) \frac{1}{r_{ij}} \phi_{n}(i) \phi_{l}(j) d\tau_j}{\phi_{k}^{*}(i) \phi_{l}(i)} \qquad \text{.....(3-20)}$$

so that equation (3-14) may be written in terms of basis orbitals $\phi's$

$$F_i = H(i) + \sum_m \sum_n \sum_q C_{qm}^{*} C_{qn} \left(\int \phi_m^{*}(j) \phi_n(j) \frac{1}{r_{ij}} d\tau_j \right.$$

$$\left. - \frac{1}{2} \int \frac{\phi_k^{*}(i) \phi_m^{*}(j) \frac{1}{r_{ij}} \phi_n(i) \phi_l(j) d\tau_j}{\phi_k^{*}(i) \phi_l(i)} \right)$$

$$= H(i) + \sum_m \sum_n \frac{P_{mn}}{2} \left(\int \phi_m^{*}(j) \phi_n(j) 1/r_{ij} d\tau_j \right.$$

$$\left. - \frac{1}{2} \int \frac{\phi_k^{*}(i) \phi_m^{*}(j) 1/r_{ij} \phi_n(i) \phi_l(j) d\tau_j}{\phi_k^{*}(i) \phi_l(i)} \right) \ldots\ldots (3\text{-}21)$$

where

$$P_{mn} = 2 \sum_q C_{qm}^{*} C_{qn} \ldots\ldots\ldots\ldots\ldots (3\text{-}22)$$

From equation (3-17), the trial orbital energies in (3-17) are given by (the expectation values):

$$\epsilon_p = \int \psi_p^{*}(i) F_i \psi_p(i) d\tau_i / \int \psi_p^2(i) d\tau_i \quad p = 1,2, \ldots\ldots \quad \ldots\ldots (3\text{-}23)$$

If we introduce the symbols

$$F_{kl} = \int \phi_k^*(i) F_i \phi_l(i) d\tau_i$$

$$= \int \phi_k^*(i) \{H(i) + \sum_m \sum_n \frac{P_{mn}}{2} (\int \phi_m^*(j) \phi_n(j) 1/r_{ij} d\tau_j$$

$$- 1/2 \int \frac{\phi_k^*(i) \phi_m^*(j) 1/r_{ij} \phi_n(i) \phi_l(j) d\tau_j}{\phi_k^*(i) \phi_l(i)} \} \phi_l(i) d\tau_i$$

$$= \int \phi_k^*(i) H(i) \phi_l(i) d\tau_i + \sum_m \sum_m \frac{P_{mn}}{2} (\iint \phi_k^*(i) \phi_m^*(j) 1/r_{ij} \phi_l(i) \phi_n(j)$$

$$x d\tau_i d\tau_j - 1/2 \int \phi_k^*(i) \phi_n^*(j) 1/r_{ij} \phi_m(i) \phi_l(j) d\tau_i d\tau_j)$$

$$= H_{kl} + \sum_m \sum_n \frac{P_{mn}}{2} (\langle kl/mn \rangle - 1/2 \langle kn/lm \rangle) \quad \ldots\ldots\ldots (3\text{-}24)$$

$$\text{also } S_{kl} = \int \phi_k^*(i) \phi_l(i) d\tau_i, \ldots\ldots\ldots\ldots\ldots\ldots\ldots\ldots (3\text{-}25)$$

then the expression for ϵ_p expectation value becomes, after putting equation (3-18) in (3-13),

$$\epsilon_p = \sum_k \sum_l C_{pk}^{\cdot} C_{pl} F_{kl} \; / \; \sum_k \sum_l C_{pk}^{\cdot} C_{pl} S_{kl}$$

or

$$\epsilon_p \sum_k \sum_l C_{pk}^{\cdot} C_{pl} S_{kl} = \sum_k \sum_l C_{pk}^{\cdot} C_{pl} F_{kl} \ldots\ldots\ldots\ldots (3\text{-}26)$$

To find the values of $C_{p1}^{\cdot}, C_{p2}^{\cdot}, \ldots, C_{pk}^{\cdot}$ which give the lowest value for ϵ_p and therefore the best approximation to the energy, we differentiate equation (3-26) with respect to each $C_{pk}^{\cdot}$ (k = 1, 2, ...):

$$\frac{\partial \epsilon_p}{\partial C_{pk}^{\cdot}} \sum_k \sum_l C_{pk}^{\cdot} C_{pl} S_{kl} + \epsilon_p \sum_l C_{pl} S_{kl} = \sum_l C_{pl} F_{kl} \ldots\ldots\ldots\ldots (3\text{-}26a)$$

The condition for the lowest value of the energy or minimum is that

$\partial \epsilon_p / \partial C_{pk}^{\cdot} = 0$ for each k index ..... (3-27)

which reduces equation (3-26a) to

$$\epsilon_p \sum_l C_{pl} S_{kl} = \sum_l C_{pl} F_{kl} \text{ otherwise } \sum_l C_{pl} (F_{kl} - \epsilon_p S_{kl}) = 0 \ldots (3\text{-}28)$$

where the S_{kl}'s are overlap integrals. In order for these equations to hold true, the determinant of the matrix must be equal to zero. Solution of the secular determinant affords the energy ϵ_p for each molecular orbital. Substitution of these energies into the set of

linear equations (3-28) provides the coefficients C_{pi}'s.

3.1.1 Matrix Elements of the SCF - MO EHT Spin Restricted Method:

A. **DIAGONAL ELEMENTS**

We shall add the subscript a or b to an orbital to indicate where that orbital is located. Diagonal element of an electron in an orbital (ϕ_{ak} on atom a), F_{kk}, from equation (3-24), is given as

$$F_{kk} = \langle\phi_{ak}| - \sum_A \frac{Z_A}{r_{Ai}} - \frac{\nabla_i^2}{2}| \phi_{ak}\rangle + \sum_m \frac{P_{mm}}{2}(\langle\phi_{ak}\phi_{ak}|\phi_{am}\phi_{am}\rangle$$

$$- 1/2\langle\phi_{ak}\phi_{am}|\phi_{ak}\phi_{am}\rangle) \ldots\ldots\ldots\ldots (3\text{-}29)$$

We shall, at this stage, define two atomic orbital parameters as follows:

$$I_{kk} = \langle\phi_{ak} /- \sum_A \frac{Z_A}{r_{Ai}} - \frac{\nabla_i^2}{2}/ \phi_{ak}\rangle \ldots\ldots\ldots\ldots (3\text{-}30)$$

and

$$\epsilon_k = \langle\phi_{ak}|-\sum_A \frac{Z_A}{r_{Ai}} - \frac{\nabla_i^2}{2}|\phi_{ak}\rangle + \sum_m (\langle\phi_{ak}\phi_{ak}|\phi_{am}\phi_{am}\rangle$$

$$- 1/2\langle\phi_{ak}\phi_{am}|\phi_{ak}\phi_{am}\rangle)$$

or

$$I_{1_i} = \langle\phi_{bl}| - \sum_A \frac{Z_A}{r_{Ai}} - \frac{\nabla_i^2}{2}|\phi_{bl}\rangle \ldots\ldots\ldots\ldots (3\text{-}30a)$$

and

$$\epsilon_l = \langle\phi_{bl}| - \sum_A \frac{Z_A}{r_{Ai}} - \frac{\nabla_i^2}{2}|\phi_{bl}\rangle + \sum_n (\langle\phi_{bl}\phi_{bl}|\phi_{bn}\phi_{bn}\rangle$$

$$- 1/2\ \langle\phi_{bl}\phi_{bn}|\phi_{bl}\phi_{bn}\rangle \ldots\ldots\ldots\ldots (3\text{-}31a)$$

If we add

$$\sum_m (\langle\phi_{ak}\phi_{ak}|\phi_{am}\phi_{am}\rangle - 1/2\langle\phi_{ak}\phi_{am}|\phi_{ak}\phi_{am}\rangle)$$

to equation (3-29) and subtract same from it (operation nothing), we obtain

$$F_{kk} = \langle\phi_{ak}|-\sum_A \frac{Z_A}{r_{Ai}} - \frac{\nabla_i^2}{2}|\phi_{ak}\rangle + \sum_m (\langle\phi_{ak}\phi_{ak}|\phi_{am}\phi_{am}\rangle$$

$$- 1/2\langle\phi_{ak}\phi_{am}|\phi_{ak}\phi_{am}\rangle)$$

$$+ \sum_m (P_{mm}/2 - 1)(\langle\phi_{ak}\phi_{ak}|\phi_{am}\phi_{am}\rangle - 1/2\langle\phi_{ak}\phi_{am}|\phi_{ak}\phi_{am}\rangle)$$

$$= \epsilon_k + \sum_m (P_{mm}/2-1)(\langle\phi_{ak}\phi_{ak}|\phi_{am}\phi_{am}\rangle - 1/2\langle\phi_{ak}\phi_{am}|\phi_{ak}\phi_{am}\rangle) \quad \ldots\ldots(3\text{-}32)$$

from the use of equation (3-31). The second term in equation (3-32) can be written in full as

$$\sum_m (P_{mm}/2-1)(\langle\phi_{ak}\phi_{ak}|\phi_{am}\phi_{am}\rangle - 1/2\langle\phi_{ak}\phi_m|\phi_{ak}\phi_{am}\rangle)$$

$$= (P_{11}/2-1)(\langle\phi_{ak}\phi_{ak}|\phi_{a1}\phi_{a1}\rangle - 1/2\langle\phi_{ak}\phi_{a1}|\phi_{ak}\phi_{a1}\rangle)$$

$$+ (P_{22}/2-1)(\langle\phi_{ak}\phi_{ak}|\phi_{a2}\phi_{a2}\rangle 1/2\langle\phi_{ak}\phi_{a2}|\phi_{ak}\phi_{a2}\rangle)$$

$$+ (P_{33}/2-1)(\langle\phi_{ak}\phi_{ak}|\phi_{a3}\phi_{a3}\rangle 1/2\langle\phi_{ak}\phi_{a3}|\phi_{ak}\phi_{a3}\rangle)$$

$$+ \ldots\ldots\ldots\

which will be difficult to handle semi-empirically. But if we make the following approximation, namely setting,

$$P_{kk} \approx P_{11} \approx P_{22} \approx P_{33} \approx \ldots\ldots \approx P_{k-1\,k-1} \approx P_{kk} \approx P_{k-1\,k-1}$$

$$\approx P_{k-2\,k-2} \approx \ldots\ldots\ldots\ldots\,,\ \ldots\ldots\ldots\ldots \quad (3\text{-}34)$$

equation (3-33) reduces to

$$\sum_{m} (P_{mm}/2-1)(\langle\phi_{ak}\phi_{ak}|\phi_{am}\phi_{am}\rangle\ 1/2\langle\phi_{ak}\phi_{am}|\phi_{ak}\phi_{am}\rangle)$$

$$\approx (P_{kk}/2-1)(\langle\phi_{ak}\phi_{ak}|\phi_{a1}\phi_{a1}\rangle\ 1/2\langle\phi_{ak}\phi_{a1}|\phi_{ak}\phi_{a1}\rangle)$$

$$+ (P_{kk}/2-1)(\langle\phi_{ak}\phi_{ak}|\phi_{a2}\phi_{a2}\rangle - 1/2\langle\phi_{ak}\phi_{a2}|\phi_{ak}\phi_{a2}\rangle)$$

$$+ (P_{kk}/2-1)(\langle\phi_{ak}\phi_{ak}|\phi_{a3}\phi_{a3}\rangle - 1/2\langle\phi_{ak}\phi_{a3}|\phi_{ak}\phi_{a3}\rangle)$$

$$+ \ldots\ldots\ldots\ldots\

+ ..... +

.....

$$= (P_{kk}/2-1)\sum_{m} (\langle\phi_{ak}\phi_{ak}|\phi_{am}\phi_{am}\rangle - 1/2\langle\phi_{ak}\phi_{am}|\phi_{ak}\phi_{am}\rangle) \quad \text{.....(3-35)}$$

which is easier to manipulate than (3-33).

Equation (3-34) is actually true for the case of even alternant hydrocarbons and odd alternant hydrocarbon radicals, even - AH and odd - AH radicals. In the even - AH and odd - AH radicals, the electronic charge density on an atomic orbital $\phi_{..}$ at atom a is, for a closed shell, given (Salem, 1966) by

$$P_{mm} = 2q_m$$

$$= \sum_{p} 2C_{pm}{}^{*}C_{pm}$$

$$= 2 \quad \textit{for all m values } (i.e.\ m = 1,2, \ldots, k, \ldots), \ldots \text{ (3-36)}$$

$q_m = \Sigma_p C_{pm} \cdot C_{pm}$

$= 1$ all MOs p ..... (3-37)

and

$P_{kk} = P_{11} = P_{22} = P_{33} = \ldots\ldots\ldots = {}_{k-1} = P_{k+1\,k+1} = \ldots\ldots$, (3 - 34a)

Equation (3-38) is true when electronic charge density is distributed uniformly over the molecule, as in the case of even AH and odd - AH radicals, and is only an approximation, in general, when that is not so.

Using equation (3-30) and (3-31), (3-35) becomes

$$(P_{kk}/2-1)\sum_{m}(\langle\phi_{ak}\phi_{ak}|\phi_{am}\phi_{am}\rangle - 1/2\langle\phi_{ak}\phi_{am}|\phi_{ak}\phi_{am}\rangle)$$

$$= (P_{kk}/2-1)(\epsilon_k - I_{kk}) \quad \ldots\ldots\ldots (3\text{-}38)$$

From equations (3-35) and (3-38), the diagonal elements F_{kk} in equation (3-32) becomes

$$F_{kk} = \epsilon_k + (P_{kk}/2-1)(\epsilon_k - I_{kk})$$

$$= (1 + \lambda_k)\epsilon_k \quad \ldots\ldots\ldots\ldots\ldots\ldots\ldots\ldots\ldots\ldots \quad (3\text{-}39)$$

where the charge dependent variable λ_k is defined as

$$\lambda_k = (P_{kk}/2-1)\frac{\epsilon_k - I_{kk}}{\epsilon_k} \quad \ldots\ldots\ldots\ldots\ldots\ldots\ldots (3\text{-}40)$$

B. **OFF-DIAGONAL ELEMENTS:**

This is a matrix element between an orbital centred on atom a and another centred on atom b. It is given by,

$$F_{kl} = \langle\phi_{ak}|-\sum_{A}\frac{Z_A}{r_{Ai}} - \frac{\nabla_i^2}{2}|\phi_{bl}\rangle + \sum_{m}\sum_{n}\frac{P_{mn}}{2}(\langle\phi_{ak}\phi_{bl}|\phi_{am}\phi_{bn}\rangle$$

$$- 1/2\langle\phi_{ak}\phi_{bn}|\phi_{bl}\phi_{am}\rangle)$$

$$= \langle\phi_{ak}|-\sum_{A}\frac{Z_A}{r_{Ai}} - \frac{\nabla_i^2}{2} + \sum_{m}\sum_{n}\frac{P_{mn}}{2}(\int\phi_{am}(j)\phi_{bn}(j)1/r_{ij}d\tau_j$$

$$- 1/2\int \frac{\phi_{ak}(i)\phi_{bl}(j)1/r_{ij}\phi_{bn}(i)\phi_{am}(j)d\tau_2}{\phi_{ak}(i)\phi_{bl}(i)} |\phi_{bl}>$$

$= <\phi_{ak}|F_i|\phi_{bl}>$, ...(3-41)

for which there are two cases:

(1) $F_{kl} = <\phi_{ak}|F_i|\phi_{bl}>$

$= 0 \quad a = b \; ; \; k \neq l$ ..... (3-42)

because $\{\phi_{ak}; k=1,2, ..., m, ... \}$ and $\{\phi_{bl}; l=1,2, ..., n, ... \}$ which are centred on atoms a and b respectively are orthonormal sub-basis sets. Thus any matrix element F_{kl} between two atomic orbitals of the sub-set $\{\phi_{ak}; k=1,2, ..., m, ... \}$ or $\{\phi_{bl}; l=1,2, ... , n, ... \}$ is zero. That is

$F_{kl} = <\phi_{ak}|F_i|\phi_{al}>$ or $F_{kl} = <\phi_{bk}|F_i|\phi_{bl}>$

$= 0 \quad k \neq l$ $\qquad\qquad$ $= 0 \quad k \neq l$ ..... (3-43)

(2) $F_{kl} = <\phi_{ak}|F_i|\phi_{bl}>$

$\neq 0 \quad a \neq b \; ; \; k \neq l$ ..... (3-44)

that is any two atomic orbitals ϕ_{ak} and ϕ_{bl} centred on atoms a and b respectively are not orthogonal and therefore matrix elements F_{kl} between them are non-zero generally. Hence from now on, when we talk about or write F_{kl}, we intend or mean this second case. Expanding (Ruedenberg, 1951),

$$\phi_{bn} = \sum_{r=1}^{\infty} S_{bl,ar}\,\phi_{ar} \; also \; \phi_{bl} = \sum_{r=1}^{\infty} S_{bl,ar}\phi_{ar} \ldots\ldots (3\text{-}45)$$

and using it in equation (3-41), we have

$$F_{kl} = \langle\phi_{ak}| - \sum_A \frac{Z_A}{r_{Ai}} - \frac{\nabla_i^2}{2} |\sum_{r=1}^{\infty} S_{bl,ar}\ \phi_{ar}\rangle + \sum_m \sum_n \frac{P_{mn}}{2}$$

$$x\ (\langle\phi_{ak}\sum_{r=1}^{\infty} S_{bl,ar}\ \phi_{ar}|\phi_{am}\sum_{r=1}^{\infty} S_{bn,ar}\ \phi_{ar}\rangle - 1/2\langle\phi_{ak}\sum_{r=1}^{\infty} S_{bn,ar}\phi_{ar}|\sum_{r=1}^{\infty} S_{bl,ar}\phi_{ar}\phi_{am}\rangle)$$

..... (3-46)

Since $\{\phi_{a_m}\ ;\ m = 1,2,\ ....,\ k,\ ...\}$ are centred on atom a, they are orthogonal and reduces (3-46) to

$$F_{kl} = \langle\phi_{ak}| - \sum_A \frac{Z_A}{r_{Ai}} - \frac{\nabla_i^2}{2} |S_{bl,ak}\phi_{ak}\rangle + \sum_m \sum_n \frac{P_{mn}}{2}$$

$$x(\langle\phi_{ak}\ S_{bl,ak}\ \phi_{ak}|\phi_{am}\ S_{ba,am}\ \phi_{am}\rangle - \tfrac{1}{2}\langle\phi_{ak}\ S_{ba,am}\ \phi_{am}|S_{bl,ak}\phi_{ak}\phi_{am}\rangle)$$

$$= S_{ak,bl}\{\langle\phi_{ak}| - \sum_A \frac{Z_A}{r_{Ai}} - \frac{\nabla_i^2}{2} |\phi_{ak}\rangle + \sum_m \sum_n \frac{P_{mn}}{2} S_{am,bn}$$

$$x(\langle\phi_{ak}\phi_{ak}|\phi_{am}\phi_{am}\rangle - \tfrac{1}{2}\langle\phi_{ak}\phi_{am}|\phi_{ak}\phi_{am}\rangle\} \ .....(3-47)$$

by bringing out the overlap integrals $S_{bl,ak}$ and $S_{ba,am}$, also using the fact that $S_{bl,ak} = \langle\phi_{bl}/\phi_{ak}\rangle = \langle\phi_{ak}/\phi_{bl}\rangle = S_{ak,bl}$ etc .....

Adding

$$S_{ak,bl}\sum_m (\langle\phi_{ak}\phi_{ak}|\phi_{am}\phi_{am}\rangle - \frac{1}{2}\langle\phi_{ak}\phi_{am}|\phi_{ak}\phi_{am}\rangle)$$

to equation (3-47) and subtracting same from it (operation nothing), we obtain.

$$F_{kl} = S_{ak,bl}[<\phi_{ak}|-\sum_{A}\frac{Z_A}{r_{Ai}} - \frac{\nabla_i^2}{2}|\phi_{ak}>$$

$$+\sum_{m}(<\phi_{ak}\phi_{ak}|\phi_{am}\phi_{am}> - 1/2<\phi_{ak}\phi_{am}|\phi_{ak}\phi_{am}>)]$$

$$+S_{ak,bl}\sum_{m}[(\sum_{n}\frac{P_{mn}}{2}S_{am,bn}-1)$$

$$x\ (<\phi_{ak}\phi_{ak}|\phi_{am}\phi_{am}> - 1/2<\phi_{ak}\phi_{am}|\phi_{ak}\phi_{am}>)]\ldots\ldots\ldots(3\text{-}48)$$

$$=S_{ak,bl}[\epsilon_k+\sum_{m}\left\{\sum_{n}\frac{P_{mn}}{2}S_{am,bn}-1)(<\phi_{ak}\phi_{ak}|\phi_{am}\phi_{am}>-1/2<\phi_{ak}\phi_{am}|\phi_{ak}\phi_{am}>\right\}]$$

$$\ldots\ldots\ldots\ldots\ldots\ldots\ldots\ldots\ (3\text{-}49)$$

From the use of equation (3-31). The second term in equation (3-49) can be written in full as

$$\sum_{m}\left\{\sum_{n}\frac{P_{mn}}{2}S_{am,bn}-1)(<\phi_{ak}\phi_{ak}|\phi_{am}\phi_{am}> - 1/2<\phi_{ak}\phi_{am}|\phi_{ak}\phi_{am}>\right\}$$

$$=(\sum_{n}\frac{P_{1n}}{2}S_{a1,bn}-1)(<\phi_{ak}\phi_{ak}|\phi_{a1}\phi_{a1}>-1/2<\phi_{ak}\phi_{a1}|\phi_{ak}\phi_{a1}>)$$

$$+ \left(\sum_n \frac{P_{2n}}{2} S_{a2,bn} - 1\right)\left(\langle \phi_{ak}\phi_{ak} | \phi_{a2}\phi_{a2}\rangle - 1/2\langle \phi_{ak}\phi_{a2} | \phi_{ak}\phi_{a2}\rangle\right)$$

$$+ \left(\sum_n \frac{P_{3n}}{2} S_{a3,bn} - 1\right)\left(\langle \phi_{ak}\phi_{ak} | \phi_{a3}\phi_{a3}\rangle - 1/2\langle \phi_{ak}\phi_{a3} | \phi_{ak}\phi_{a3}\rangle\right)$$

$$+ \text{.....} +$$

$$\text{.....}$$

$$+ \left(\sum_n \frac{P_{k-1n}}{2} S_{ak-1,bn} - 1\right)\left(\langle \phi_{ak}\phi_{ak} | \phi_{ak-1}\phi_{ak-1}\rangle - 1/2\langle \phi_{ak}\phi_{ak-1} | \phi_{ak}\phi_{ak-1}\rangle\right)$$

$$+ \left(\sum_n \frac{P_{kn}}{2} S_{ak,bn} - 1\right)\left(\langle \phi_{ak}\phi_{ak} | \phi_{ak}\phi_{ak}\rangle - 1/2\langle \phi_{ak}\phi_{ak} | \phi_{ak}\phi_{ak}\rangle\right)$$

$$+ \left(\sum_n \frac{P_{k+1n}}{2} S_{ak-1,bn} - 1\right)\left(\langle \phi_{ak}\phi_{ak} | \phi_{ak-1}\phi_{ak+1}\rangle - 1/2\langle \phi_{ak}\phi_{ak-1} | \phi_{ak}\phi_{ak-1}\rangle\right)$$

$$+ \text{.....}+$$

$$\text{..... (3-50)}$$

where $S_{a1,bn} = \langle \phi_{a1} | \phi_{bn}\rangle$, $S_{a2,bn} = \langle \phi_{a2} | \phi_{bn}\rangle$, $S_{a3,bn} = \langle \phi_{a3} | \phi_{bn}\rangle$, ..., $S_{ak-1,bn} = \langle \phi_{ak-1} | \phi_{bn}\rangle$, $S_{ak,bn} = \langle \phi_{ak} | \phi_{bn}\rangle$, $S_{ak+1,bn} = \langle \phi_{ak+1} / \phi_{bn}\rangle$, ... This sum, equation (3-50), will be very difficult to handle semi-empirically, therefore, we shall make the following approximation to simplify it:

$$\sum_n \frac{P_{kn}}{2} S_{ak,bn} \approx \sum_n \frac{P_{1n}}{2} S_{a1,bn} \approx \sum_n \frac{P_{2n}}{2} S_{a2,bn} \approx \sum_n \frac{P_{3n}}{2} S_{a3,bn}$$

$$\approx\sum_n \frac{P_{k-1n}}{2}\, S_{ak-1,bn}\approx\sum_n \frac{P_{kn}}{2}\, S_{ak,bn}\approx\sum_n \frac{P_{k+1n}}{2}\, S_{ak-1,bn}$$

$$\approx\sum_n \frac{P_{k-2n}}{2}\, S_{ak-2,bn}\approx\ldots\ldots\ldots

$$+\left(\sum_n \frac{P_{kn}}{2} S_{ak,bn}-1\right)\left(\langle\phi_{ak}\phi_{ak}/\phi_{ak}\phi_{ak}\rangle-\frac{1}{2}\langle\phi_{ak}\phi_{ak}/\phi_{ak}\phi_{ak}\rangle\right)$$

$$+----------+$$

$$----------$$

$$=\left(\sum_n \frac{P_{kn}}{2} S_{ak,bn}-1\right)\sum_m \left(\langle\phi_{ak}\phi_{ak}/\phi_{am}\phi_{am}\rangle-\frac{1}{2}\langle\phi_{ak}\phi_{am}/\phi_{ak}\phi_{am}\rangle\right)\ldots\ldots(3\text{-}52)$$

Using equations (3-30) and (3-31), this becomes

$$\left(\sum_n \frac{P_{kn}}{2} S_{ak,bn}-1\right)\sum_m \left(\langle\phi_{ak}\phi_{ak}/\phi_{am}\phi_{am}\rangle-\frac{1}{2}\langle\phi_{ak}\phi_{am}/\phi_{ak}\phi_{am}\rangle\right)$$

$$=\left(\sum_n \frac{P_{kn}}{2} S_{ak,bn}-1\right)(\epsilon_k-I_{kk})\ldots\ldots\ldots(3\text{-}53)$$

From equations (3-52) and (3-53), the off-diagonal elements F_{kl} in equation (3-49) becomes

$$F_{kl}=S_{ak,bl}\left[\epsilon_k+\left(\sum_n \frac{P_{kn}}{2} S_{ak,bn}-1\right)(\epsilon_k-I_{kk})\right]\ldots\ldots\ldots\ldots(3\text{-}54)$$

Similarly expanding (Ruedenberg, 1951),

$$\phi_{am}=\sum_{r=1}^{\infty} S_{am,br}\phi_{br} \quad also \quad \phi_{ak}=\sum_{r=1}^{\infty} S_{ak,br}\phi_{br}\ldots\ldots\ldots\ldots(3\text{-}55)$$

and folowing the steps from equation (3-46) to (3-54), we obtain

$$F_{kl} = S_{ak,bl}[\epsilon_l + (\sum_m \frac{P_{ml}}{2} S_{am,bl} - 1)(\epsilon_l - I_{l_l})] \ldots\ldots\ldots\ldots (3\text{-}56)$$

Therefore, from equations (3-54) and (3-56), the off-diagonal element F_{kl} becomes:

$$F_{kl} = \frac{S_{ak,bl}}{2}[(\epsilon_k + \epsilon_l) + (\sum_n \frac{P_{kn}}{2} S_{ak,bn} - 1)(\epsilon_k - I_{kk})$$

$$+ (\sum_m \frac{P_{ml}}{2} S_{am,bl} - 1)(\epsilon_l - I_{l_l})]$$

$$= (1 + \sigma_{BOND}^{a\text{-}b}) S_{ak,bl}(\epsilon_k + \epsilon_l)/2 \ldots\ldots\ldots\ldots\ldots\ldots (3\text{-}57)$$

where $\sigma_{BOND}^{a\text{-}b}$ *is called a - b bond function and is defined as:*

$$\sigma_{BOND}^{a\text{-}b} = (\sum_n \frac{P_{kn}}{2} S_{ak,bn} - 1)\ (\frac{\epsilon_k - I_{kk}}{\epsilon_k + \epsilon_l}) + (\sum_m \frac{P_{ml}}{2} S_{am,bl} - 1) \frac{\epsilon_l - I_{l_l}}{\epsilon_k + \epsilon_l} \ldots\ldots (3\text{-}58)$$

3.2.0 **A Self-Consistent Field Molecular Orbital Spin-Polarized Extended Huckel theory: SCF-MO EHT-SP Method**

This is for the generalized open shell system in which the ground state can be represented by a single determinant wave function. For such a state we may associate M electrons with orthonormal orbitals $\psi_1^{\alpha} \ldots\ldots\ldots\ldots \psi_M^{\alpha}$ and α-spin functions and the remaining N electrons with orbitals $\psi_1^{\beta} \ldots\ldots\ldots \psi_N^{\beta}$ and β-spin functions. There is no a prior reason, however, why any of the

orbitals in one set should be identical with any in the other. The total determinantal wavefunction (Pople and Nesbet, 1954) is, then,

$$\psi_{sp} = \frac{1}{\sqrt{(M+N)!}} \sum_R (-1)^R \hat{R}[\psi_1^\alpha(1)\alpha(1)\ldots\ldots\ldots\ldots\ldots\psi_N^\alpha(M)\alpha(M)$$

$$X\ \psi_1^\beta(M+1)\beta(M+1)\ldots\ldots\ldots\psi_N^\beta(M+N)\beta(M+N)]\ldots\ldots\ldots(3\text{-}59)$$

Using the total electronic Hamiltonian (3-3), the corresponding total electronic energy is found by the standard reduction procedure and has the following expression:

$$E_{sp} = \sum_p^\alpha (H_{pp} + \sum_q^{\alpha+\beta} J_{pq} - \sum_q^\alpha K_{pq}^\alpha) + \sum_p^\beta (H_{pp} + \sum_q^{\alpha+\beta} J_{pq} - \sum_q^\beta K_{pq}^\beta)\ldots\ldots\ldots(3\text{-}60)$$

where

$$\sum_p^\alpha H_{pp} = \sum_p^\alpha \int \psi_p^{*\alpha}(i) H(i) \psi_p^\alpha(i) d\tau_i \ldots\ldots\ldots\ldots(3\text{-}61)$$

$$\sum_p^\alpha \sum_q^{\alpha+\beta} J_{pq} = \sum_p^\alpha \int \psi_p^{*\alpha}(i) [\sum_q^\alpha \int \psi_q^{*\alpha}(j) \psi_q^\alpha(j) 1/r_{ij} d\tau_j$$

$$+ \sum_q^\beta \int \psi_q^{*\beta}(j) \psi_q^\beta(j) 1/r_{ij} d\tau_j] \psi_p^\alpha(i) d\tau_i$$

$$\sum_{p}^{\alpha}\int\psi_p^{*\alpha}(i)\sum_{q}^{\alpha+\beta}J_q\psi_p^{\alpha}(i)d\tau_i \quad \text{.....(3-62)}$$

and

$$\sum_{p}^{\alpha}\sum_{q}^{\alpha}K_{pq}^{\alpha} = \sum_{p}^{\alpha}\int\psi_p^{*\alpha}(i)\left[\sum_{q}^{\alpha}\int\frac{\psi_p^{*\alpha}(i)\psi_q^{*\alpha}(j)1/r_{ij}\psi_q^{\alpha}(i)\psi_p^{\alpha}(j)d\tau_j}{\psi_p^{*\alpha}(i)\psi_p^{\alpha}(i)}\right.$$

$$\left.x\psi_p^{\alpha}(i)d\tau_i\right.$$

$$= \sum_{p}^{\alpha}\int\psi_p^{*\alpha}(i)\sum_{q}^{\alpha}K_q^{\alpha}\psi_p^{\alpha}(i)d\tau_i \quad \text{.....(3-63)}$$

with similar expression for the second term $\sum_p^\beta$ in equation (3-60).

Using equation (3-60), the total electronic energy becomes:

$$E_{sp}=\sum_{p}^{\alpha}\int\psi_p^{*\alpha}(i)\left[H(i)+\sum_{q}^{\alpha+\beta}J_q-\sum_{q}^{\alpha}K_q^{\alpha}\right]\psi_p^{\alpha}(i)d\tau_i$$

$$+\sum_{p}^{\beta}\int\psi_p^{*\beta}(i)\left[H(i)+\sum_{q}^{\alpha+\beta}J_q-\sum_{q}^{\beta}K_q^{\beta}\right]\psi_p^{\beta}(i)d\tau_i \quad \text{.....(3-64)}$$

which can be written as

$$E_{sp} = \sum_{p}^{\alpha}\int\psi_p^{*\alpha}(i)F_i^{\alpha}\psi_p^{\alpha}(i)d\tau_i+\sum_{p}^{\beta}\int\psi_p^{*\beta}(i)F_i^{\beta}\psi_p^{\beta}(i)d\tau_i, \quad \text{.....(3-65)}$$

where the one-electron operators F_i^α and F_i^β, called the spin-

polarized Hartree-Fock-Roothaan operators, are defined from (3-64) as

$$F_i^{\alpha} = H(i) + \sum_{q}^{\alpha\cdot\beta} J_q - \sum_{q}^{\alpha} K_q^{\alpha} \quad \text{.....(3-66)}$$

and

$$F_i^{\beta} = H(i) + \sum_{q}^{\alpha\cdot\beta} J_q - \sum_{q}^{\beta} K_q^{\beta} \quad \text{.....(3-67)}$$

The summations

$$\sum_{p}^{\alpha} \int \psi_p^{*\alpha}(i) F_i^{\alpha} \psi_p^{\alpha}(i) d\tau_i \text{ also } \sum_{p}^{\beta} \int \psi_p^{*\beta}(i) F_i^{\beta} \psi_p^{\beta} \psi_p^{\beta}(i) d\tau_i$$

in equation (3-65), individually, contain independent terms which, according to quantum mechanics, each can be written as

$$\int \psi_p^{*\alpha}(i) F_i^{\alpha} \psi_p^{\alpha}(i) d\tau_i = \epsilon_p^{\alpha} \quad p=1,2,\ldots\ldots\ldots\ldots,M \quad \text{.....(3-68)}$$

$$\text{also } \int \psi_p^{\beta}(i) F_i^{\beta}(i) \psi_p^{\beta}(i) d\tau_i = \epsilon_p^{\beta} \ldots\ldots p=1,2,\ldots\ldots,N\ldots\ldots \text{(3-69)}$$

or in other words, equation (3-65) becomes

$$\sum_{p}^{\alpha} \epsilon_p^{\alpha} + \sum_{p}^{\beta} \epsilon_p^{\beta} = E_{sp} \quad \text{.....(3-70)}$$

From equations (3-68) and (3-69), the molecular orbitals [ψ_p^{α}; p = 1,2,.....,M] and [ψ_p^{β}; p=1,2,.....,N] are the eigenfunctions of the one-electron spin-polarized Hartree-Fock-Roothaan operators F_i^{α}

and F_i^{β} with (real) energies [ϵ_p^{α}; p=1,2,....., M] and [ϵ_p^{β}; p=1, 2,....., N] that satisfy the spin-polarized Hartree-Fock-Roothaan equations

$$F_i^{\alpha}\psi_p^{\alpha}(i) = \epsilon_p^{\alpha}\psi_p^{\alpha}(i) \quad p=1,2,.....,M \quad .....(3-71)$$

and

$$F_i^{\beta}\psi_p^{\beta}(i) = \epsilon_p^{\beta}\psi_p^{\beta}(i) \quad p=1,2,.....,N,.....(3-72)$$

the total energy E_{sp} being simply given by equation (3-70). Using equation (3-18), the correlation terms in (3-66) become (Pople and Nesbet, 1954).

$$\sum_q^{\alpha\text{-}\beta} J_q = \sum_q^{\alpha}\int\psi_q^{*\alpha}(j)\psi_q^{\alpha}(j)1/r_{ij}d\tau_j+\sum_q^{\beta}\int\psi_q^{*\beta}(j)\psi_q^{\beta}(j)1/r_{ij}d\tau_j$$

$$= \sum_q^{\alpha}\int\sum_m C_{qm}^{*\alpha}\phi_m^{*}(j)\sum_n C_{qn}^{\alpha}\phi_n(j)1/r_{ij}d\tau_j+\sum_q^{\beta}\int\sum_m C_{qm}^{*\beta}\phi_m^{*}(j)\sum_n C_{qn}^{\beta}\phi_n(j)1/r_{ij}d\tau_j$$

$$= \sum_m\sum_n(\sum_q^{\alpha} C_{qm}^{*\alpha}C_{qn}^{\alpha}+\sum_q^{\beta} C_{qn}^{*\beta}C_{qn}^{\beta})\int\phi_m^{*}(j)\phi_n(j)1/r_{ij}d\tau_j$$

$$= \sum_m\sum_n(P_{mn}^{\alpha}+P_{mn}^{\beta})\int\phi_m^{*}(j)\phi_n(j)1/r_{ij}d\tau_j.....(3-73)$$

$$\text{where } P_{mn}^{\alpha} = \sum_q^{\alpha} C_{qm}^{*\alpha}C_{qn}^{\alpha} \text{ also } P_{mn}^{\beta} = \sum_q^{\beta} C_{qm}^{*\beta}C_{qn}^{\beta}.....(3-74)$$

Similarly, (Pople and Nesbet, 1954)

$$\sum_q^{\alpha} K_q^{\alpha} = \sum_q^{\alpha} \int \frac{\psi_p^{*\alpha}(i)\psi_q^{*\alpha}(j)1/r_{ij}\psi_q^{\alpha}(i)\psi_p^{\alpha}(j)d\tau_j}{\psi_p^{*\alpha}(i)\psi_p^{\alpha}(i)}$$

$$\sum_q^{\alpha} K_q^{\alpha} = \sum_q^{\alpha} \int \frac{\sum_k C_{pk}^{*\alpha}\phi_k^*(i)\sum_m C_{qm}^{*\alpha}\phi_m^*(j)1/r_{ij}\sum_n C_{qn}^{\alpha}\phi_n(i)\sum_l C_{pl}^{\alpha}\phi_l(j)d\tau_j}{\sum_k C_{pk}^{*\alpha}\phi_k^*(i)\sum_l C_{pl}^{\alpha}\phi_l(i)}$$

$$= \sum_m \sum_n \sum_q^{\alpha} C_{qm}^{*\alpha} C_{qn}^{\alpha} \int \frac{\phi_k^*(i)\phi_m^*(j)1/r_{ij}\phi_n(i)\phi_l(j)d\tau_j}{\phi_k^*(i)\phi_l(i)}$$

$$= \sum_m \sum_n P_{mn}^{\alpha} \int \frac{\phi_k^*(i)\phi_m^*(j)1/r_{ij}\phi_n(i)\phi_l(j)d\tau_j}{\phi_k^*(i)\phi_l(i)} \quad \text{.....(3-75)}$$

So that equation (3-66) becomes

$$F_i^{\alpha} = H(i) + \sum_m \sum_n (P_{mn}^{\alpha} + P_{mn}^{\beta}) \int \phi_m^*(j)\phi_n(j)1/r_{ij}d\tau_j$$

$$- \sum_m \sum_n P^{\alpha}_{mn} \int \frac{\phi^*_k(i)\phi^*_m(j)1/r_{ij}\phi_n(i)\phi_l(j)d\tau_j}{\phi^*_k(i)\phi_l(i)}$$

$$= H(i) + \sum_m \sum_n (P^{\alpha}_{mn} + P^{\beta}_{mn}) \{ \int \phi^*_m(j)\phi_n(j)1/r_{ij}d\tau_j$$

$$- \alpha_{mn} \int \frac{\phi^*_k(i)\phi^*_m(j)1/r_{ij}\phi_n(i)\phi_l(j)d\tau_j}{\phi^*_k(i)\phi_l(i)} \} \ldots\ldots\ldots (3\text{-}76)$$

where the quantity α_{mn} is defined as

$$\alpha_{mn} = P^{\alpha}_{mn}/(P^{\alpha}_{mn} + P^{\beta}_{mn}) \ldots\ldots\ldots (3\text{-}77)$$

Similarly F_i^{β} is obtained as

$$F^{\beta}_i = H(i) + \sum_m \sum_n (P^{\alpha}_{mn} + P^{\beta}_{mn}) \{ \int \phi^*_m(j)\phi_n(j)1/r_{ij}d\tau_j$$

$$- \sum_m \sum_n P^{\beta}_{mn} \int \frac{\phi^*_k(i)\phi^*_m(j)1/r_{ij}\phi_n(i)\phi_l(j)d\tau_j}{\phi^*_k(i)\phi_l(i)}$$

$$= H(i) + \sum_m \sum_n (P^{\alpha}_{mn} + P^{\beta}_{mn}) [\int \phi^*_m(j)\phi_n(j)1/r_{ij}d\tau_j$$

$$\beta_{mn} \int \frac{\phi^*_k(i)\phi^*_m(j)1/r_{ij}\phi_n(i)\phi_l(j)d\tau_j}{\phi^*_k(i)\phi_l(i)}]$$

where also $\beta_{mn} = P_{mn}{}^{\beta}/(P_m{}^{\alpha} + P_{mn}{}^{\beta})$ .....(3-79)

From equation (3-71), the trial orbital energies in (3-71) are

given by (the expectation values):

$$\epsilon_p^\alpha = \int \psi_p^{*\alpha}(i) F_i^\alpha \psi_p^\alpha(i) d\tau_i / \int \psi_p^{\alpha 2}(i) d\tau_i \quad p = 1,2,\ldots,M \quad \ldots\ldots\ldots (3\text{-}80)$$

If we introduce the symbols

$$F_{kl}^\alpha = \int \phi_k^*(i) F_i^\alpha \phi_l(i) d\tau_i$$

$$= \int \phi_k^*(i) [H(i) + \sum_m \sum_n (P_{mn}^\alpha + P_{mn}^\beta) [\int \phi_m^*(j) \phi_n(j) 1/r_{ij} d\tau_j$$

$$- \alpha_{mn} \int \frac{\phi_k^*(i) \phi_m^*(j) 1/r_{ij} \phi_n(i) \phi_l(j) d\tau_j}{\phi_k^*(i) \phi_l(i)}]] \phi_l(i) d\tau_i$$

$$= \int \phi_k^*(i) H(i) \phi_l(i) d\tau_j + \sum_m \sum_n (P_{mn}^\alpha + P_{mn}^\beta) [\iint \phi_k^*(i) \phi_m^*(j) 1/r_{ij}$$

$$x\ \phi_l(j) \phi_n(i) d\tau_i d\tau_j - \alpha_{mn} \iint \phi_k^*(i) \phi_m^*(j) 1/r_{ij} \phi_n(i) \phi_l(j) d\tau_i d\tau_j]$$

$$= H_{kl} + \sum_m \sum_n (P_{mn}^\alpha + P_{mn}^\beta) (\langle \phi_k \phi_l / \phi_m \phi_n \rangle$$

$$- \alpha_{mn} \langle \phi_k \phi_n / \phi_l \phi_m \rangle) \ldots\ldots\ldots\ldots (3\text{-}81)$$

and $S_{kl} = \int \phi_k^*(i) \phi_l(i)\ d\tau_i$, ... (3-82)

then the expression for the expectation value ϵ_p^α in (3-80) becomes

$$\epsilon_p^\alpha = \sum_k \sum_l C_{pk}^{*\alpha} C_{pl}^\alpha F_{kl}^\alpha / \sum_k \sum_l C_{pk}^{*\alpha} C_{pl}^\alpha S_{kl}$$

or

$$\epsilon_p^{\alpha} \sum_k \sum_l C_{pl}^{*\alpha} C_{pl}^{\alpha} S_{kl} = \sum_k \sum_l C_{pk}^{*\alpha} C_{pl}^{\alpha} F_{kl}^{\alpha} \quad \text{.....(3-83)}$$

To find the values of $C_{p1}^{*\alpha}$, $C_{p2}^{*\alpha}$, ..., $C_{pk}^{*\alpha}$ which give the lowest value for ϵ_p^{α} and therefore the best approximation to the energy $E_{\alpha p}$, we differentiate equation (3-83) with respect to each $C_{pk}^{*\alpha}$ (k=1,2,....,M):

$$\frac{\partial \epsilon_p^{\alpha}}{\partial C_{pk}^{*\alpha}} \sum_k \sum_l C_{pk}^{*\alpha} C_{pl}^{\alpha} S_{kl} + \epsilon_p^{\alpha} \sum_l C_{pl}^{\alpha} S_{kl} = \sum_l C_{pl}^{\alpha} F_{kl}^{\alpha} \quad \text{.....(3-84)}$$

$$\frac{\partial \epsilon_p^{\alpha}}{\partial C_{pk}^{*\alpha}} = 0 \quad \textit{for each k index} \quad \text{.....(3-85)}$$

The condition for the lowest value of the energy or minimum is that which reduces equation (3-84) to

$$\epsilon_p^{\alpha} \sum_l C_{pl}^{\alpha} S_{kl} = \sum_l C_{pl}^{\alpha} F_{kl}^{\alpha} \textit{ otherwise } \sum_l C_{pl}^{\alpha} (F_{kl}^{\alpha} - \epsilon_p^{\alpha} S_{kl}) = 0 \quad \text{....(3-86)}$$

Similarly following the same procedure for equation (3-72), we obtain

$$\epsilon_p^{\beta} \sum_l C_{pl}^{\beta} S_{kl} = \sum_l C_{pl}^{\beta} F_{kl}^{\beta} \textit{ otherwise } \sum_l C_{pl}^{\beta} (F_{kl}^{\beta} - \epsilon_p^{\beta} S_{kl}) = 0 \quad \text{...(3-87)}$$

where the S_{kl}'s are overlap integrals. In order for these equations to hold true, the determinant of the matrices must be equal to zero. Solution of the secular determinants affords the energies ϵ_p^{α} and ϵ_p^{β} for each molecular orbital. Substitution of these energies

into the sets of linear equations (3-86) and (3-87) provides the coefficients C_{p1}^{α} and C_{p1}^{β}.

3.2.1 Matrix elements of the S C F - M O E H T Spin-Polarized Method

A. DIAGONAL ELEMENTS

Following equations (3-28) and (3-81) the spin-polarized diagonal element F_{kk}^{α} is

$$F_{kk}^{\alpha} = \langle\phi_{ak}/-\sum_{A}\frac{Z_A}{r_{Ai}} - \frac{\nabla_i^2}{2}/\phi_{ak}\rangle + \sum_{m}(P_{mm}^{\alpha} + P_{mm}^{\beta})(\langle\phi_{ak}\phi_{ak}/\phi_{am}\phi_{am}\rangle$$

$$- \alpha_{mm}\langle\phi_{ak}\phi_{am}/\phi_{ak}\phi_{am}\rangle).....(3\text{-}88)$$

Let's now define the spin-polarized atomic orbital quantities

$$\epsilon_k^{\alpha} = \langle\phi_{ak}/-\sum_{A}\frac{Z_A}{r_{Ai}} - \frac{\nabla_i^2}{2}/\phi_{ak}\rangle + \sum_{m}(\langle\phi_{ak}\phi_{ak}/\phi_{am}\phi_{am}\rangle$$

$$- \alpha_{mm}\langle\phi_{ak}\phi_{am}/\phi_{ak}\phi_{am}\rangle).....(3\text{-}89)$$

while I_{kk} is as defined in equation (3-30). Adding

$$\sum_{m}(\langle\phi_{ak}\phi_{ak}/\phi_{am}\phi_{am}\rangle - \alpha_{mm}\langle\phi_{ak}\phi_{am}/\phi_{ak}\phi_{am}\rangle).....(3\text{-}90)$$

to equation (3-88) and subtracting same from it (operation nothing), we have

$$F^{\alpha}_{kk} = \langle\phi_{ak}/-\sum_{A}\frac{Z_A}{r_{Ai}} - \frac{\nabla_i^2}{2}/\phi_{ak}\rangle + \sum_{m}(\langle\phi_{ak}\phi_{ak}/\phi_{am}\phi_{am}\rangle - \alpha_{mm}\langle\phi_{ak}\phi_{am}/\phi_{ak}\phi_{am}\rangle$$

$$+ \sum_{m}[(P^{\alpha}_{mm} + P^{\beta}_{mm}-1)(\langle\phi_{ak}\phi_{ak}/\phi_{am}\phi_{am}\rangle - \alpha_{mm}\langle\phi_{ak}\phi\text{-}am/\phi_{ak}\phi_{am}\rangle).....(3\text{-}91)$$

Invoking the approximation of equation (3-35),

$$\sum_{m}[(P^{\alpha}_{mm} + P^{\beta}_{mm}-1)(\phi_{ak}\phi_{ak}/\phi_{am}\phi_{am}\rangle - \alpha_{mm}\langle\phi_{ak}\phi_{am}/\phi_{ak}\phi_{am}\rangle)]$$

$$\approx(P^{\alpha}_{kk} + P^{\beta}_{kk}-1)\sum_{m}(\langle\phi_{ak}\phi_{ak}/\phi_{am}\phi_{am}\rangle - \alpha_{mm}\langle\phi_{ak}\phi_{am}/\phi_{ak}\phi_{am}\rangle)$$

$$= (P^{\alpha}_{kk} + P^{\beta}_{kk}-1)(\epsilon^{\alpha}_{k} - I_{kk}).....(3\text{-}92)$$

using equations (3-89) and (3-30). Thus the spin-polarized diagonal element $F_{kk}{}^{\alpha}$ takes the final form

$$F^{\alpha}_{kk} = \epsilon^{\alpha}_{k} + (P^{\alpha}_{kk}+P^{\beta}_{kk}-1)(\epsilon^{\alpha}_{k}-I_{kk})$$

$$= (1 + \lambda^{\alpha}_{k})\epsilon^{\alpha}_{k}.....(3\text{-}93)$$

where the charge dependent variable $\lambda_{k}{}^{\alpha}$ is defined as

$$\lambda^{\alpha}_{k} = (P^{\alpha}_{kk} + P^{\beta}_{kk}-1)\frac{\epsilon^{\alpha}_{k} - I_{kk}}{\epsilon^{\alpha}_{k}}.....(3\text{-}94)$$

Following the same procedure for the diagonal element $F_{kk}{}^{\beta}$, we obtain

$$F_{kk}^{\beta} = (1 + \lambda_k^{\beta})\epsilon_k^{\beta} \quad \text{.....(3-95)}$$

$$\text{where } \lambda_k^{\beta} = (P_{kk}^{\alpha} + P_{kk}^{\beta} - 1)\frac{\epsilon_k^{\beta} - I_{kk}}{\epsilon_k^{\beta}} \quad \text{.....(3-96)}$$

B. **OFF-DIAGONAL ELEMENTS**

The explanations emanating from equations (3-42), (3-43) and (3-44) apply to the spin-polarized off-diagonal elements and the F_{kl}^{α} is given by

$$F_{kk}^{\alpha} = \langle\phi_{ak}/ - \sum_A \frac{Z_A}{r_{Ai}} - \frac{\nabla_i^2}{2}/\phi_{bl}\rangle + \sum_m \sum_n (P_{mn}^{\alpha} + P_{mn}^{\beta})(\langle\phi_{ak}\phi_{bl}/\phi_{am}\phi_{bn}\rangle$$
$$- \alpha_{mn}\langle\phi_{ak}\phi_{bn}/\phi_{bl}\phi_{am}\rangle) \quad \text{.....(3-97)}$$

Following the procedures of (3-45) to (3-47), we have for F_{kl}^{α}

$$F_{kl}^{\alpha} = S_{ak,bl}[\langle\phi_{ak}/ - \sum_A \frac{Z_A}{r_{Ai}} - \frac{\nabla_i^2}{2}/\phi_{ak}\rangle + \sum_m \sum_n (P_{mn}^{\alpha} + P_{mn}^{\beta})S_{am,bn}$$

$$x\ (\langle\phi_{ak}\phi_{ak}/\phi_{am}\phi_{am}\rangle - \alpha_{mn}\langle\phi_{ak}\phi_{am}/\Phi_{ak}\phi_{am}\rangle)] \quad \text{.....(3-98)}$$

Adding

$$S_{ak,bl}\sum_m (\langle\phi_{ak}\phi_{ak}/\phi_{am}\phi_{am}\rangle - \alpha_{mm}\langle\phi_{ak}\phi_{am}/\phi_{ak}\phi_{am}\rangle) \quad \text{.....(3-99)}$$

to equation (3-98) and subtracting same from it (operation nothing), we get

$$F^{\alpha}_{kl} = S_{ak,bl}[<\phi_{ak}/ - \sum_{A}\frac{Z_A}{r_{Ai}} - \frac{\nabla^2_i}{2}/\phi_{ak}> + \sum_{m}(<\phi_{ak}\phi_{ak}/\phi_{am}\phi_{am}>$$

$$- \alpha_{mn}<\phi_{ak}\phi_{am}/\phi_{ak}\phi_{am}>)]$$

$$+ S_{ak,bl}[\sum_{m}\sum_{n}(P^{\alpha}_{mn} + P^{\beta}_{mn})S_{am,bn}(<\phi_{ak}\phi_{ak}/\phi_{am}\phi_{am}> - \alpha_{mn}<\phi_{ak}\phi_{am}/\phi_{ak}\phi_{am}>)$$

$$- \sum_{m}(<\phi_{ak}\phi_{ak}/\phi_{am}\phi_{am}> - \alpha_{mm}<\phi_{ak}\phi_{am}/\phi_{ak}\phi_{am}>)]$$

$$= S_{ak,bn}[\epsilon^{\alpha}_{k} + \sum_{m}\sum_{n}(P^{\alpha}_{mn} + P^{\beta}_{mn})S_{am,bn}(<\phi_{ak}\phi_{ak}/\phi_{am}\phi_{am}>$$

$$- \alpha_{mn}<\phi_{ak}\phi_{am}/\phi_{ak}\phi_{am}>) - \sum_{m}(<\phi_{ak}\phi_{ak}/\phi_{am}\phi_{am}>$$

$$- \alpha_{mm}<\phi_{ak}\phi_{am}/\phi_{ak}\phi_{am}>)]\ldots\ldots\ldots(3\text{-}100)$$

by using (3-89). Invoking the approximation of equation (3-52),

$$\sum_{m}\sum_{n}(P^{\alpha}_{mn} + P^{\beta}_{mn})S_{am,bn}(<\phi_{ak}\phi_{ak}/\phi_{am}\phi_{am}> - \alpha_{mn}<\phi_{ak}\phi_{am}/\phi_{ak}\phi_{am}>)$$

$$\approx \sum_{n}(P^{\alpha}_{kn} + P^{\beta}_{kn})S_{ak,bn}\sum_{m}(<\phi_{ak}\phi_{ak}/\phi_{am}\phi_{am}> - \alpha_{mn}<\phi_{ak}\phi_{am}/\phi_{ak}\phi_{am}>)\ldots(3\text{-}101)$$

equation (3-100) reduces to

$$F^{\alpha}_{kl} = S_{ak,bl}[\epsilon^{\alpha}_{k} + \sum_{n}(P^{\alpha}_{kn} + P^{\beta}_{kn})S_{ak,bn}\sum_{m}(<\phi_{ak}\phi_{ak}/\phi_{am}\phi_{am}>$$

$$- \alpha_{mn}\langle\phi_{ak}\phi_{am}/\phi_{ak}\phi_{am}\rangle) - \sum_{m}(\langle\phi_{ak}\phi_{ak}/\phi_{am}/\phi_{ak}\phi_{am}\rangle$$

$$- \alpha_{mm}\langle\phi_{ak}\phi_{am}/\phi_{ak}\phi_{am}\rangle)]$$

$$\approx S_{ak,bl}[\epsilon_k^{\alpha} + [\sum_{n}(P_{kn}^{\alpha} + P_{kn}^{\beta})S_{ak,bn}-1]\sum_{m}(\langle\phi_{ak}\phi_{ak}/\phi_{am}\phi_{am}\rangle$$

$$- \alpha_{mm}\langle\phi_{ak}\phi_{am}/\phi_{ak}\phi_{am}\rangle)]$$

$$= S_{ak,bl}[\epsilon_k^{\alpha} + [\sum_{n}(P_{kn}^{\alpha} + P_{kn}^{\beta})S_{ak,bn}-1](\epsilon_k^{\alpha} - I_{kk})]$$

using equations (3-89) and (3-30) and by making further approximation that

$$\alpha_{mm} \approx \alpha_{mn} \quad \ldots\ldots\ldots\ldots\ldots\ldots\ldots\ldots (3\text{-}103)$$

Actually $\alpha_{aa} = \alpha_{ss}$ for closed shell or spin-restricted systems. It is also true for spin-polarized system with $n_\alpha \neq 0$ and $n_\beta = 0$.

Similarly following the steps of equation (3-55) applying the same procedure, from equation (3-97) to (3-103), we obtain

$$F_{kl}^{\alpha} = S_{ak,bl}[\epsilon_l^{\alpha} + [\sum_{m}(P_{ml}^{\alpha} + P_{ml}^{\beta})S_{am,bl}-1](\epsilon_l^{\alpha} - I_{l_l})] \ldots . (3\text{-}104)$$

From equations (3-102) and (3-104), we have the final expression for the off-diagonal element F_{kl}.

$$F_{kl}^{\alpha} = (1+{}^{\alpha}\sigma_{BOND}^{a-b})\, S_{ak,bl}(\epsilon_k^{\alpha} + \epsilon_l^{\alpha})/2 \ldots\ldots\ldots (3\text{-}105)$$

where the spin-polarized $^{\alpha}\sigma_{BOND}^{a-b}$ is defined as

$$\{^{\alpha}\sigma_{BOND}^{a-b}\} = [\sum_{n}(P_{kn}^{\alpha} + P_{kn}^{\beta})S_{ak,bn} - 1]\frac{\epsilon_k^{\alpha} - I_{kk}}{\epsilon_k^{\alpha}+\epsilon_l^{\alpha}} + [\sum_{m}(P_{ml}^{\alpha}+P_{ml}^{\beta})S_{am,bn} - 1]$$

$$\times \frac{\epsilon_l^{\alpha} - I_{l_1}}{\epsilon_k^{\alpha}+\epsilon_l^{\alpha}} \ldots\ldots\ldots (3\text{-}106)$$

In the same fashion, we obtain for F_{kl}^{β}

$$F_{kl}^{\beta} = (1+{}^{\beta}\sigma_{BOND}^{a-b})S_{ak,bl}(\epsilon_k^{\beta}+\epsilon_l^{\beta})/2 \ldots\ldots\ldots (3\text{-}107)$$

where also

$$\{^{\beta}\sigma_{BOND}^{a-b}\} = [\sum_{n}(P_{kn}^{\alpha}+P_{kn}^{\beta})S_{ak,bn} - 1]\frac{\epsilon_k^{\beta} - I_{kk}}{\epsilon_k^{\beta}+\epsilon_l^{\beta}} + [\sum_{m}(P_{ml}^{\alpha}+P_{ml}^{\beta})S_{am,bl} - 1]$$

$$\times \frac{\epsilon_l^{\beta} - I_{l_1}}{\epsilon_k^{\beta}+\epsilon_l^{\beta}} \ldots\ldots\ldots\ldots (3\text{-}108)$$

3.3 OPTIMIZATION OF NUMERICAL VALUES FOR THE MATRIX ELEMENTS

From equation (3-31), ϵ_k is given by

$$\epsilon_k = \langle\phi_{ak}/ - \sum_{A}\frac{Z_A}{r_{Ai}} - \frac{\nabla_i^2}{2}/\phi_{ak}\rangle + \sum_{m}(\langle\phi_{ak}\phi_{ak}/\phi_{am}\phi_{am}\rangle$$

$$-\frac{1}{2}\langle\phi_{ak}\phi_{am}/\phi_{ak}\phi_{am}\rangle)$$

$$= \langle \phi_{ak} / -\sum_A \frac{Z_A}{r_{Ai}} - \frac{\nabla_i^2}{2} + \sum_m [\int \phi_{am}^*(j)\phi_{am}(j) 1/r_{ij} d\tau_j$$

$$- \frac{1}{2}\int \frac{\phi_{ak}^*(i)\phi_{am}^*(j) 1/r_{ij}\phi_{ak}(j)\phi_{am}(i) d\tau_j}{\phi_{ak}^*(i)\phi_{ak}(i)}] / \phi_{ak} \rangle$$

$$= \langle \phi_{ak} / H_{eff}(i) / \phi_{ak} \rangle \ldots\ldots\ldots\ldots\ldots\ldots\ldots\ldots (3\text{-}109)$$

where the one-electron effective Hamiltonian $H_{eff}(i)$ is defined as

$$H_{eff}(i) = -\frac{\nabla_i^2}{2} - \sum_A \frac{Z_A}{r_{Ai}} + \sum_m [\int \phi_{am}^*(j)\phi_{am}(j) 1/r_{ij} d\tau_j$$

$$- \frac{1}{2}\int \frac{\phi_{ak}^*(i)\phi_{am}^*(j) 1/r_{ij}\phi_{ak}(j)\phi_{am}(i) d\tau_j)}{\phi_{ak}^*(i)\phi_{ak}(i)}]$$

$$= -\frac{\nabla_i^2}{2} + v_i \ldots\ldots\ldots\ldots\ldots\ldots\ldots\ldots\ldots (3\text{-}110)$$

v_i is the potential of electron i mathematically defined as

$$v_i = -\sum_A \frac{Z_A}{r_{Ai}} + \sum_m [\int \phi_{am}^*(j)\phi_{am}(j) 1/r_{ij} d\tau_j$$

$$- \frac{1}{2}\int \frac{\phi_{ak}^*(i)\phi_{am}^*(j) 1/r_{ij}\phi_{ak}(j)\phi_{am}(i) d\tau_j}{\phi_{ak}^*(i)\phi_{ak}(i)}] \ldots\ldots\ldots (3\text{-}111)$$

and represents the field of the nuclei and the effect of all the other electrons. It is also a function of the coordinates of electron i alone, independent of the position of other electrons. Thus, the effective one-electron Hamiltonian H_{eff} (i) and the corresponding one-electron potential v_i assumed by the Huckel theory in equation (2-6) are now physically and mathematically defined by equations (3-110) and (3-111) respectively. Therefore, the parameter ϵ_k

$$\epsilon_k = \langle \phi_{ak}(i) / -\frac{\nabla_i^2}{2} + v_i / \phi_{ak}(i) \rangle$$

$$= \langle \phi_{ak}(i) / H_{eff}(i) / \phi_{ak}(i) \rangle \quad \ldots\ldots\ldots\ldots\ldots\ldots (3\text{-}112)$$

represents the effective energy of a bound electron i in orbital ϕ_{ak} and can be equated to the energy required to remove such an electron from ϕ_{ak} to infinity (i.e. ionization potential, please see (2-20)):

$$\epsilon_k = \langle \phi_{ak}(i) / H_{eff}(i) / \phi_{ak}(i) \rangle$$

$$= - IP_k \quad \ldots\ldots\ldots\ldots\ldots\ldots\ldots\ldots\ldots\ldots\ldots\ldots (3\text{-}113)$$

In similar fashion, ϵ_k^α and ϵ_k^β are also given by (please see (3-89)]

$$\epsilon_k^\alpha = \langle \phi_{ak} / -\frac{\nabla_i^2}{2} + v_i^\alpha / \phi_{ak} \rangle$$

$$= \langle \phi_{ak} / H^{\alpha}_{eff}(i) / \phi_{ak} \rangle$$

$$= -IP^{\alpha}_{k} \quad \ldots\ldots\ldots\ldots\ldots\ldots\ldots\ldots\ldots\ldots\ldots\ldots (3\text{-}114)$$

and

$$\epsilon^{\beta}_{k} = \langle \phi_{ak} / H^{\beta}_{eff}(i) / \phi_{ak} \rangle$$

$$= -IP^{\beta}_{k} \quad \ldots\ldots\ldots\ldots\ldots\ldots\ldots\ldots\ldots\ldots\ldots\ldots (3\text{-}115)$$

where the spin-polarized one-electron potentials V_i^{α} and V_i^{β} are defined as

$$V^{\alpha}_{i} = -\sum_{A} \frac{Z_A}{r_{Ai}} + \sum_{m} [\int \phi^{*}_{am}(j) \phi_{am}(j) 1/r_{ij} d\tau_j$$

$$- \alpha_{mm} \int \frac{\phi^{*}_{ak}(i) \phi^{*}_{am}(j) 1/r_{ij} \phi_{ak}(j) \phi_{am}(i) d\tau_j}{\phi^{*}_{ak}(i) \phi_{ak}(i)}] \ldots\ldots\ldots\ldots (3\text{-}116)$$

and

$$V^{\beta}_{i} = -\sum_{A} \frac{Z_A}{r_{Ai}} + \sum_{m} [\int \phi^{*}_{am}(j) \phi_{am}(j) 1/r_{ij} d\tau_j$$

$$- \beta_{mm} \int \frac{\phi^{*}_{ak}(i) \phi^{*}_{am}(j) 1/r_{ij} \phi_{ak}(j) \phi_{am}(i) d\tau_j}{\phi^{*}_{ak}(i) \phi_{ak}(i)}] \ldots\ldots\ldots\ldots (3\text{-}117)$$

respectively and the corresponding one-electron spin-polarized

effective Hamiltonians $H_{eff}^{\alpha}(i)$ and $H_{eff}^{\beta}(i)$ are given by

$$H_{eff}^{\alpha}(i) = -\frac{\nabla_i^2}{2} + V_i^{\alpha} \quad an,d \quad H_{eff}^{\beta}(i) = -\frac{\nabla_i^2}{2} + V_i^{\beta} \text{.....(3-118)}$$

Hence, the matrix elements of the SCF-MO EHT-spin Restricted method are optimized from, using equations (3-39), (3-57) and (3-113),

$$F_{kk} = -(1+\lambda_k)IP_k \text{.....(3-118)}$$

$$F_{kl} = -(1+\sigma_{BOND}^{a-b})S_{ak,bl}(IP_k+IP_l)/2 \text{.....(3-120)}$$

whereas those of the SCF-MO EHT-Spin Polarized Method from, using equations (3-93), (3-95), (3-105), (3-107), (3-114) and (3-115),

$$F_{kk}^{\alpha} = -(1+\lambda_k^{\alpha})IP_k^{\alpha} \text{.....(3-121)}$$

$$F_{kl}^{\alpha} = -(1+{}^{\alpha}\sigma_{BOND}^{a-b})S_{ak,bl}(IP_k^{\alpha}+IP_l^{\alpha})/2 \text{.....(3-121)}$$

and

$$F_{kk}^{\beta} = -(1+\lambda_k^{\beta})IP_k^{\beta} \text{.....(3-122)}$$

$$F_{kl}^{\beta} = -(1+{}^{\beta}\sigma_{BOND}^{a-b})\ S_{ak,bl}(IP_k^{\beta}+P_l^{\beta})/2 \text{.....(3-122)}$$

respectively. The charge dependent variables λ_k, λ_k^{α} and λ_k^{β} are calculated analytically from equations (3-40), (3-94) and (3-96) easily by some initial guess of the charges P_{kk}, P_{kk}^{α} and P_{kk}^{β}, after

which calculation continues to self-consistency.

3.4 Determination of σ_{BOND}^{a-b} and its Physical Significance

From equation (3-16), the total molecular energy, for a closed shell system, is given by

$$E = 2\sum_p \epsilon_p$$

$$= 2\sum_p \langle \psi_p^*(i)/F_i/\psi_p(i)\rangle$$

$$= 2\sum_p \langle \sum_k C_{pk}^* \phi_k^*(i)/F_i/\sum_l C_{pl}\phi_l(i)\rangle$$

$$= \sum_k \sum_l \sum_p 2C_{pk}^* C_{pl}\langle \phi_k^*(i)/F_i/\phi_l(i)\rangle$$

$$= \sum_k \sum_p 2C_{pk}^2 \langle \phi_k^*(i)/F_i/\phi_k(i)\rangle + \sum_k \sum_{<l} \sum_p 2C_{pk}^* C_{pl}\langle \phi_k(i)/F_i/\phi_l(i)\rangle$$

$$= \sum_k P_{kk}F_{kk} + \sum_k \sum_{<l} P_{kl}F_{kl} \quad \ldots\ldots\ldots\ldots\ldots\ldots\ldots (3\text{-}123)$$

Using the results of equations (3-39) and (3-57) for F_{kk} and F_{kl}, we have for the total molecular energy

$$E = \sum_k P_{kk}(1+\lambda_k)\epsilon_k + \sum_k \sum_{<l} P_{kl}(1 + \sigma_{BOND}^{a-b})S_{ak,bl}(\epsilon_k+\epsilon_l)/2 \ldots\ldots (3\text{-}124)$$

Consider now the energy required to dissociate the molecule into widely separated atoms, that is the energy of atomization ΔE. The energy of the dissociated atoms will be given by the sum $\sum_k P_{kk}$ $(1 + \lambda_k)\epsilon_k$ for the electrons in them. Hence the atomization or binding energy of the molecule is given by

$$\Delta E = \sum_{k}\sum_{<l} P_{kl}(1+\sigma_{BOND}^{a-b})\, S_{ak,bl}(\epsilon_k+\epsilon_l)/2 \quad \text{.....(3-125)}$$

The sum consists of a number of terms, each referring to AOs of one pair of atoms a and b; it is natural to associate the term associated with one pair of AOs, (ϕ_{ak}, ϕ_{bn}), (ϕ_{am}, ϕ_{bl}) or (ϕ_{ak}, ϕ_{bl}), with the corresponding contribution to the total "bonding" in the molecule. This in turn is proportional to the bond orders {P_{kn}, P_{ml} or P_{kl}}, a-b bond function σ_{BOND}^{a-b} and {$S_{ak,bn}$, $S_{am,bl}$ or $S_{ak,bl}$}, therefore when they are all zero, ΔE is zero.

{P_{kn}, P_{ml} or P_{kl}} have the physical significance of bond orders since the product of coefficients of two AOs on adjacent atoms a and b in the MOs, are reasonable measures of finding an electron in the a-b region. If they are negative, this means there is a very low probability of finding electrons in the a-b region. However, if the {P_{kn}, P_{ml} or P_{kl}} are all zero, the electron distribution in the a-b region will be zero and this, in other words, is a nonbonding situation where a and b are separated atoms. Identically under this (separated atoms or nonbonding) situation all the overlap integrals {$S_{ak,bn}$, $S_{am,bl}$ or $S_{ak,bl}$} and the a-b bond functions σ_{BOND}^{a-b} must also be both zero.

Thus when

all {P_{kn}, P_{ml} or P_{kl}} = 0, ...(3-126)

physically, the a-b bond function σ_{BOND}^{a-b} must also be zero, that is

$\sigma_{BOND}^{a-b} = 0$ .....(3-127)

Therefore, the mathematically analytical expression of σ_{BOND}^{a-b} function,

$$\sigma_{BOND}^{a\text{-}b} = \left(\sum_n \frac{P_{kn}}{2}\, S_{ak,bn} - 1\right) \frac{\epsilon_k - I_{kk}}{\epsilon_k + \epsilon_l} + \left(\sum_m \frac{P_{ml}}{2}\, S_{am,bl} - 1\right) \frac{\epsilon_l - I_{l_1}}{\epsilon_k + \epsilon_l}$$

$$= \frac{\epsilon_k - I_{kk}}{\epsilon_k} \sum_n \frac{P_{kn}}{2} (S_{ak,bn} - 1) + \frac{\epsilon_l - I_{l_1}}{\epsilon_k + \epsilon_l} \sum_m \frac{P_{ml}}{2} (S_{am,bl} - 1)$$

$$+ \frac{\epsilon_k - I_{kk}}{\epsilon_k + \epsilon_l} \left(\sum_n \frac{P_{kn}}{2} - 1\right) + \frac{\epsilon_l - \epsilon_{I_{l_1}}}{\epsilon_k + \epsilon_l} \left(\sum_m \frac{P_{ml}}{2} - 1\right),$$

$$= \sigma_{a\text{-}b}' + \sigma_{a\text{-}b}'' \quad \text{.....(3-128)}$$

where

$$\sigma_{a\text{-}b}' = \frac{\epsilon - I_{kk}}{\epsilon_k + \epsilon_l} \sum_n \frac{P_{kn}}{2} (S_{ak,bn} - 1) + \frac{\epsilon - I_{l_1}}{\epsilon_k + \epsilon_l} \sum_m \frac{P_{ml}}{2} (S_{am,bl} - 1) \text{.....(3-130)}$$

and

$$\sigma_{a\text{-}b}'' = \frac{\epsilon_k - I_{kk}}{\epsilon_k + \epsilon_l} \left(\sum_n \frac{P_{kn}}{2} - 1\right) + \frac{\epsilon_l - I_{l_1}}{\epsilon_k + \epsilon_l} \left(\sum_m \frac{P_{ml}}{2} - 1\right), \text{.....(3-130)}$$

must be zero when, using equation (3-126), we substitute for the bond orders $\{P_{kn}, P_{ml}, \ldots\ldots\}$- in equation (3-128)- with zero values. This implies that $\sigma_{a\text{-}b}'$ and $\sigma_{a\text{-}b}''$ must both physically vanish when a and b are separated atoms, that is

$$\sigma_{a\text{-}b}' = \frac{\epsilon_k - I_{kk}}{\epsilon_k + \epsilon_l} \sum_n \frac{P_{kn}}{2} (S_{ak,bn} - 1) + \frac{\epsilon_l - I_{l_1}}{\epsilon_k + \epsilon_l} \sum_m \frac{P_{ml}}{2} (S_{am,bl} - 1)$$

= 0 when all $\{P_{kn}, P_{ml}, \ldots\ldots\}$ are zero, a and b separated atoms, i.e. charge distribution in the a-b region zero.

but

$$\sigma_{a\text{-}b}// = \frac{\epsilon_k - I_{kk}}{\epsilon_k + \epsilon_l}\left(\sum_n \frac{P_{kn}}{2} - 1\right) + \frac{\epsilon_l - I_{ll}}{\epsilon_k + \epsilon_l}\left(\sum_m \frac{P_{ml}}{2} - 1\right)$$

$\neq 0$ even when all $\{P_{ka}, P_{al}, \ldots\}$ are zero, a and b separated atoms, i.e. charge distribution in the a-b region zero.

Since the a-b bond function $\sigma_{BOND}^{a\text{-}b}$ must vanish, physically when a and b are separated atoms, the mathematically analytical expression (of $\sigma_{BOND}^{a\text{-}b}$) that satisfies this physical requirement is

$$\sigma_{BOND}^{a\text{-}b} \approx \sigma_{a\text{-}b}/$$

$$= \frac{\epsilon_k - I_{kk}}{\epsilon_k + \epsilon_l} \sum_n \frac{P_{kn}}{2} (S_{ak,bn} - 1) + \frac{\epsilon_l - I_{kk}}{\epsilon_k + \epsilon_l} \sum_m \frac{P_{ml}}{2} (S_{am,bl} - 1), \ldots (3\text{-}131)$$

dropping $\sigma_{a\text{-}b}$" because it is non-zero even when a and b atoms are not bonded.

Similarly, ${}^{\alpha}\sigma_{BOND}^{a\text{-}b}$ and ${}^{\beta}\sigma_{BOND}^{a\text{-}b}$, imposing this physical requirement, reduce to

$$({}^{\alpha}\sigma_{BOND}^{a\text{-}b}) = \frac{\epsilon_k^{\alpha} - I_{kk}}{\epsilon_k^{\alpha} + \epsilon_l^{\alpha}} \sum_n (P_{kn}^{\alpha} + P_{kn}^{\beta})(S_{ak,bn} - 1) + \frac{\epsilon_l^{\alpha} - I_{ll}}{\epsilon_k^{\alpha} + \epsilon_l^{\alpha}} \sum_m (P_{ml}^{\alpha} + P_{ml}^{\beta})(S_{am,bl} - 1)$$

..... (3-132)

and

$$({}^{\beta}\sigma_{BOND}^{a\text{-}b}) = \frac{\epsilon_k^{\beta} - I_{kk}}{\epsilon_k^{\beta} + \epsilon_l^{\beta}} \sum_n (P_{kn}^{\alpha} + P_{kn}^{\beta})(S_{ak,bn} - 1)$$

$$+\frac{\epsilon_1^{\beta}-I_{1_1}}{\epsilon_k^{\beta}+\epsilon_1^{\beta}}\sum_{m}(P_{m1}^{\alpha}+P_{m1}^{\beta})(S_{am,b1}-1).....(3\text{-}133)$$

Therefore, $\sigma_{a\text{-}b}{}^{a\text{-}b}$, ${}^{a}\sigma_{a\text{-}b}{}^{a\text{-}b}$ and ${}^{\beta}\sigma_{a\text{-}b}{}^{a\text{-}b}$ have the physical significance of bond functions since they have non-zero values when atoms a and b are chemically bonded and zero when they are not chemically bonded. They are calculated from these equations by some initial guess of the $\{P_{kk}, P_{m1}\}$'s and $\{P_{kk}{}^{\alpha}, P_{kk}{}^{\beta}; P_{m1}{}^{\alpha}, P_{m1}{}^{\beta}\}$'s after which calculation continues to self-consistency.

These self-consistent field molecular orbital extended Huckel methods and the familiar extended Huckel method (using the Wolfberg-Helmholz approximation) are employed in the study of $H^{\cdot}$, OH^{-} and NH_3 chemisorptions by α-Fe_2O_3 using $FeO_6{}^{n-}$ cluster model (where A^{n} is an adsorbate and n the charge it carries). The calculations are performed in the all valence electron approximation in which all the occupied valence orbitals of $FeO_6{}^{n-}$, $H^{\cdot}$, OH^{-} and NH_3 systems are used. Their basis orbitals are given in the table below:

Table 3.0: The Basis set for $FeO_6{}^{n-}$, $H^{\cdot}$, OH^{-} and NH, Systems

System	Valence Orbitals	IP_k (eV)	Symmetry
$F_eO_6{}^{n-}$	(i) $2t_{2g}$ ($IP_k{}^{\alpha}$)	7.8000	Π
	(ii) $3e_g$ ($IP_k{}^{\alpha}$)	5.9000	σ
OH^{-}	(i) 3σ($IP_k{}^{\alpha}$, $IP_k{}^{\beta}$)	6.9006	σ
	(ii) 1Π ($IP_k{}^{\alpha}$, $IP_k{}^{\beta}$)	2.9050	Π
NH_3	(i) 3a ($IP_k{}^{\alpha}$, $IP_k{}^{\beta}$)	11.6362	σ
	(ii) 1e ($IP_k{}^{\alpha}$, $IP_k{}^{\beta}$)	17.2720	Π
$H^{\cdot}$	Is (EA) ($IP_k{}^{\alpha}$, $IP_k{}^{\beta}$)	13.600	σ

Table 3.1: O2p σ-Nonbonding Orbital of the FeO_6^{9-} System

O2p σ-Nonbonding Orbital	IP(eV)	Symmetry
$6t_{1u}$ (IP_k^{α}, IP_k^{β})	8.4890	σ

Table 3.2. The Basis Set Used for FeO_3^{7-} and OH^- in $FeO_3.OH^{9-}$ System

System	Orbital	IP or EA (eV)	Symmetry
FeO_3^{7-}	$4S(Fe^{3+})(IP_k^{\alpha}, IP_k^{\beta})$	7.9110	σ
OH^-	$3\sigma(IP_k^{\alpha}, IP_k^{\beta}$	6.9006	σ

Table 3.3: The Basis Set Used for FeO_3^{7-} and H^+ in $FeO_3.H^{8-}$

System	Orbital	IP or EA(eV)	Symmetry
FeO_3^{7-}	$3dz^2(Fe^{3+})(IP_k^{\alpha})$	78.1900	σ
H^+	1s (IP_k^{α}, IP_k^{β})	13.6000	σ

Table 3.4: The Orbitals of the Various Irreducible Representations

System	FeO_6^{9-}		OH-		NH_3	
Irred. Representation	$2t_{2g}$	$3e_g$	3σ	1Π	3a	1e
Orbitals	ϕ_{xz} ϕ_{yz} ϕ_{xy}	ϕ_{z^2} $\phi_{x^2-y^2}$	ϕ_z	ϕ_x ϕ_y	ϕ_z	ϕ_x ϕ_y

1s (H^+) is simply ϕ_s and $6t_{1u}$ = $\{\phi_z, \phi_x, \phi_y\}$.

(1) **Form of the Orbitals: FeO_6^{9-} System:**

ϕ_{z^2} = 0.7071 ($3d_{z^2}$) - 0.1667 ψ_{z^2}

$\phi_{x^2-y^2}$ = 0.7071 ($3d_{x^2-y^2}$) - 0.3536 $\psi_{x^2-y^2}$

ϕ_{xz} = 0.7071 ($3d_{xz}$) - 0.3536 ψ_{xz}

ϕ_{yz} = 0.7071 ($3d_{yz}$) - 0.3536 ψ_{yz}

ϕ_{xy} = 0.7071 ($3d_{xy}$) - 0.3536 ψ_{xy}

where ψ_{z^2}, $\psi_{x^2-y^2}$, ψ_{xz}, ψ_{yz} and ψ_{xy} are linear combinations of O - ligands atomic

orbitals transforming as the same irreducible representation with $3d_{z^2}$, $3d_{x^2-y^2}$, $3d_{xz}$, $3d_{yz}$ and $3d_{xy}$ respectively. They are

$$\psi_{z^2} = 2(2p_{z_3} + 2p_{z_6}) - 2p_{z_1} - 2p_{z_2} - 2p_{z_4} - 2p_{z_5}*$$

$$\psi_{x^2-y^2} = 2p_{z_1} - 2p_{z_2} - 2p_{z_4} - 2p_{z_5}$$

$$\psi_{xz} = 2p_{x_3} + 2p_{y_1} + 2p_{x_4} + 2p_{y_6}$$

$$\psi_{yz} = 2p_{x_2} + 2p_{y_3} + 2p_{x_6} + 2p_{y_5}$$

$$\psi_{xy} = 2p_{x_1} + 2p_{y_2} + 2p_{x_5} + 2p_{y_4}$$

* For the numbering, please see figure 3.0.

$$\phi_z = \frac{1}{\sqrt{2}}(2p_{z_3} - 2p_{z_6})$$

$$\phi_y = \frac{1}{\sqrt{2}}(2p_{z_2} - 2p_{z_5})$$

$$\phi_x = \frac{1}{\sqrt{2}}(2p_{z_1} - 2p_{z_4})$$

(2) OH- System

$$\phi_z = -0.0384(1s) - 0.6572(2s) + 0.5229(2p_z) + 0.7179(1s_H)$$

$$\phi_x = 2p_x$$

$$\phi_y = 2p_y$$

(3) **NH_3 System**

$$\phi_z = -0.551(2s) - 0.855(2p_z) + 0.261(3^{-\frac{1}{2}}[h_1+h_2+h_3])^{**}$$

$$\phi_x = 0.633(2p_x) + 0.600(6^{-\frac{1}{2}}[2h_1-h_2-h_3])$$

$$\phi_y = 0.633(2p_y) + 0.600(6^{-\frac{1}{2}}[2h_1-h_2-h_3])$$

(4) **H^+ System**

ϕ_s = 1s

** hi (i=1,2,3) is the 1s orbital of H atom i in NH_3 molecule.

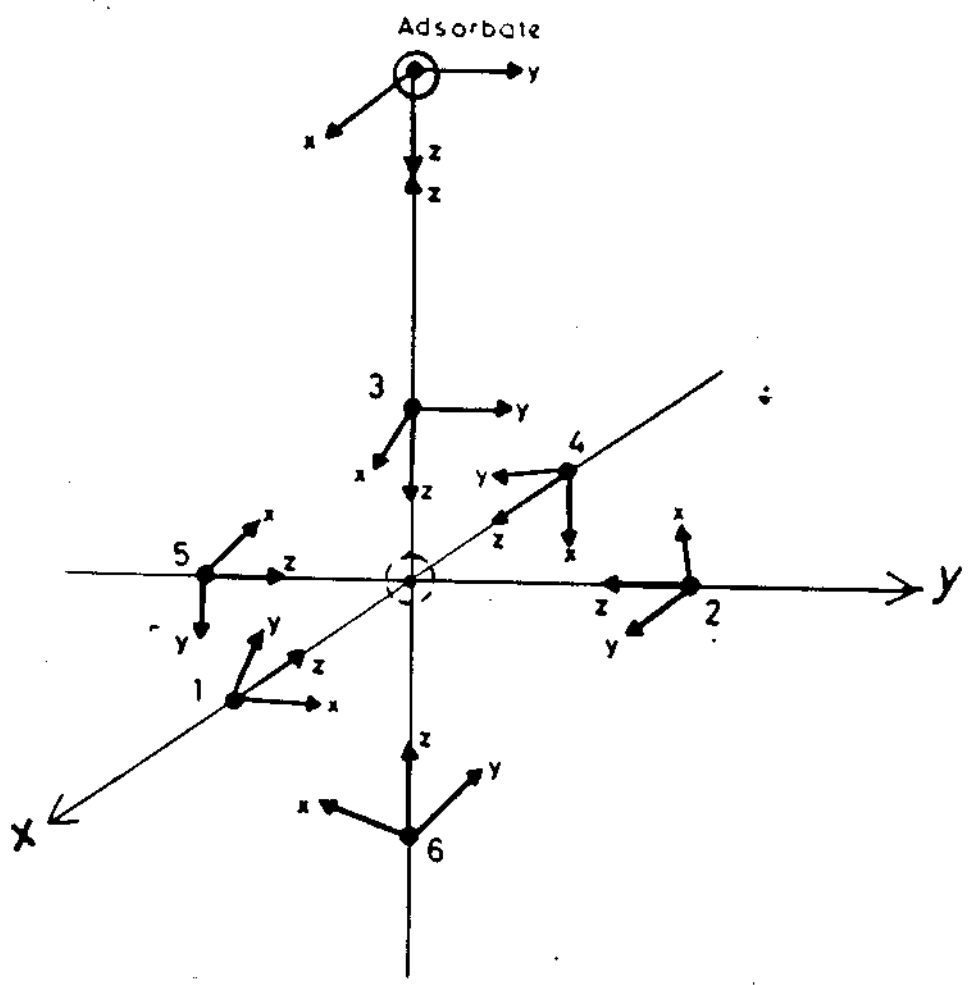
N.B: All atomic orbitals were taken to be normalized Slater Type Orbitals (STO) in the calculations.

The coordinate systems in figure 3.0 are constructed in such a fashion that the following principles are fulfilled:

(1) The numbering of ligands follows Van Vleck [44].

(2) The Z axis is always pointing toward the metal atom.

Hence, all of the σ-bonds are described by using the z coordinate, and the Π-bonds by using the x and y coordinates.



KEY

● = O^{2-} anion

(•) = Fe^{3+} cation

◯ = Adsorbate, A^.

Figure 3·0: The σ- and π- Bonds in FeO_6A^{-9} Cluster

(3) All of the FeO_4^{3-} coordinate system are right handed coordinate systems. Adsorbate coordinate system is left handed. This choice has been made because of the fact that overlap integrals usually are evaluated by using one right- and one left-handed coordinate system.

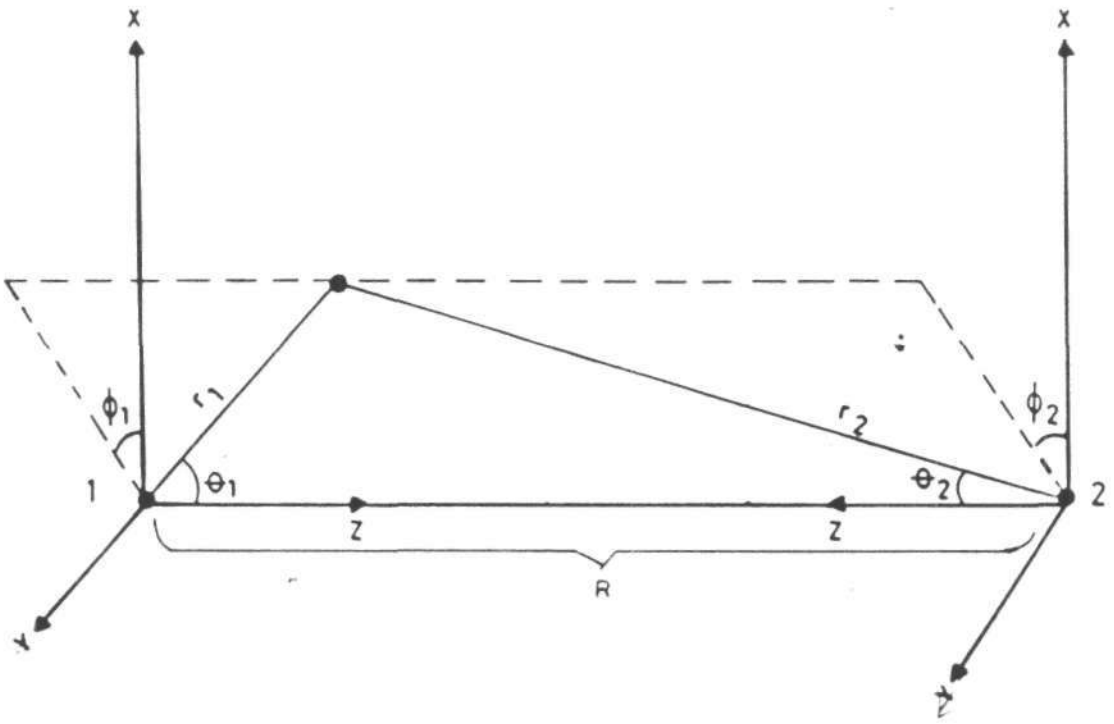


Figure 3.1: Sphenidal Coodinate System

Conditions 1,2 and 3 therefore fix the coordinate systems of the FeO_6A^{n-} cluster.

In table 3.5 we have collected the various possibilities for molecular-orbital formation between the adsorbates under study and the FeO_6^{9-} cluster.

Table 3.5: The Possible Molecular-Orbitals Combinations in FeO_6A^{n-} Cluster Adsorbent - Adsorbate Systems

Symmetry	FeO_6^{9-} Orbitals	H^- Orbital	OH^- Orbitals	NH_3 Orbitals
σ $(3e_g)$	ϕ_z $(\phi_{x^2-y^2})$	ϕ_s	ϕ_z	ϕ_z
$\Pi(2t_{2g})$	ϕ_{xz} ϕ_{yz} (ϕ_{xy})	-	ϕ_x ϕ_y	ϕ_x ϕ_y

By taking linear combinations of the orbitals in table 3.5, the MOs ψ_{k-n} of FeO_6H^{9-}, $FeO_6.OH^{10-}$ and $FeO_6.NH_3^{9-}$ adsorbent - adsorbate systems are:

FeO_6H^{9-}: $1a_{1g} = C_{11}(\phi_{z^2}) + C_{12}(\phi_s)$

$2a_{1g} = C_{21}(\phi_{z^2}) + C_{22}(\phi_s)$

$1b_{1g} = \phi_{x^2-y^2}$

$2t_{2g} = (\phi_{xz}, \phi_{yz}, \phi_{xy})$

FeO_6H^{9-}: (02p σ-Nonbonding with H^-)

$3e_g = (\phi_{z^2}, \phi_{x^2-y^2})$

$2t_{2g} = (\phi_{xz}, \phi_{yz}, \phi_{xy})$

$1a_{1g} = C_{11}(\phi_z) + C_{12}(\phi_s)$

$2a_{1g} = C_{21}(\phi_z) + C_{22}(C\phi_s)$

$4e_g = (\phi_x, \phi_y)$

$FeO_6.OH^{10-}$: $1a_{1g} = C_{11}(\phi_{z^2}) + C_{12}(\phi_s)$

$2a_{1g} = C_{21}(\phi_z) + C_{22}(\phi_s)$

$1b_{1g} = \phi_{x^2-y^2}$

$5e_g = C_{44}(e_d) + C_{45}(e_p)$

$6e_g = C_{54}(e_d) + C_{55}(e_p)$

$1b_{2g} = \phi_{xy}$

where the orbitals e_d and e_p are:

$e_d = (\phi_{xz}, \phi_{yz})$
$e_p = (\phi_x, \phi_y)$ of OH^-

$FeO_6.NH_3^{9-}$: $1a_{1g} = C_{11}(\phi_{z^2}) + C_{12}(\phi_z)$

$2a_{1g} = C_{21}(\phi_{z^2} + C_{22}(\phi_z$

$1b_{1g} = \phi_{x^2-y^2}$

$5e_g = C_{44}(e_d) + C_{45}(e_p)$

$6e_g = C_{54}(e_d) + C_{55}(e_p)$

$1b_{2g} = \phi_{xy}$

where the orbitals e_d and e_p are:

$e_d = (\phi_{xz}, \phi_{yz})$

$e_p = (\phi_x, \phi_y)$ of NH_3

Since the Π-orbitals do not point toward the FeO_6^{9-} cluster along z-axis, they usually give a much weaker bonding than σ-orbitals give. In many cases it is even possible to neglect the Π-bonds and consider only σ-bonds in the bonding scheme (Baullhausen, 1962). If this is done, the Π-orbitals are treated as nonbonding.

Because of the above reasons, we have considered σ- and Π-bonding schemes separately. For example:

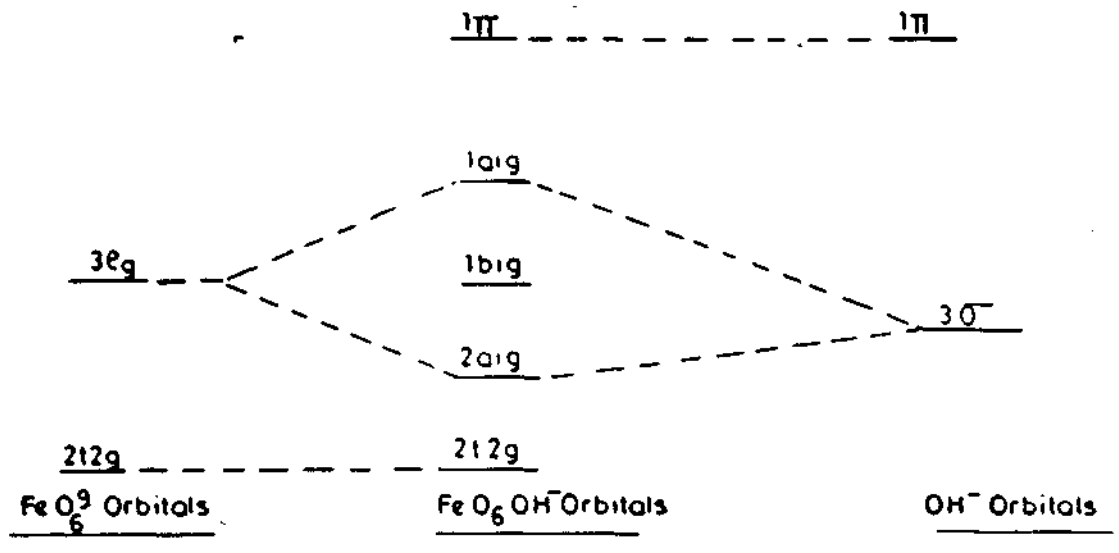


Figure 3·2: Bonding Scheme for the $Fe O_6 OH^{10-}$ Cluster in which only σ-Bonding is Operative

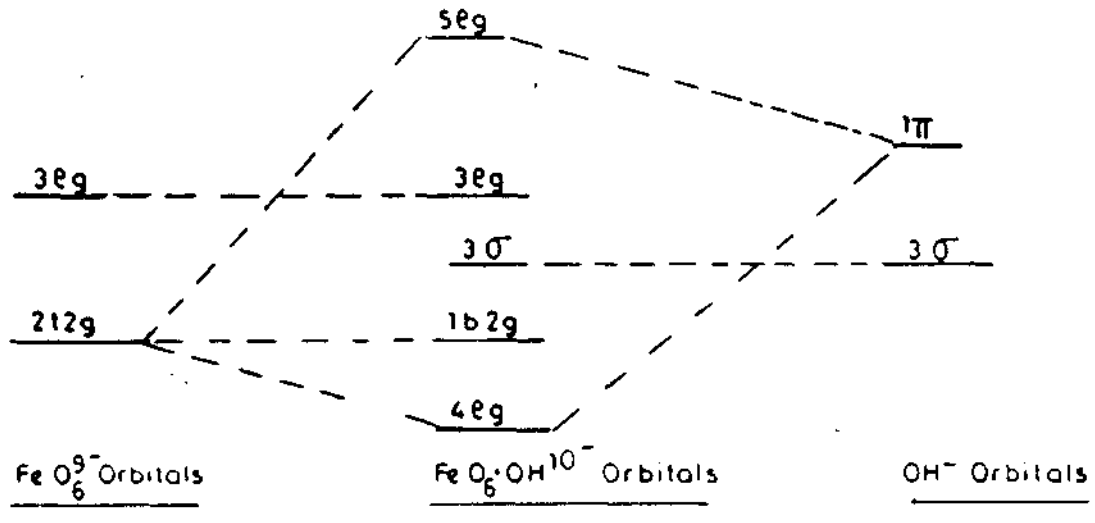


Figure 3·3: Bonding Scheme for the $Fe O_6 OH^{10-}$ Cluster in which only π-Bonding is Operative

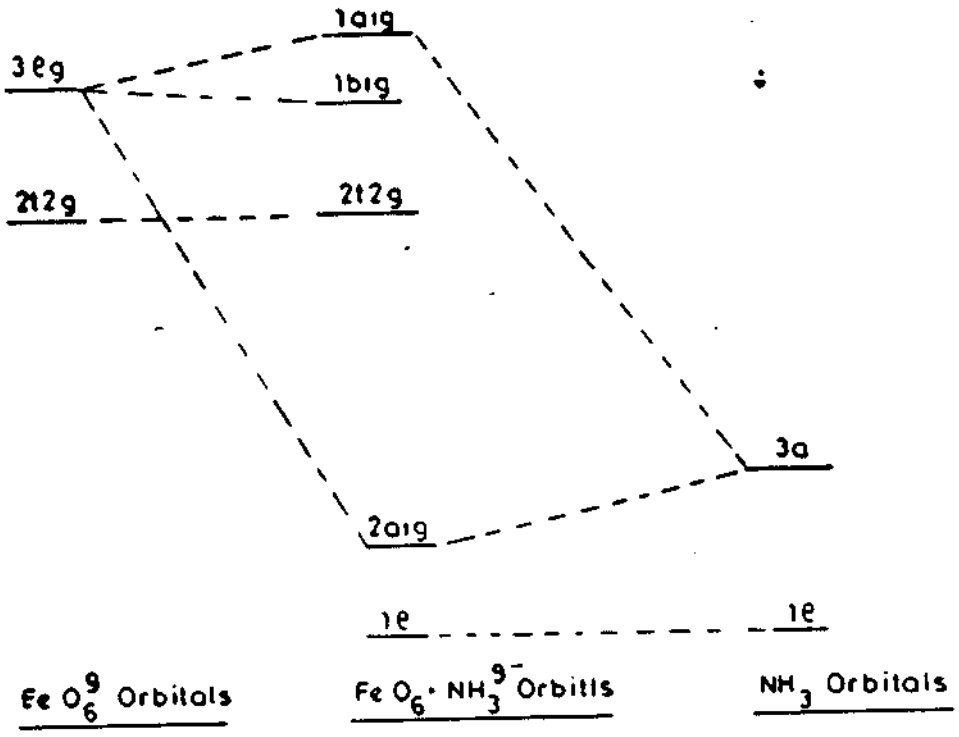


Figure.3.4: Bonding Scheme for the $FeO_6NH_3^{9-}$ Cluster in which only σ-Bonding is Operative

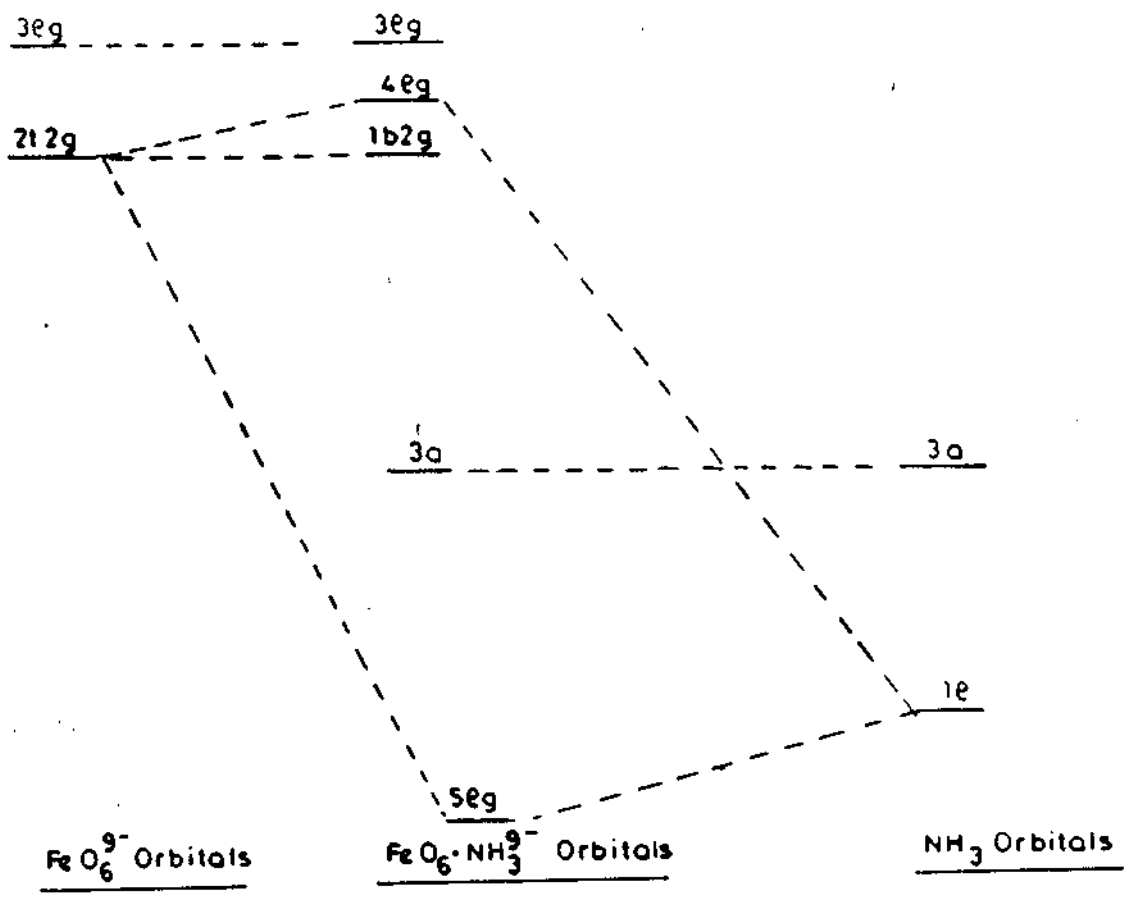


Figure 3.5: Bonding Scheme for the $FeO_6NH_3^{9-}$ Cluster in which only π-Bonding is Operative

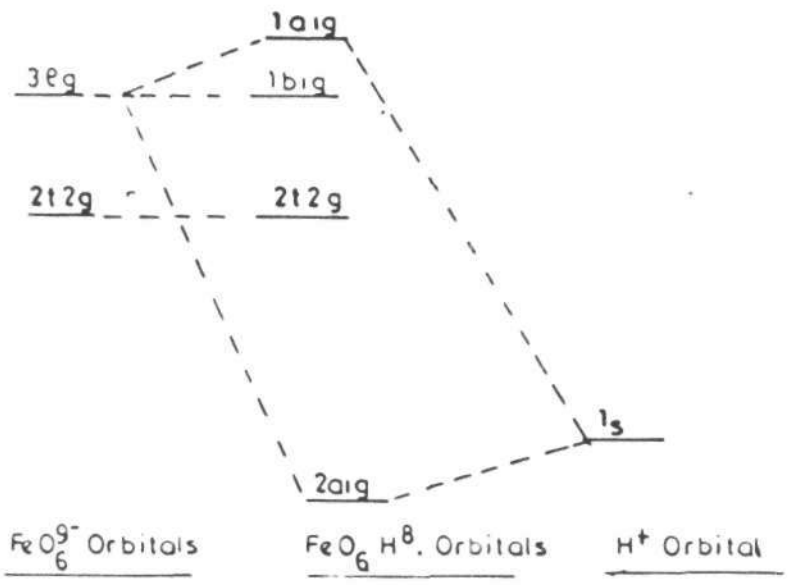


Figure 3·6: Bonding Scheme for the FeO_6H^{8-} Cluster

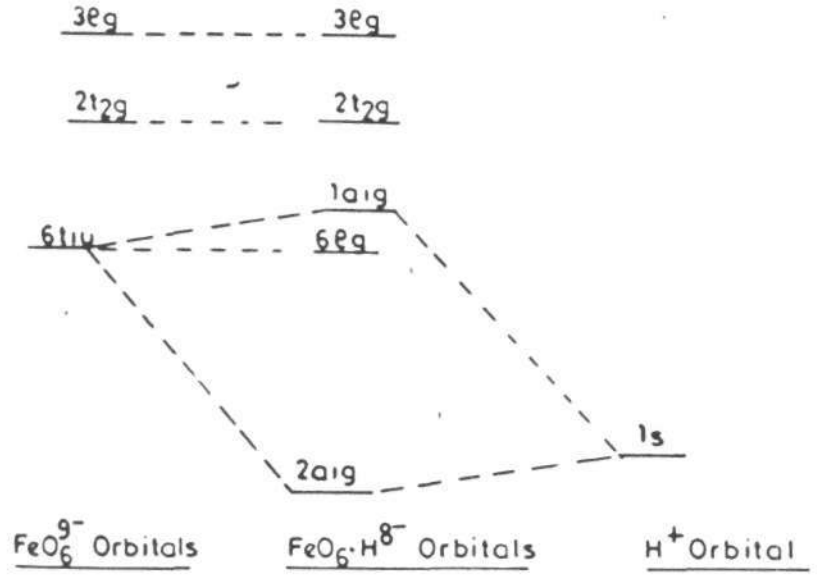


Figure 3·7: Bonding Scheme for the FeO_6H^{8-} Cluster in which only O_{2p} σ-Nonbonding is Operative

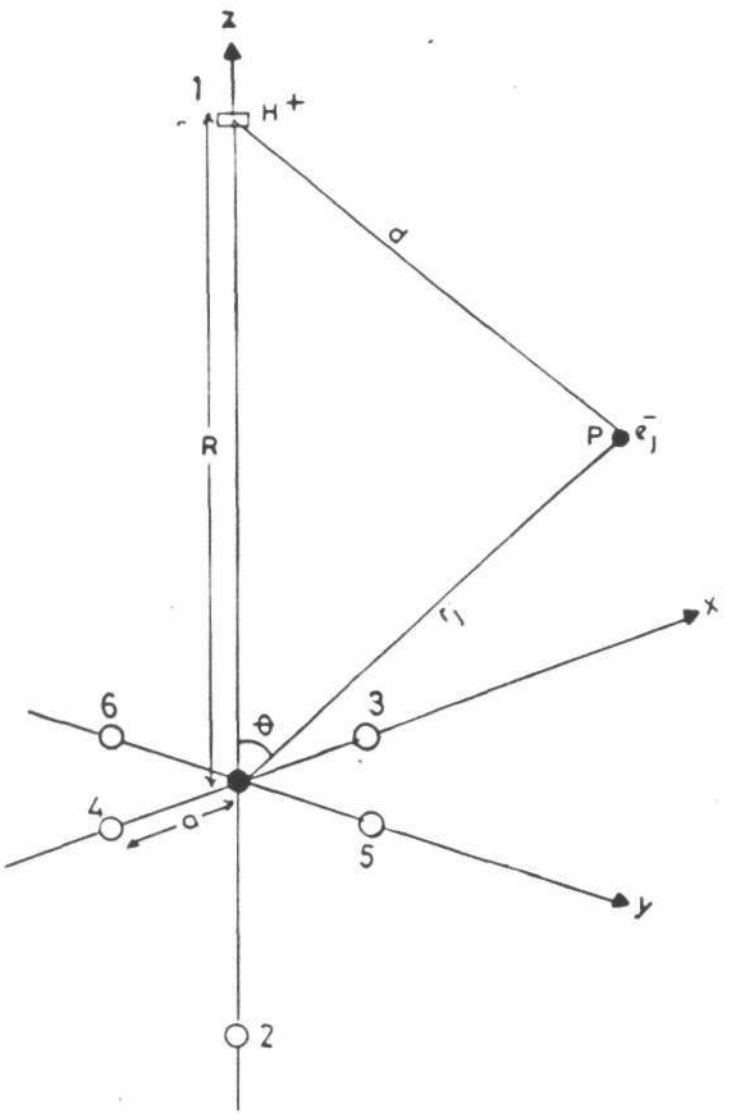
The calculations of the $FeO_4.H^{9-}$, $FeO_4.OH^{10-}$ and $FeO_4.NH_3^{9-}$ molecular-orbital energies is persued by the extended Hückel theory (using the Wolfberg - Helmholz approximation) and the SCF-MO EHT methods.

CHAPTER FOUR

4. RESEARCH METHODS II: QUANTUM ADSORPTION METHODS

4.1.0 PHYSISORPTION OF $H^{\cdot}$ ION BY $FeO_3A^{\cdot\cdot}$ PHYSISORPTIVE INTERACTION MODEL

The physisorption of $H^{\cdot}$ ion on the (111) surface of ferric oxide, as proposed in section 1.6, is simulated by cluster physisorptive interaction model. The (111) surface in the physisorption scheme is represented by $FeO_3^{\cdot\cdot}$ cluster and FeO_3H^{6-} is, therefore, the physisorptive interaction model for the physical adsorption of $H^{\cdot}$ ion. The physisorptive interaction is simulated through a modified crystal field theory. In the crystal field theory formalism, FeO_3H^{6-} is regarded as an ionic molecule. The spatial arrangement of ligands (the five O^{2-} anions plus $H^{\cdot}$ ion) around the central $Fe^{3\cdot\cdot}$ cation is shown in figure 4.1.0 below. Thence the $Fe^{3\cdot\cdot}$ ion is subjected to an electric field originating from the surrounding Five O^{2-} plus $H^{\cdot}$ ions, analogous to what would take place if $Fe^{3\cdot\cdot}$ ion were located in a little cavity inside a crystaline lattice.



KEY

□ = H^+

○ = O^{2-}

● = Fe^{3+} ion

Ligands' Coordinates

Ligand	V	θ	ϕ
1	R	0	0
2	a	π/2	0
3	a	π/2	0
4	a	π/2	π
5	a	π/2	π/2
6	a	π/2	3π/2

Figure 4.1.0 : The Physisorption of H^+ ion by FeO_5H^{6-} Model

Such crystal field would destroy the spherical symmetry of the free ferric ion. The consequences of this situation are dealt with by the crystal field theory. In the crystal field model, the electrons of the Fe^{3+} ion are considered to be subjected to an electric field originating from the surrounding five O^{2-} plus H^{+} ligands. The electrons of the ligands are not allowed to overlap and mix with the electrons of the ferric ion and are supposed to provide a constant electric potential possessing the symmetry of the arrangement of the five O^{2-} plus H^{+} nuclei, in which the electrons of the ferric ion can move.

The quantal treatment for such a model is easily formulated (Baullhausen, 1962). The Hamiltonian for the valence electrons of the ferric ion consists of two terms.

$$H_{3d} = H_{3d}' + \sum_{j=1}^{5} U(r_j) \qquad (4\text{-}1)$$

where

$$H_{3d}' = \sum_{j=1}^{5} \left(-\frac{\nabla_j^2}{2} - \frac{Z^*}{r_j} \right) + \sum_{j} \sum_{<i} 1/r_{ij} \qquad (4\text{-}1a)$$

is the Hamiltonian for the free 3d electrons of the ferric ion and $\Sigma U(r_j)$ is the potential provided by its ligands. It is supposed that the eigenfunctions and eigenvalues of H_{3d}' are known (and indeed are known).

Written out in greater detail, we have for the Hamiltonian:

$$H_{3d} = \sum_{j=1}^{5} \left(-\frac{\nabla_j^2}{2} - \frac{Z^*}{r_j} \right) + \sum_{j} \sum_{<i} 1/r_{ij} + \sum_{j=1}^{5} U(r_j) \ldots\ldots\ldots (4\text{-}2)$$

without spin-orbit terms. With the exception of the term $\Sigma U(r_j)$, the Hamiltonian (4-2) is exactly the Hamiltonian for the valence electrons of the free ferric ion. The solution to this problem is already known (i.e. without $\Sigma U(r_j)$). However, we are going to perturb the eigenvalues of the free ferric ion with $\Sigma U(r_j)$, it is, of course, very important to know how $\Sigma U(r_j)$ compares in order of magnitude with the other perturbing quantity in (4-2), the electronic repulsion term $\Sigma\ 1/r_{ij}$. For strong ligands such as O^{2-} ions,

$$\sum 1/r_{ij} < \sum U(r_j) \ldots\ldots\ldots\ldots\ldots\ldots (4\text{-}3)$$

This is customerily called the strong crystalline field case.

The potential $U(r_j)$, provided by the five O^{2-} plus H^{+} ions to a 3d electron j of the ferric ion situated at some general point P in space, is given by

$$U(r_j) = \sum_{i=2}^{6} \frac{Ze^2}{|a_i - r_j|} - \frac{e^2}{|R - r_j|} \ldots\ldots\ldots (4\text{-}4)$$

where the first term on the right hand side of (4-4) represents the potential energy of electron j due to the five O^{2-} ligands and the last term due to H^{+} adsorbate. Z is the charge on the O^{2-} ligands, and a_i's and R are the vectorial distances of the O^{2-} ligands and H^{+} adsorbate respectively whereas r_j is that of the general point P in

space.

Normally, $U(r_j)$ is expanded in normalized spherical harmonics, thus

$$U(r_j) = \sum_{i=1}^{6}\sum_{k=0}^{\infty}\sum_{m=-k}^{m=k} \frac{4\pi ze^2}{2k+1} R_k(r_j) Y_k^m(\theta_j,\phi_j) Y_k^{m*}(\theta_i,\phi_i)$$

$$- \sum_{k=0}^{\infty}\sum_{m=-k}^{m=k} \frac{4\pi e^2}{2k+1} F_k(r_j) Y_k^m(\theta_j,\phi_j) Y_k^{m*}(\theta_1,\phi_1) \quad \text{.....(4-5)}$$

where

$$R_k(r_j) = r_j^k/a_i^{k-1}, F_k(r_j) = r_j^k/R^{k-1} \quad \text{.....(4-6a)}$$

Since the O^{2-} ligands are simply regarded as point charges, they are viewed classically so that their coordinates (a_i, θ_i, ϕ_i) are also fixed (Gerloch and Slade, 1973) (also see figure 4.1.0 for table of ligands' coordinates). In the case of H^+ ion, while (θ_1, ϕ_1) are fixed - see figure 4.1.0, R varies since the adsorbate is initially in the gas (or liquid) phase. These developments make the following to be constants (Gerloch and Slade, 1973):

$$C_k^m = \sum_{i=2}^{6} \frac{4\pi ze^2}{2k+1} Y_k^{m*}(\theta_i,\phi_i) \text{ for } O^{2-} \text{ligands} \quad \text{.....(4-6b)}$$

and

$$G_k^m = \frac{4\pi e^2}{2k+1} Y_k^{m*}(\theta_1,\phi_1) \text{ for } H^- \text{ adsorbate} \quad \text{.....(4-6c)}$$

Using these definitions, equation (4-5) reduces to

$$U(r_j) = \sum_{k=0}^{\infty} \sum_{m=-k}^{m=k} [C_k^m R_k(r_j) Y_k^m(\theta_j, \phi_j)$$

$$- G_k^m F_k(r_j) Y_k^m(\theta_j, \phi_j)] \ldots\ldots\ldots\ldots\ldots (4-7)$$

It now becomes important to know the disposition of ligands around the ferric ion, because $U(r_j)$ must transform as the totally symmetric representation in the symmetry group of $FeO_6H_6^{3-}$.

4.1.1: $U(r_j)$ in the Symmetry Group of FeO_5H^{6-} System

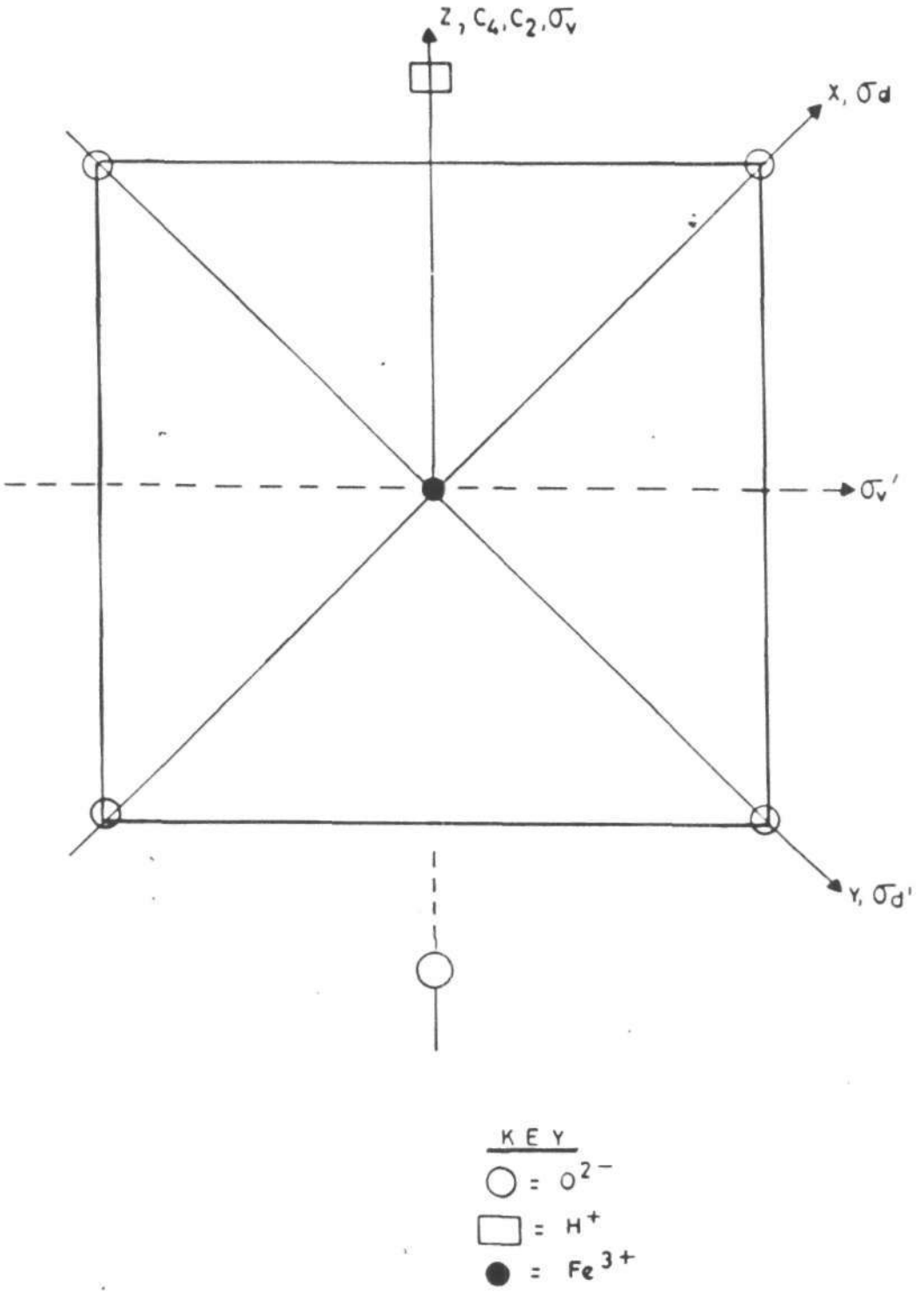


Figure 4.1.1: The Symmetry Elements of $Fe\,O_5\,H^{6-}$ System

The only symmetry elements that bring the FeO_5H^{4-} system into itself are the, E, C_2, $2C_4$, $2\sigma_v$, $2\sigma_d$, symmetry operators and belongs to the C_{4v} point group. The symmetry requirement that $U(r_j)$ must satisfy is that, for the Hamiltonian (4-2) to remain totally symmetric, it should remain invariant under all the symmetry operations of the C_{4v} point group. Since reflection or rotation carry the spherical polar coordinates through some angle, the requirement now becomes that the spherical harmonic in (4-7) must not change sign when $U(r_j)$ is acted upon by a rotation or reflection operator (of the C_{4v} point group), viz

$$\hat{P}\, Y_k^m(\theta_j,\phi_j) = Y_k^m(\theta_j,\phi_j) \qquad (4\text{-}8)$$

where P in equation (4-8) is a symmetry operator. The symmetry requirement expressed by (4-8) holds only for

$k = 0, 2, 4, 6, 8, \ldots\ldots\ldots$

and

$m = 0, \pm 4, \pm 8, \pm 12, \ldots\ldots\ldots$

Using the result of (4-8) $U(r_j)$ reduces to, ignoring terms higher than $k = 4$ and $m = \pm 4$.

$$U(r_j) = C_0^0 R_0(r_j) Y_0^0(\theta_j,\phi_j) + C_2^0 R_2(r_j) Y_2^0(\theta_j,\phi_j)$$

$$+ C_4^{-4} R_4(r_j) Y_4^{-4}(\theta_j,\phi_j) + C_4^0 R_4(r_j) Y_4^0(\theta_j,\phi_j)$$

$$+ C_4^4 R_4(r_j) Y_4^4(\theta_j,\phi_j)$$

$$- G_o^o F_o(r_j) Y_o^o(\theta_j,\phi_j - G_2^o F_2(r_j) Y_2^o(\theta_j,\phi_j)$$

$$- G_4^{-4} F_4(r_j) Y_4^{-4}(\theta_j,\phi_j) - G_4^o F_4(r_j) Y_4^o(\theta_j,\phi_j)$$

$$- G_4^4 F_4(r_j) Y_4^4(\theta_j,\phi_j) \ldots\ldots\ldots\ldots\ldots\ldots\ldots\ldots (4\text{-}9).$$

We can now make the following definitions (since we have the final form of $U(r_j)$)

$$U_{0^2\cdot}(r_j) = C_o^o R_o(r_j) Y_o^o(\theta_j,\phi_j) + C_2^o R_2(r_j) Y_2^o(\theta_j,\phi_j) + C_4^{-4} R_4(r_j)$$

$$x\ Y_4^{-4}(\theta_j,\phi_j) + C_4^o R_4(r_j) Y_4^o(\theta_j,\phi_j) - C_4^4 R_4(r_j) Y_4^4(\theta_j,\phi_j) \ldots (4\text{-}10)$$

and

$$U_{H^+}(r_j) = - G_o^o F_o(r_j) Y_o^o(\theta_j,\phi_j) - G_2^o F_2(r_j) Y_2^o(\theta_j,\phi_j) - G_4^{-4}$$

$$x\ F_4(r_j) Y_4^{-4}(\theta_j,\phi_j) - G_4^o F_4(r_j) Y_4^o(\theta_j,\phi_j) - G_4^4 F_4(r_j) Y_4^4(\theta_j,\phi_j) \ldots (4\text{-}11)$$

From the definitions of (4-10) and (4-11), the potential $U(r_j)$ may be written as

$$U(r_j) = U_{0^2\cdot}(r_j) + U_{H^+}(r_j) \ldots\ldots\ldots\ldots\ldots\ldots (4\text{-}12)$$

Having found the potential energy acting on the 3d-electrons of the ferric ion, the complete Hamiltonian (4-2) can be written, via (4-12), as

$$H_{3d} = \sum_{j=1}^{5} \left(-\frac{\nabla_j^2}{2} - \frac{Z^*}{r_j}\right) + \sum_{j}\sum_{<i} 1/r_{ij} + \sum_{j=1}^{5} U_{O^{2-}}(r_j) + \sum_{j=1}^{5} U_{H^+}(r_j) \quad \ldots\ldots(4\text{-}13)$$

Since the distance between the oxygen ligands to the ferric ion is fixed, the matrix element of the potential due to the oxygens is a constant. On the other hand, the potential energy due to H^+ adsorbate is not constant because it varies with R-its distance of approach to the surface from infinity.

Thus we can rewrite the Hamiltonian (4-13) into

$$H' = \sum_{j=1}^{5} \left(-\frac{\nabla_j^2}{2} - \frac{Z^*}{r_j}\right) + \sum_{j}\sum_{<i} 1/r_{ji} + \sum_{j=1}^{5} U_{O^{2-}}(r_j) \quad \ldots\ldots\ldots\ldots\ldots(4\text{-}13a)$$

whose matrix element is a constant, and

$$U_{H^+}(r) = \sum_{j=1}^{5} U_{H^+}(r_j) \quad \ldots\ldots\ldots\ldots\ldots\ldots(4\text{-}13b)$$

whose matrix element varies with R. (through the $F_k(r_j)$ functions of equation (4-6a)]. Thus

$$H_{3d} = H' + U_{H^+}(r) \quad \ldots\ldots\ldots\ldots\ldots\ldots\ldots\ldots(4\text{-}14)$$

$U_{H^+}(r)$ is regarded as perturbaton caused by the approach of H^+ adsorbate to the surface of α-Fe_2O_3. When the $U_{H^+}(r)$ perturbation is calculated, it should yield a potential energy curve for the physisorption of H^+ ion by ferric oxide surface, giving binding energy and equilibrium surface - H^+ ion distance.

4.1.2. The Physisorption Energy of H^+ ion by FeO_5H^{4-} Model

As we saw in the last section, all that we need to do, in order to find the physisorption energy of H^+ ion on ferric oxide surface, is to calculate the perturbation $U_{H^+}(r)$ for the ground state of the FeO_5H^{4-} system. To do that, we need to know the ground electronic state and the corresponding wavefunction.

In order to get the ground electronic state and the corresponding wavefunction, we should have to first find the ground state electronic configuration of the ferric ion in the strong field of the C_{4v} point group. The 3d orbitals of the free ferric ion are five fold degerate and the orbitals are

$$\psi_{3,2,m} = f_{3,2}(r)P_2^m(\cos\theta)\frac{e^{im\phi}}{\sqrt{2\pi}} \qquad \text{.....(4-15)}$$

with $\mid m \mid \leq 2$.

We take these five orthogonal functions as our basis set ψ_1.....ψ_5 and investigate how they transform under the operations of the point group C_{4v}. The most general rotation is that around an arbitrary axis through the angle Φ. The simplest way of investigating how the five 3d orbitals behave is by always quantizing ψ_1.....ψ_5 with respect to the axis about which we rotate. If this is the case, our rotation will carry ϕ over in $\phi + \Phi$ and take

$$\psi_{3,2,m} = f_{3,2}(r)P_2^m(\cos\theta)\frac{e^{im\phi}}{\sqrt{2\pi}}$$

over into

$$f_{3,2}(r)P_2^m(\cos\theta)e^{im(\phi+\Phi)}$$

The rotation is thus given by the matrix

$$\begin{bmatrix} e^{il\Phi} & 0 & 0 \\ 0 & e^{i(l-1)\Phi} & \cdots\cdots \\ \cdots\cdots & \cdots\cdots & \cdots\cdots \\ 0 & \cdots\cdots & e^{-il\Phi} \end{bmatrix}$$

that is, the character of the rotation $X(\Phi)$ is given by

$$X(\Phi) = e^{il\Phi} + e^{i(l-1)\Phi} + \cdots\cdots + e^{-il\Phi} \cdots\cdots (4\text{-}17)$$

$$= e^{-il\Phi}\sum_{n=0}^{2l}(e^{i\Phi})^n$$

$$= \frac{Sin(l+\frac{1}{2})\Phi}{Sin(\Phi/2} \cdots\cdots\cdots\cdots (4\text{-}18)$$

The character of the identity operator E is given by the l Hospital rule

$$X(E) = \frac{(l+\frac{1}{2})Cos(l+\frac{1}{2})O}{\frac{1}{2}Cos(\frac{1}{2}O)}$$

$$= 2l+1 \cdots\cdots\cdots\cdots\cdots (4\text{-}19)$$

For the 3d orbitals, l=2 so that

$$X(E) = 2x2+1$$

$$= 5$$

Also for $\Phi = \Pi$ $\quad X(C_2) = X(\sigma_v)$

$$= X(\sigma_d)$$

$$= \mathrm{Sin}(2+\tfrac{1}{2})\Pi/\mathrm{Sin}(\Pi/2)$$

$$= 1.$$

$$\Phi = \pi/2,\ X\ (C_4) = \frac{Sin(2+\frac{1}{2})\pi/2}{Sin(\pi/4)} = -1$$

The character of the representations spanned by the five 3d orbitals in the point group C_{4v} are then

E	C_2	$2C_4$	$2\sigma_v$	$2\sigma_d$
5	1	-1	1	1

Using the reduction formula for working out the number of times an ineducible representation occurs in a given reducible representation

$$n^i = \frac{1}{h} \sum_p X_{p^i} \cdot X_p \ldots\ldots\ldots\ldots\ldots\ldots (4\text{-}20)$$

where h is the order of the group (i.e. the number of symmetry operators in the point group), X_{p^i} the character of the irreducible representation and X_p as the character of the reducible representation, the five fold degenerate 3d orbitals of the ferric ion are found to split into e, b_2, b_1 and a_1 levels.

Now, Fe^{3+} has been experimentally detected (Baullhausen, 1962) to have a high spin electronic configuration of $(t_{2g})^3(e_g)^2$ in the

perfect octahedral complex FeO_6^{9-} and a low spin electronic configuration $(e_g)^4(b_2)^1$ when the FeO_6^{9-} complex is tetragonally distorted. Thus the descent in symmetry from cubic (O_h) -------> tetragonal (C_{4v} or D_{4v}) lead to low spin configuration of Fe^{3+} in the FeO_6^{9-} system. Since FeO_5H^{6-} is also a complex with a tetragonal symmetry (C_{4v}), we assume the tetragonal distortion on the Fe^{3+} ion to produce a low spin electronic configuration $(e)^4(b_2)^1$ based on the experimental evidence above. We therefore take $(e)^4(b_2)^1$ to be the ground state configuration of Fe^{3+} ion in the FeO_5H^{6-} system.

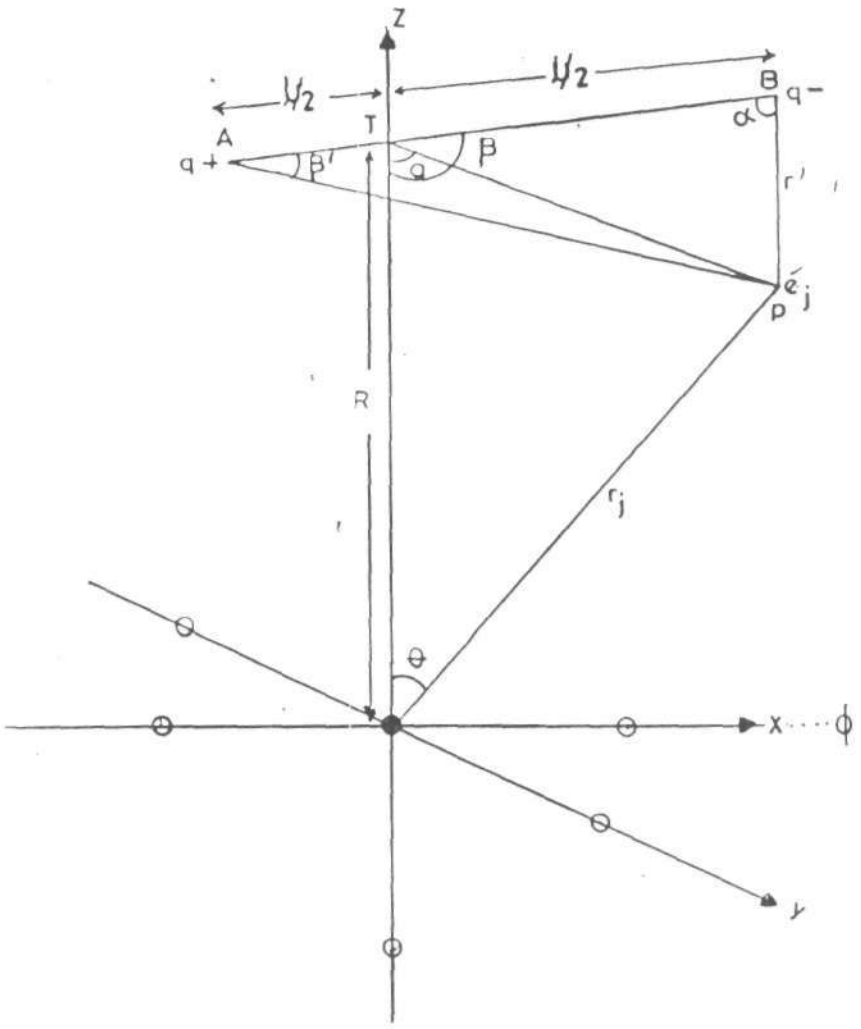
Since $(e)^4(b_2)^1$ configuration has only one unpaired electron, we obtained ^2E, $^2B_2$, $^2B_1$ and $^2A_1$ terms for the configuration in C_{4v} field. Using Hund's rule for electronic states, the ground electronic state of the ferric ion in the C_{4v} point group is ^2E. The wavefunction corresponding to the ^2E ground state term, $\psi(^2E)$ doubly degenerate, is the {3dxz, 3dyz} set.

Therefore the physisorption energy of the H^+ ion, which is regarded as a perturbation to the ground electronic state of the FeO_6H^{6-} system, is given by

$$\Delta H = \langle \psi(^2E) | U_{H^+}(r) | \psi(^2E) \rangle \text{.....(4-21)}$$

4.2.0 The Physisorption of NH_3 and OH^- by FeO_5A^{n-7} Physisorptive Interaction Model

The physisorption of OH^- ion and NH_3 molecule on α-Fe_2O_3 (111) surface is also simulated by the FeO_5 A^{n-9} model, where A is OH^- or NH_3 adsorbate. Unlike H^+, which was taken as a simple point charge



Dipole Coordinates		
r	θ	ϕ
R	0	÷0

A = dipole

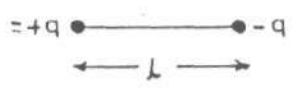


Figure 4.2.0: The Physisoption of a Dipole by FeO_5A^{n-7} Model

in section 4.1, OH^- and NH_3 adsorbates are dipoles (1.66 D and 1.47 D respectively), and the valence electrons of the ferric ion are considered to be subjected to an electric field originating from the five O_{2-} plus OH^- (or NH_3) dipole ligands: The physisorptive interaction is schematically shown in figure 4.2.0.

The dipole is assumed to interact with the valence electrons of the ferric ion along the z-axis, which passes through the midpoint of its charge separation, of some coordinates centred on the central ion with β as its oreintation with respect to the Z-axis. From (4-13), the Hamiltonian for the 3d-electrons is given by

$$H_{3d} = \sum_{j=1}^{5} \left(-\frac{\nabla_j^2}{2} - \frac{Z^*}{r_j}\right) + \sum_{j}\sum_{<j} 1/r_{ij} + \sum_{j=1}^{5} U_{o^{2-}}(r_j)$$

$$+ \sum_{j=1}^{5} U_{\mu}(r_j) \qquad \text{.....(4-22)}$$

Using the argument and definition of (4-12a), (4-22) becomes

$$H_{3d} = H' + U_{\mu}(r) \qquad \text{.....(4-23)}$$

where

$$U_{\mu}(r) = \sum_{j=1}^{5} U_{\mu}(r_j) \qquad \text{.....(4-23a)}$$

The potential $U_{\mu}(r_j)$, provided by the dipole to a 3d-electron j of the ferric ion situated at some general P in space (see figure

4.2.0), is given by

$$U_\mu(r_j) = eq\left\{\frac{1}{r'} - \frac{1}{AP}\right\} \quad \ldots\ldots\ldots\ldots\ldots (4\text{-}24)$$

From ΔBTP and ΔABP using sine rule

$$\frac{1}{r'} = \frac{Sin\alpha}{TP\ Sin(\beta\text{-}a)} \quad also \quad \frac{1}{AP} = \frac{Sin\beta'}{TP\ Sin(\beta\text{-}a)} \quad \ldots\ldots\ldots\ldots\ldots (4\text{-}25)$$

So that (4-24) becomes

$$U_\mu(r_j) = eq\left\{\frac{Sin\alpha}{TP\ Sin(\beta\text{-}a)} - \frac{Sin\ \beta'}{TP\ Sin(\beta\text{-}a)}\right\}$$

$$= \frac{eq}{TP\ Sin(\beta\text{-}a)}\ (Sin\alpha - Sin\beta') \quad \ldots\ldots\ldots\ldots\ldots\ldots (4\text{-}26)$$

From ΔBTP,

$$\frac{TP}{Sin\alpha} = \frac{1/2}{Sin(180\text{-}\alpha\text{-}\beta\text{+}a)} \quad \ldots\ldots\ldots (4\text{-}27)$$

rearranging we obtain

$$Sin\ \alpha = \frac{TP\ Sin\ (180\text{-}\alpha\text{-}\beta\text{+}a)}{1/2}$$

$$= \frac{TP\ Sin\ (\alpha\text{+}\beta\text{-}a)}{1/2}$$

$$= \frac{TP[Sin\alpha Cos(\beta\text{-}a) + Cos\alpha Sin(\beta\text{-}a)]}{1/2} \quad \ldots\ldots\ldots (4\text{-}28)$$

Rearranging (4-28), taking out Sin α in the left hand side

$$[1/2 - TP\ Cos(\beta\text{-}a)]\ Sin\alpha = TP\ Sin(\beta\text{-}a)\ Cos\alpha$$

which gives

$$\frac{Sin\alpha}{Cos\alpha} = \frac{Sin\alpha}{(1-Sin^2\alpha)^{\frac{1}{2}}}$$

$$= \frac{TPSin(\beta-a)}{[1/2-TP\ Cos(\beta-a)]} \quad \ldots\ldots\ldots\ldots\ldots\ldots (4\text{-}29)$$

Squaring both sides of (4-29) gives

$$\frac{Sin^2\alpha}{1 - Sin^2\alpha} = \frac{TP^2\ Sin^2(\beta-a)}{[1/2 - TPCos(\beta-a)]^2} \quad \ldots\ldots\ldots (4\text{-}30)$$

Rearranging also gives

$$\{ \frac{[1/2-TPcos(\beta-a)]^2 + TP^2sin^2(\beta-a)}{[1/2-TPcos(\beta-a)]} \} sin^2\alpha$$

$$= \frac{TP^2\ Sin^2(\beta-a)}{[1/2 - TP\ Cos(\beta-a)]^2} \quad \ldots\ldots\ldots (4\text{-}31)$$

which, making Sin α subject of the formula, gives

$$Sin\alpha = \frac{[TP^2\ Sin^2(\beta-a)]^{\frac{1}{2}}}{[TP^2\ Sin^2(\beta-a) + (1/2 - TPCos(\beta-a))^2]^{\frac{1}{2}}} \quad \ldots\ldots\ldots\ldots (4\text{-}32)$$

Similarly, from ΔATP

$$\frac{AP}{Sin(180-\beta+a)} = \frac{TP}{Sin\ \beta'} = \frac{1/2}{Sin(\beta-\beta'-a)} \quad \ldots\ldots\ldots\ldots\ldots (4\text{-}33)$$

Equation (4-33) gives, for Sin β', the following expression

$$Sin\beta' = \frac{TP\ Sin(\beta-\beta'-a)}{1/2} \quad \ldots\ldots\ldots\ldots\ldots (4\text{-}34)$$

$$= \frac{TP[-Sin\beta'\ Cos(\beta-a) + Cos\beta'\ Sin\ (\beta-a)]}{1/2} \quad \ldots\ldots\ldots (4\text{-}35)$$

which, on rearrangement, gives

$$[1/2 + TP\ Cos\ (\beta-a)]\ Sin\ \beta' = TP\ Sin(\beta-a)Cos\ \beta'$$

that further yields

$$\frac{Sin\ \beta'}{Cos\ \beta'} = \frac{Sin\ \beta'}{(1 - Sin^2\beta')^{\frac{1}{2}}}$$

$$= \frac{TP\ Sin(\beta-a)}{[1/2 + TP\ Cos(\beta-a)]} \quad \ldots\ldots\ldots (4\text{-}36)$$

Equation (4-35) is equivalent to (4-29), and following the same procedure, from (4-30) to (4-32), we obtained

$$Sin\ \beta' = \frac{[TP^2\ Sin^2(\beta-a)]^{\frac{1}{2}}}{[TP^2\ Sin^2(\beta-a) + (1/2 + TP\ Cos(\beta-a))^2]^{\frac{1}{2}}} \quad \ldots\ldots\ldots (4\text{-}37)$$

Now, using the values of Sin α and Sin β' from (4-32) and (4-37), the equation for the dipole potential (4-26) becomes

$$U_{\mu}(r_j) = \frac{eq\,[TP^2\,Sin^2(\beta-a)]^{\frac{1}{2}}}{TP\,Sin(\beta-a)}\{\frac{1}{[TP^2\sin^2(\beta-a)+(1/2-TP\cos(\beta-a))^2]^{\frac{1}{2}}}$$

$$-\frac{1}{TP^2\,Sin^2(\beta-a)+(1/2+TP\,Cos(\beta-a))^2]^{\frac{1}{2}}}\}....(4\text{-}38)$$

Let's expand $(1/2 - TPCos\ (\beta-a))^2$ and $(1/2 + TP\ Cos\ (\beta-a))^2$:

$$(1/2 - TP\,Cos(\beta-a))^2 = \frac{1^2}{4} - 1TP\,Cos\,\beta-a) + TP^2\,Cos^2(\beta-a)$$

$$= TP^2\{\frac{1^2}{4TP^2} - \frac{1\,Cos\,(\beta-a)}{TP}\} + TP^2\,Cos^2(\beta-a)$$

$$= TP^2K_1 + TP^2\,Cos^2(\beta-a).....(4\text{-}39)$$

where K_1 is defined as

$$K_1 = \frac{1^2}{4TP^2} - \frac{1\,Cos(\beta-a}{TP}.....(4\text{-}40)$$

Similarly,

$$(1/2 + TP\,Cos\ (\beta-a))^2 = \frac{1^2}{4} + 1TP\,Cos(\beta-a) + TP^2\,Cos^2(\beta-a)$$

$$= TP^2K_2 + TP^2\cos^2(\beta-a).....(4\text{-}41)$$

where K_2 is also given by

$$K_2 = \frac{l^2}{4TP^2} + \frac{l\,Cos(\beta-a)}{TP} \quad \ldots\ldots\ldots\ldots\ldots\ldots (4-42)$$

Using (4-39) and (4-41), the denominators of (4-38) become

$$[TP^2\,Sin^2(\beta-a) + TP^2K_1 + TP^2\,Cos^2(\beta-a)]^{\frac{1}{2}}$$

$$= TP[Sin^2(\beta-a) + Cos^2(\beta-a) + K_1]^{\frac{1}{2}}$$

$$= TP(1+K_1)^{\frac{1}{2}} \quad \ldots\ldots\ldots\ldots\ldots\ldots\ldots\ldots (4-43)$$

and

$$(TP^2\,Sin^2(\beta-a) + TP^2K_2 + TP^2Cos^2(\beta-a)]^{\frac{1}{2}}$$

$$= TP[Sin^2(\beta-a) + Cos^2(\beta-a) + K_2]^{\frac{1}{2}}$$

$$= TP(1 + K_2)^{\frac{1}{2}} \quad \ldots\ldots\ldots\ldots (4-44)$$

With the results of (4-43) and (4-44), (4-38) simplifies to

$$U_\mu\,(r_j) = \frac{eq\,[TP^2\,Sin^2(\beta-a)]^{\frac{1}{2}}}{TP\,Sin\,(\beta-a)} \left\{ \frac{1}{TP(1+K_1)^{\frac{1}{2}}} \right.$$

$$\left. - \frac{1}{TP(1+K_2)^{\frac{1}{2}}} \right\}$$

$$= \frac{\pm eq}{TP}\left\{\frac{1}{(1+K_1)^{\frac{1}{2}}} - \frac{1}{(1+K_2)^{\frac{1}{2}}}\right\}, \ldots\ldots\ldots (4\text{-}45)$$

taking the root.

Expanding equation (4-45), we obtain

$$U_\mu(r_j) = \frac{\pm\, eq}{TP}\{\, 1 + (-\tfrac{1}{2})K_1 + (-\tfrac{1}{2})(\tfrac{-3}{2})K_1^2/2! + \ldots\ldots\ldots$$

$$-1 - (-\tfrac{1}{2})K_2 - (-\tfrac{1}{2})(-\tfrac{3}{2})K_2^2/2! + \ldots\ldots\ldots\}$$

$$= \frac{\pm\, eq}{TP}\left\{\frac{1}{2}(K_2 - K_1) + \frac{3}{8}(K_1^2 - K_2^2) + \textit{higher terms}\right\}\ldots\ldots (4\text{-}46)$$

Using the values of K_1 and K_2 from (4-40) and (4-42), we get

$$U_\mu\,(r_j) = \frac{\pm\, e}{TP^2}\,\{\mu\, Cos(\beta - a) + \textit{multipole terms}\}\ldots\ldots\ldots\ldots (4\text{-}47)$$

where μ is the magnitude of the electric dipole moment, defined as

$$\mu = ql\ldots\ldots\ldots\ldots\ldots\ldots (4\text{-}48a)$$

In dipole approximation, multipole terms are neglected. The justification for this is that their contribution to (4-47) is very much small since multipole interactions are very weaker interactions. This reduces (4-47) to

$$U_\mu(r_j) = \frac{\pm\, \mu\, e\, Cos\,(\beta - a)}{TP^2}\ldots\ldots\ldots\ldots (4\text{-}48b)$$

Now,

$$Cos(\beta - a) = Cos\,\beta\, Cos\, a + Sin\,\beta\, Sin\, a\ldots\ldots\ldots\ldots (4\text{-}49)$$

and from Δ ROP

$$\frac{r_j}{Sin\ a} = \frac{TP}{Sin\ \theta_j} \qquad \text{.....(4-50)}$$

giving

$$Sin\ a = \frac{r_j\ Sin\ \theta_j}{TP} \qquad \text{.....(4-51)}$$

Also,

$$Cos\ a = (1-Sin^2\ a)^{\frac{1}{2}}$$

$$= (1 - r_j^2\ Sin^2\theta_j/TP^2)^{\frac{1}{2}} \qquad \text{.....(4-52)}$$

$$= 1 - \frac{r_j^2\ Sin^2\theta_j}{2TP^2} - \frac{1}{8}\ \frac{r_j^4 Sin^4\theta}{TP^4} + higher\ terms \qquad \text{.....(4-53)}$$

Using (4-51) and (3-53), equation (4-49) becomes

$$Cos(\beta-a) = Cos\beta\ \{1 - \frac{r_j^2 Sin^2\theta_j}{TP^2} + \frac{3}{8}\ \frac{r_j^4 Sin^4\theta_j}{TP^4} + higher\ terms\}$$

$$+ Sin\ \beta(r_j\ \sin\theta_j/TP) \qquad \text{.....(4-54)}$$

If the ratio r_j Sin θ_j/TP is very small compared to unity, then

$$1> > r_j^2\ Sin^2\theta_j/2TP^2$$

So that (4-54) reduces to

$$Cos(\beta-a) \simeq Cos\ \beta - Sin\ \beta(r_j \sin\theta_j/TP) \quad \text{.....(4-55)}$$

From (4-48) and (4-55), the dipole potential $U_\mu(r_j)$ becomes

$$U_\mu(r_j) = \pm \left(\frac{\mu\ e\ Cos\ \beta}{TP^2} + \frac{\mu\ e\ \sin\beta(r_j \sin\theta_j)}{TP^3}\right) \quad \text{.....(4-56)}$$

Since μ is defined as the "magnitude" of the electric dipole moment, then the correct equation that predicts the dipole - surface interaction is the -ve root (of equation (4-56). Thus

$$U_\mu\ (r_j) = -\frac{\mu\ Cos\ \beta}{TP^2} - \frac{\mu\ \sin\beta\ (r_j \sin\theta_j}{TP^3} \quad \text{.....(4-57)}$$

From ΔTOP (using cosine rule)

$$TP^2 = R^2 + r_j^2 - 2Rr_j \cos\theta_j \quad \text{.....(4-58)}$$

which gives

$$\frac{1}{TP} = \frac{1}{R}\ \left(1 + \left(\frac{r_j}{R}\right) - 2\left(\frac{r_j}{R} \cos\theta_j\right)^{\frac{1}{2}}\right) \quad \text{.....(4-59)}$$

Expanding (4-59) in Legendre functions, we have

$$\frac{1}{TP} = \sum_{k=0}^{\infty} \frac{r_j^k}{R^{k+1}} P_k(\cos\theta_j) \quad \text{.....(4-60)}$$

Equation (4-60) can also be expanded in terms of spherical harmonics (Gerloch and Slade,1973) in the coordinates of the dipole (R, Θ_1, ϕ_1) and those of the 3d-electron j (r_j, Θ_j, ϕ_j):

$$\frac{1}{TP} = \sum_{k=0}^{\infty} \sum_{m=-k}^{m=k} \frac{4\pi}{2k+1} \frac{r_j^k}{R^{k+1}} Y_k^{m*}(\theta_1,\phi_1)\, Y_k^m(\theta_j,\phi_j) \quad \text{.....(4-61)}$$

Since the angular coordinates of the dipole are fixed, see figure 4.2.0, we can define the constant (Gerloch and Slade, 1973)

$$C_k^m = \frac{4\pi}{2k+1} Y_k^{m*}(\theta_1,\phi_1) \quad \text{.....(4-62)}$$

and the function

$$F_k(r_j) = \frac{r_j^k}{R^{k+1}} \quad \text{.....(4-63)}$$

Using (4-61), (4-62) and (4-63), the potential energy due to the dipole (4-57) becomes

$$U_\mu(r_j) = -\mu\, e\, Cos\, \beta \sum_{k=0}^{\infty} \sum_{k=-m}^{k=m} C_k^m C_k^m F_k(r_j) F_k(r_j) Y_k^m(\theta_j,\phi_j) Y_k^m(\theta_j,\phi_j)$$

$$-\mu\, e\, Sin\, \beta\, r_j\, Sin\, \theta_j \sum_{k=0}^{\infty} \sum_{k=-m}^{k=m} C_k^m C_k^m C_k^m F_k(r_j) F_k(r_j) F_k(r_j) Y_k^m(\theta,\phi_j)$$

$$x\, Y_k^m(\theta_j,\phi_j) Y_k^m(\theta_j,\phi_j) \quad \text{.....(4-64)}$$

For H_{sa} to remain invariant, U_μ (r_j) must transform as the totally symmetric representation under the symmetry operations of FeO_5A^{a-7} system point group (where A^a is a dipole). That being the case, it becomes important, then, to know the symmetry of the five O^{2-} plus dipole ligand around the central ferric ion.

4.2.1: $U_\mu(r_j)$ in the Symmetry Group of $FeO_5 A^{n-7}$ System

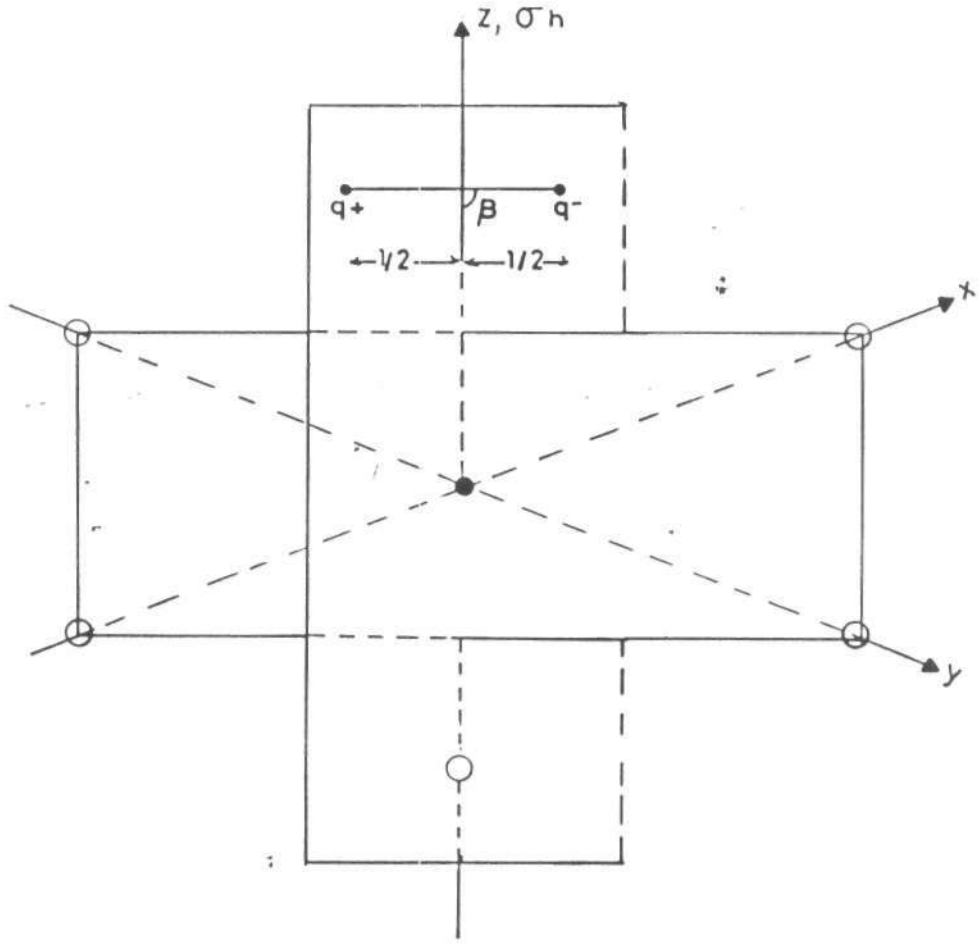


Figure 4·2·1: The Symmetry Elements of $FeO_5 A^{n-7}$ System

The symmetry elements that leave the FeO_3A^{n-7} system invariant are the E and σ_h operators only. It therefore belongs to the C_{1h} point group. The symmetry requirement that $U_\mu(r_j)$ must satisfy is that it must remain symmetric or $Y_k^m(\theta_j, \phi_j)$ must remain totally symmetric

$$\hat{P}Y_k^m(\theta_j,\phi_j) = Y_k^m(\theta_j,\phi_j)$$

in equation (4-64) under all the symmetry operations of the C_{1h} point group. This was found to hold only for

$k = 0, 2, 4, 6, 8, \ldots\ldots\ldots$

$m = 0, \pm4, \pm8, \ldots\ldots\ldots\ldots$

values.

This makes $U_\mu(r_j)$ to take its final form as the dipole potential energy to the 3d-electron j in the C_{1h} point group:

$$U_\mu(r_j) = -\mu\cos\beta[C_o^oC_o^oF_o(r_j)F_o(r_j)Y_o^o(\theta_j,\phi_j)Y_o^o(\theta_j,\phi_j)$$

$$+ C_2^oC_2^oF_2(r_j)F_2(r_j)Y_2^o(\theta_j,\phi_j)Y_2^o(\theta_j,\phi_j)$$

$$+ C_4^{-4}C_4^{-4}F_4(r_j)F_4(r_j)Y_4^{-4}(\theta_j,\phi_j)Y_4^{-4}(\theta_j,\phi_j)$$

$$+ C_4^oC_4^oF_4(r_j)F_4(r_j)Y_4^o(\theta_j,\phi_j)Y_4^o(\theta_j,\phi_j)$$

$$+ C_4^4C_4^4F_4(r_j)F_4(r_j)Y_4^4(\theta_j,\phi_j)Y_4^4(\theta_j,\phi_j)$$

$$-\mu e\sin\beta\, r_j\sin\theta_j[C_o^oC_o^oC_o^oF_o(r_j)F_o(r_j)F_o(r_j)Y_o^o(\theta_j,\phi_j)Y_o^o(\theta_j,\phi_j)$$

$$x\ Y_o^o(\theta_j,\phi_j) + C_2^oC_2^oC_2^oF_2(r_j)F_2(r_j)F_2(r_j)Y_2^o(\theta_j,\phi_i)Y_2^o(\theta_j,\phi_j)Y_2^o(\theta_j,\phi_j)$$

$$+ C_4^{-4}C_4^{-4}C_4^{-4}F_4(r_j)F_4(r_j)F_4(r_j)Y_4^{-4}(\theta_j,\phi_j)Y_4^{-4}(\theta_j,\phi_j)Y_4^{-4}(\theta_j,\phi_j)$$

$$+C_4^0C_4^0C_4^0F_4(r_j)F_4(r_j)F_4(r_j)Y_4^0(\theta_j,\phi_j)Y_4^0(\theta_j,\phi_j)Y_4^0(\theta_j,\phi_j)$$

$$+C_4^4C_4^4C_4^4F_4(r_j)F_4(r_j)F_4(r_j)Y_4^4(\theta_j,\phi_j)Y_4^4(\theta_j,\phi_j)Y_4^4(\theta_j,\phi_j)]\ldots\ldots(4\text{-}65)$$

The total potential energy due to the dipole, through 4-65, is thus given by

$$U_\mu(r) = \sum_{j=1}^{5} U_\mu(r_j)\ldots\ldots\ldots\ldots\ldots(4\text{-}66)$$

From equation (4-66), the Hamiltonian for the 3d-electrons of the ferric ion can be written as

$$H_{3d} = H_{3d}/ + U_\mu(r)\ldots\ldots\ldots\ldots\ldots(4\text{-}67)$$

This equation, (4-67), is analogous to (3-14) with $U_\mu(r)$ as the perturbation which is caused due to the approach of the dipole to the ferric oxide surface. Therefore when $U_\mu(r)$ is calculated, the potential energy curve for the physisorption of the dipole shall be obtained, yielding its binding energy and equilibrium surface-dipole separation.

4.2.2 The Dipole Physisorption Energy by the FeO_5A^{n-7} Model

The physisorption energy of the dipole can be obtained only if the perturbation $U_\mu(r)$, to the ground state of FeO_5A^{n-7}, is calculated. As in section 4.1.2, we must therefore know the ground electronic state and the corresponding wavefunction of the system.

Following the procedures of (4-15) to (4-19), we find the reducible representation spanned by the 3d orbitals in the C_{1h} point group to be:

E	σ_h
5	1

By using the reduction formula (4-20), the five fold degenerate 3d orbitals of the ferric ion split into five three a' and two a" non-degenrate levels. As in the FeO_5H^{6-} case, we assume a low spin electronic configuration because of the further descent in symmetry from C_{4v} -----> C_{1h}. We found the doubly degenerate level e in C_{4v} to split into two a" nondegerate levels when descending from C_{4v} ---------> C_{1h}, so the ground electronic configuration of Fe^{3+} ion in the FeO_5.[dipole]$^{7-}$ system is $(a")^2\ (a")^2\ (a')^1$. This configuration has only one unpaired electron so we obtained $3^2A'$ and $2^2A"$ terms for the configuration in C_{1h} field. Since upon descent of symmetry from C_{4v} ---------> C_{1h} e level splits into two a" levels, we also found ^2E, which is the ground state term of Fe^{3+} in C_{4v} field, to split into $2^2A"$ terms in the C_{1h} field. Based on this, we therefore take $^2A"$ as the ground electronic state term of the ferric ion in C_{1h} field.

The physisorption energy of the dipole, which is taken as the perturbation to the ground electronic state, is given by

$$\Delta H = \langle \psi(^2A'') | U_\mu(r) | \psi(^2A'') \rangle \ldots\ldots\ldots\ldots (4\text{-}68)$$

where the corresponding wavefunction $\psi(^2A'')$ is any of the {$3dx^2$, 3dyz} set. When this perturbation is calculated, the physisorption energy of the dipole shall be obtained as the binding energy of the P.E. curve.

4.3.0 The Chemisorption of NH_3 by $FeO_6.NH_3^{7-}$ Model

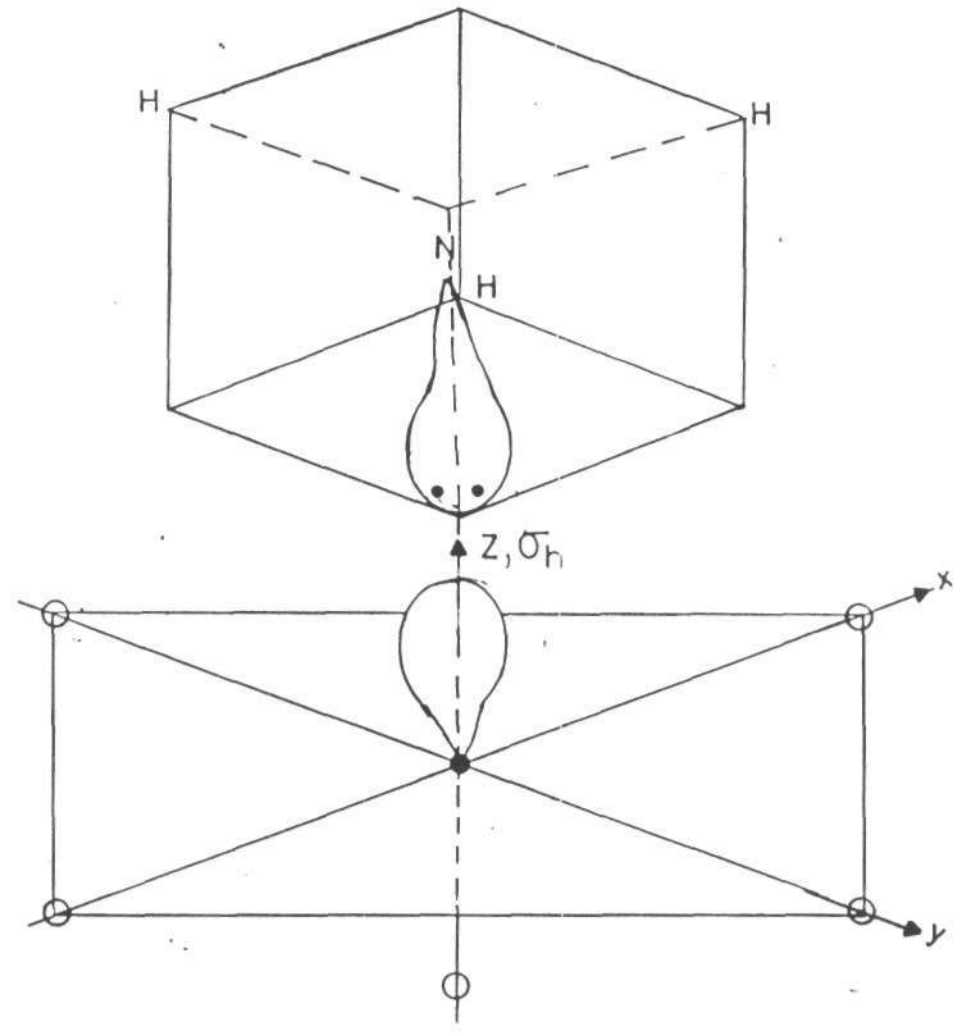
The chemisorption of ammonia is simulated as a pseudo-diatomic molecular type interaction, where an electron pair bond is envisioned to be formed between the lone pair on the nitrogen atom of ammonia molecule and the ferric ion. As in the two previous cases, the five O^{2-} anions are assumed to provide a constant electric potential to the valence electrons of the ferric ion.

Following the model of (4-14) and (4-67), the Hamiltonian for the pseudo-diatomic molecule, without the O^{2-} crystal potential, is given by

$$H_{pseudo} = \sum_j \left(-\frac{\nabla_j^2}{2} - \sum_A \frac{Z_A^*}{r_{Aj}} \right) + \sum_j \sum_{<i} 1/r_{ij} + \frac{Z_N^* Z_{Fe}^*}{R_{Fe-N}} \ldots (4\text{-}69)$$

where the summation is over the lone pair electrons on the N atom and the valence electrons of the ferric ion, whereas Σ_A is over the N and Fe frozen core charges Z_N^* and Z_{Fe}^* respectively.

Having found the Hamiltonian for the pseudo-diatomic molecule, Fe^{3+} ----: NH_3, the Schrödinger equation and the energy of the



KEY

● = Fe^{3+}

○ = O^{2-}

Symmetry	Elements
E	σ_h

Figure 4.3.0: The Chemisorption of NH_3 by $FeO_5NH_3^{7-}$ Model

interaction are given by

$$H_{pseudo}\ \psi_{pseudo} = E_{pseudo}\ \psi_{pseudo} \text{.....(4-70)}$$

$$E_{pseudo} = \int \psi^{*}_{pseudo}\, H_{pseudo}\, \psi_{\psi_{pseudo}}\, d\tau / \int \psi^{2}_{pseudo} d\tau \text{.....(4-71)}$$

where ψ_{pseudo} is the electron pair bond wavefunction corresponding to the ground state of the pseudo-diatomic molecule, Fe^{3+}------:NH_3.

4.3.1 Chemisorption Energy of NH_3 by the $FeO_5NH_3^{7-}$ Model

The chemisorption energy of NH_3 molecule can be obtained from the potential energy curve of the interaction, if the quantity on the right hand side of (4-71) can be calculated. It therefore becomes mandatory to know the wavefunction Ψ_{pseudo} representing the ground state of the pseudo-diatomic molecule.

From figure 4.3.0, the only symmetry elements that leaves the $FeO_5NH_3^{7-}$ system invariant are the E and σ_h symmetry operators. The configuration of the ferric ion in this field, C_{1h}, is already given in section 4.2.2 {$a''^2\ a''^2\ a'^1$ or $(3dxz)^2\ (3dyz)^2\ (3dxy)^1$}. Thus the $3dz^2$ orbital is empty and available for sharing lone pair electrons from donors such as :NH_3.

Since the electron pair bond Fe^{3+}------:NH_3 and the lone pair on the nitrogen atom of ammonia are directed along the z-axis (please see figure 4.3.0) the basis set of the electron pair bond wavefunction Ψ_{pseudo} is {$3dz^2$, 2Pz}. Here, the 2Pz orbital, which contain the lone pair, is centred on the nitrogen atom of ammonia

molecule while the $3dz^2$, which is empty, is centred on the ferric ion. The antisymmetric wavefunction of the electron pair bond is written as

$$\psi_{pseudo} = \frac{1}{\sqrt{2!}} \sum_R (-1)^R R \sum_P (1)^P P \, \phi_1(1) \, \phi_2(2)\alpha(1)\beta(2) \ldots\ldots (4\text{-}72)$$

where

$$\phi_1 = 2P_2 \quad also \quad \phi_2 = 3dz^2 \ldots\ldots\ldots\ldots\ldots\ldots (4\text{-}73)$$

and R and P are permutation operators that exchange spin and electronic coordinates respectively.

Putting the value of Ψ_{pseudo} from (4-72) into (4-71) and integrating, we obtain

$$E_{pseudo} = E(\phi_1) + E(\phi_2) + Q + \alpha \ldots\ldots\ldots\ldots (4\text{-}74)$$

where (the one-electron quantities are)

$$E(\phi_1) = \langle \phi_1 | - \frac{\nabla_1^2}{2} - \frac{Z_N^*}{r_1} | \phi_1 \rangle \ldots\ldots\ldots\ldots (4\text{-}75)$$

$$E(\phi_2) = \langle \phi_2 | - \frac{\nabla_2^2}{2} - \frac{Z_{Fe^*}}{r_2} | \phi_2 \rangle \ldots\ldots\ldots\ldots (4\text{-}76)$$

and the Coulomb and exchange terms (two-electron quantities are)

$$Q = \frac{J}{1+S^2} \quad also \; \alpha = \frac{K}{1+S^2} \ldots\ldots\ldots\ldots\ldots\ldots (4\text{-}77)$$

The J and K parameters are called Coulomb and exchange integral respectively and have the following expressions:

$$J = \int \phi_1^*(1)\phi_2^*(2)\{ - \frac{Z_{Fe}^*}{r_1} - \frac{Z_N^*}{r_2} + \frac{1}{r_{12}} + \frac{Z_{Fe}^* Z_N^*}{R_{Fe-N}}\}\phi_1(1)\phi_2(2)d\tau_1 d\tau_2$$

.....(4-78)

and

$$K = \int \phi_1^*(1)\phi_2^*(2)\{ - \frac{Z_{Fe}^*}{r_1} - \frac{Z_N^*}{r_2} + \frac{1}{r_{12}} + \frac{Z_{Fe}^* Z_N^*}{R_{Fe-N}}\}\phi_1(2)\phi_2(1)d\tau_1 d\tau_2$$

.....(4-79)

The overlap integral S in the denominator of (4-77) is defined by

$$S = \int \phi_1^* \phi_2 d\tau \text{.....(4-80)}$$

It is seen that the one-electron quantities, E (ϕ_1) and E(ϕ_2), defined by equations (4-75) and (4-76) are independent of the Fe-N nuclear separation, and as such may be regarded as constants which provide only a constant shift to the energy, E_{pseudo}. They could be taken as the zero (or reference) position in calculating the potential energy curve of the pseudo diatomic molecule. To calculate the potential energy curve, it is necessary to make transformation from spherical polar coordinates to elliptical coordinates, (r, θ, ϕ) -------> (μ, v, ϕ). As a result of this transformation, the Coulomb and exchange terms (Q + α) are calculated at successive Fe - N nuclear separations. The potential energy curve, so obtained, yield the binding energy, chemisorption energy, and equilibrium separation of the Fe - N nuclei in the pseudo diatomic molecule.

CHAPTER FIVE

5. RESULTS AND DISCUSSION I: ENERGY LEVELS OF THE ADSORBENT -ADSORBATE SYSTEMS

5.0 The Electronic Structure of the FeO_6A^{n-9} and FeO_5A^{n-7} Adsorbent-Adsorbate Systems

In this chapter, the electronic structure of the FeO_6A^{n-9} and FeO_5A^{n-7} adsorbent-adsorbate systems, where A^n represents either H^+ OH^- or NH_3, are presented and discussed. The results of the extended Hückel theory (EHT) and the self-consistent field molecular orbital extended Hückel theory (SCF-MO EHT) methods for the FeO_6A^{n-9} systems will first be presented. Then results for FeO_5A^{n-7}, for both chemisorption and physisorption, follow. The energy levels of the FeO_6A^{n-9} and FeO_5A^{n-7} clusters for spin up and spin down electrons are shown in MO diagrams. All orbital energies are in electron volts (eV) unit.

5.1 Results for FeO_6H^{9-} Cluster

The calculated MO levels (in eV), together with other quantities for the FeO_6H^{9-} adsorbent-adsorbate system are given in Table 5.1 below:

Table 5.1: Results for the FeO_6H^{n-} System: Orbital Energies and Other Quantities - Sigma Interaction

MO energy (eV) etc MOs and other quantities	EHT	SCF-MO EHT -SP
$1a_{1g}\uparrow$	-5.9517	-6.3124
$2a_{1g}\uparrow$	-12.2981	-13.6290
$1b_{1g}\uparrow$	-5.9000	-5.9000
$2t_{2g}\uparrow$	-7.8000	-7.8000
$6t_{1u}\uparrow$	-8.4890	-8.4890
$6t_{1u}\downarrow$	-8.4890	-8.4890
$\{^{\alpha}\sigma_{BOND}^{a-b}\}$	NE	0.2088
λ_1^{α}	NE	0.0392
λ_2^{α}	NE	0.0000
Eigenvectors	0.9999 -0.0003 0.0003 0.9999	0.9985 0.0508 -0.0508 0.9987

where NE means no equivalent of the quantity in the EHT method. The corresponding MO diagrams for the FeO_6H^{n-} system in the EHT and SCF -MO EHT spin polarized levels of calculation are shown in figures 5.1 and 5.2 respectively.

The $2a_{1g}\uparrow$ MO is essentially H^+ 1s orbital while $1a_{1g}\uparrow$ MO is primarily FeO_6^{9-} $3e_g$ $(\phi_{z^2})\uparrow$ orbital with a slight H^+ 1s orbital admixture in both the EHT and SCF-MO EHT-SP levels of calculation, though the orbital mixing is stronger in the latter method. These

levels are lower in energy by the SCF-MO EHT-SP method than by the EHT. The lowering is brought about due to the contribution of the charge dependent quantity λ_k in the diagonal elements

$$F_{kk} = (1 + \lambda_k) IP_k \qquad .....(5\text{-}1)$$

in the SCF-MO EHT methods which is absent in the EHT formalism. The $1b_{1g}$, $2t_{2g}$ and $6t_{1u}$ orbitals are non-bonding in FeO_6H^{8-} σ-bonding. The value of $1 + {}^{\alpha}\sigma^{a-b}_{BOND}$ is however less than 1.75 of the EHT method

showing that the latter method has probably over-estimated the K parameter.

Table 5.2: Results for the $FeO_6H^{\cdot}$- System: Orbital Energies and Other Quantities - *O2p* σ -Nonbonding Interaction with H· Adsorbate

MO energy (eV) etc MOs and other quantities	EHT	SCF-MO EHT -SR
$1a_{1g}\uparrow$	-9.5418	-1.4878
$1a_{1g}\downarrow$	-9.5418	-1.4878
$2a_{1g}\uparrow$	-16.8014	-20.0682
$2a_{1g}\downarrow$	-16.8014	-20.0682
$3e_g\uparrow$	-5.9000	-5.9000
$6e_g\uparrow$	-8.4890	-8.4890
$6e_g\downarrow$	-8.4890	-8.4890
$2t_{2g}\uparrow$	-7.8000	-7.8000
σ_{BOND}^{a-b}	NE	0.9203
λ_1	NE	0.0073
λ_2	NE	0.0000
Eigenvectors	0.9905 -0.1373 0.1373 0.9905	0.7219 -0.5900 0.5275 0.8074

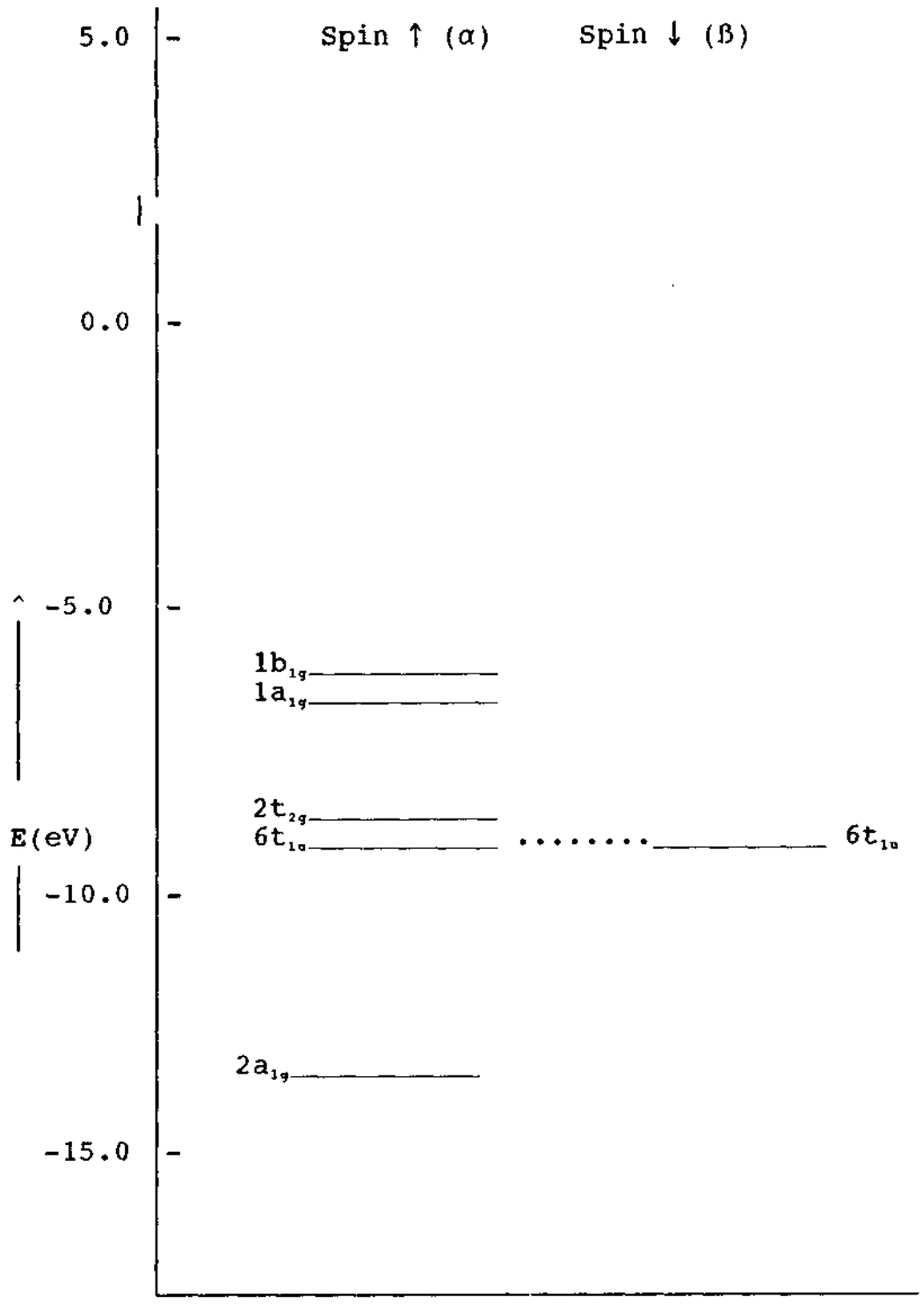


Figure 5.1: **The Energy Levels of the Adsorbent-Adsorbate system of FeO_6H^{9-} Cluster: Calculated by SCF-MO-EHT-SP.**

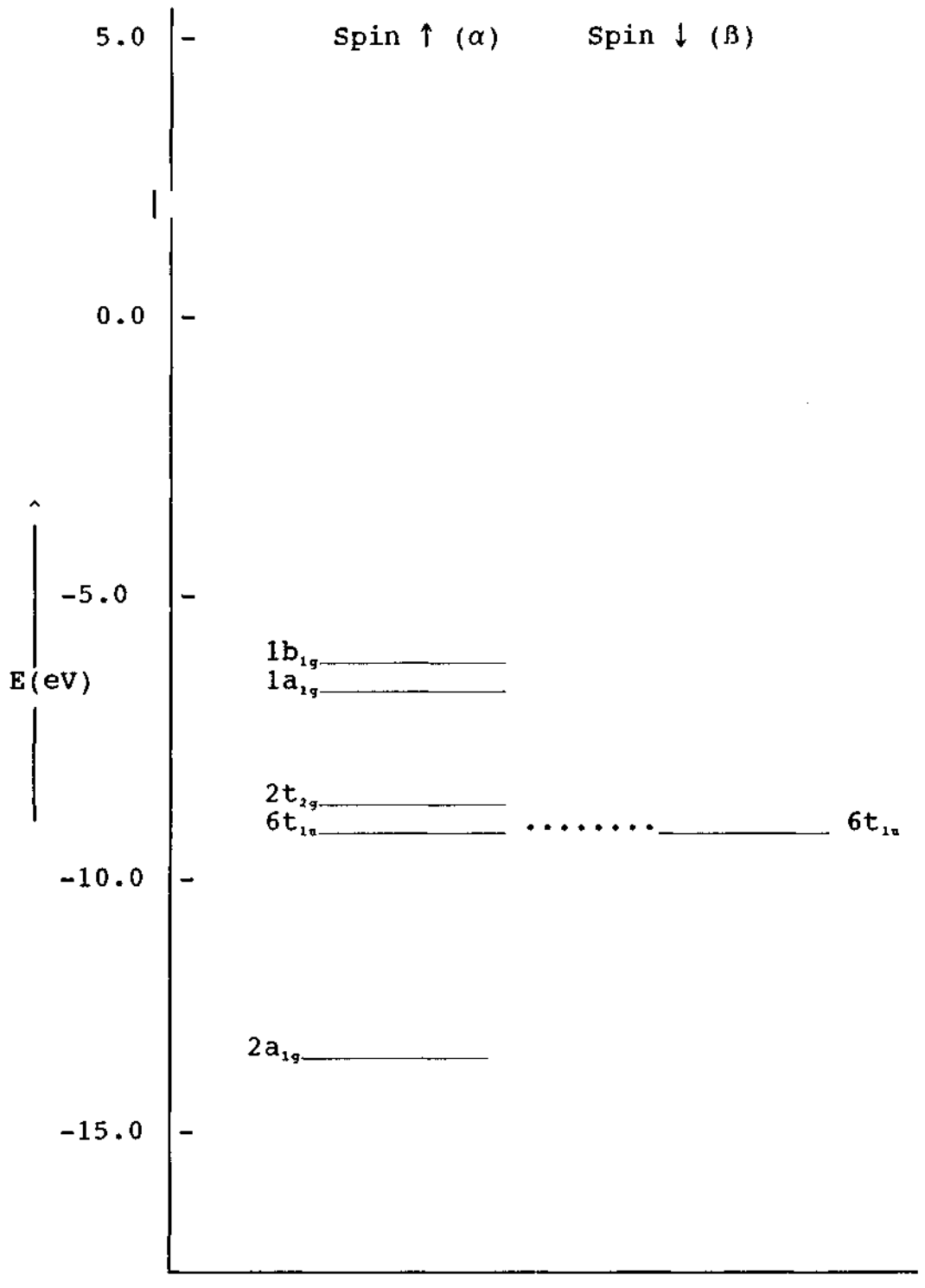


Figure 5.2: **The Energy Levels of the Adsorbent-Adsorbate system of FeO_6H^{9-} Cluster: Calculated by EHT.**

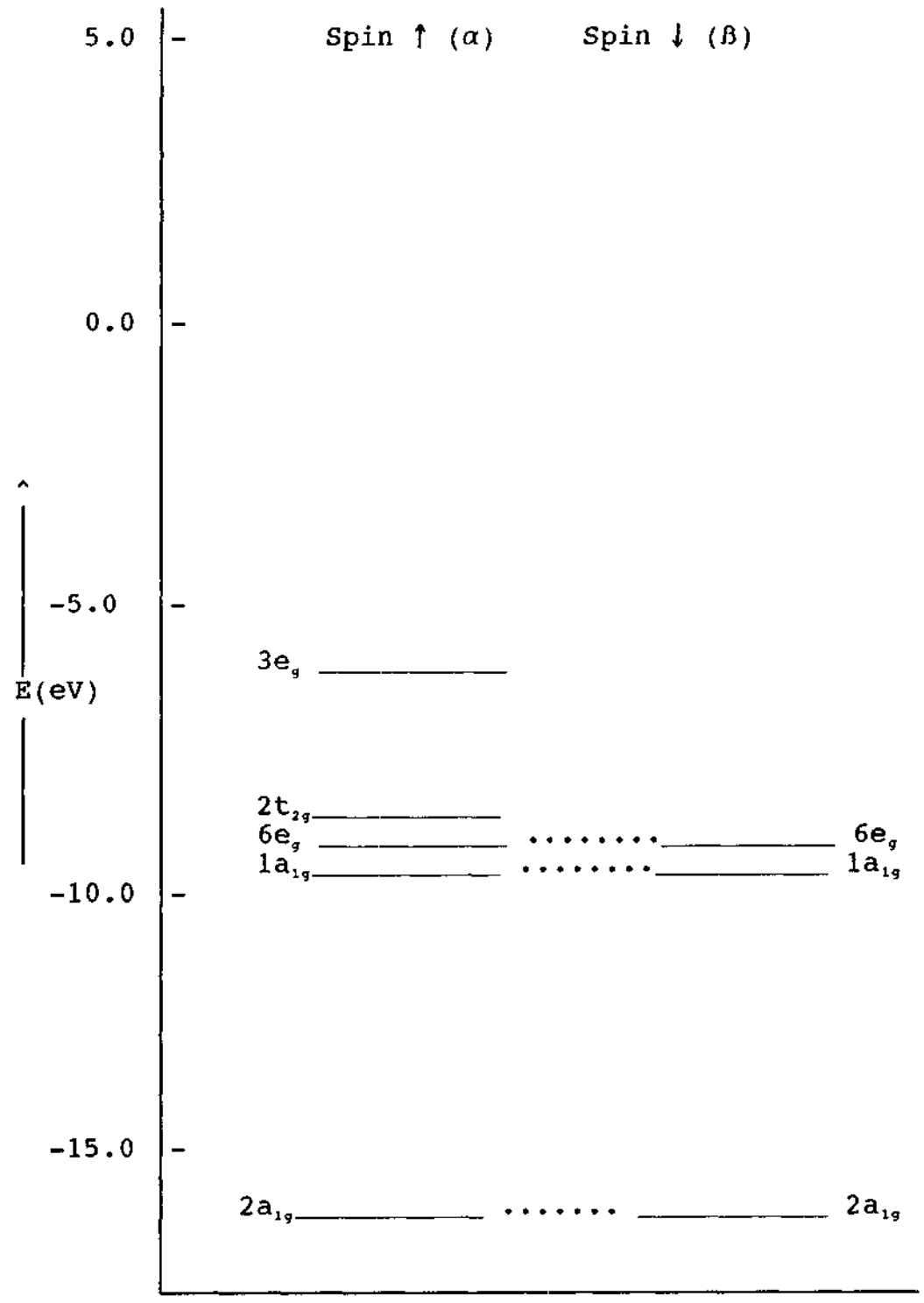


Figure 5.3: **The Energy Levels of the Adsorbent-Adsorbate system of $FeO_4H^{\cdot}$ Cluster: ($H^{\cdot}$ ion Chemisorption by the oxygens) Calculated by EHT.**

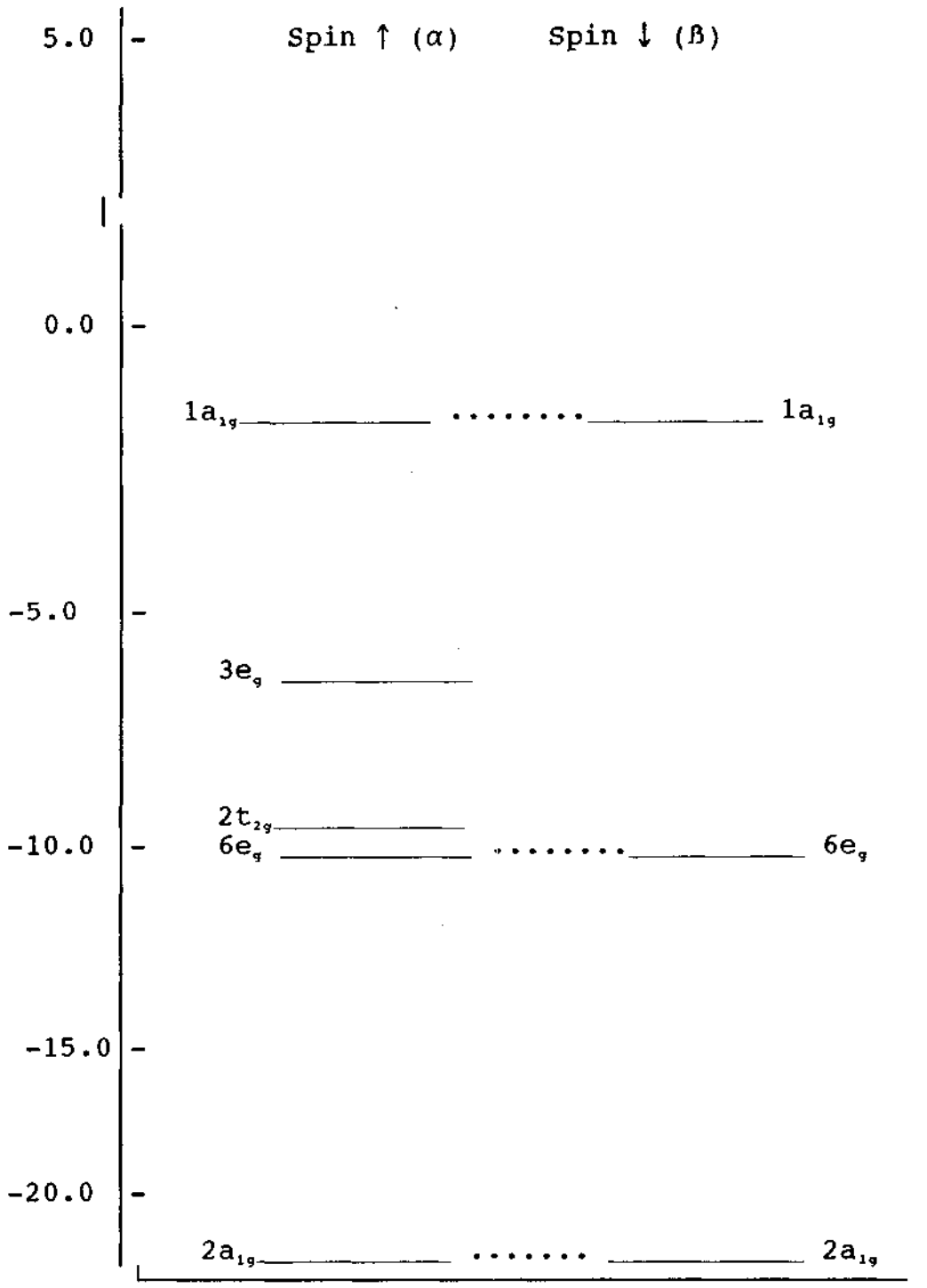


Figure 5.4: **The Energy Levels of the Adsorbent-Adsorbate system of FeO_5H^{9-} Cluster: (H^+ ion Chemisorption by the oxygens) Calculated by SCF-MO EHT-SR.**

Table 5.2 collects orbital energies and other quantities for the FeO_6H^{9-} adsorbent-adsorbate system, H^+ bonding simulated through the O2p σ-nonbonding orbital of the surface oxygens. The results of both EHT and SCF-MO EHT-SR methods predict a rather very high affinity to H^+ ions by the surface oxygens. The corresponding MO diagrams are shown in figures 5.3 and 5.4 for the two levels of calculation.

The H^+ 1s and the O2p non-bonding orbital $6t_{1u}$ (ϕ_z) are very well mix-up, more especially as shown by the SCF-MO EHT-SR method. The $1a_{1g}$ and $2a_{1g}$, bonding-antibonding orbitals of the interaction, levels clearly show a serious disagreement between the two methods of calculation. The $2a_{1g}$ is far lower (by about 3eV) in the SCF-MO EHT-SR method than in the EHT, while $1a_{1g}$ is far lower in energy by EHT (with about 8eV) than by the former. However large the disagreement is, the two methods predict orbital lowering of order of a very strong ionic bond. The $3e_g$, $6e_g$ and $2t_{2g}$ orbitals are non-bonding in this case.

Another prominent feature of the SCF-MO EHT-SR method in this system is that $1 + \sigma_{BOND}^{a-b}$ is greater than the 1.75 value of K assumed by the EHT. Infact the very large value of $1 + \sigma_{BOND}^{a-b}$ suggests that the strength of the H^+ - surface oxygens bond exceeds normal convalent character if we were to compare it with the

corresponding value obtained in the FeO_6H^{8-} cluster σ-interaction results:

$$1 + {}^{a}\sigma_{BOND}^{a-b} = 1.2088 \text{ for } FeO_6H^{8-} \ \sigma\text{-Bond} \quad .....(5\text{-}2)$$

$$1 + \sigma_{BOND}^{a-b} = 1.9203 \text{ for } FeO_6H^{8-} \ O2p\text{-Bond} \quad .....(5\text{-}3)$$

This strong affinity of the surface oxygens towards H^+ adsorbate perhaps suggests that most of the H^+ ion bonding on the surface is done by the O^{2-} anions in the surface than by the surface Fe^{3+} ion.

5.2 Results for $FeO_6.OH^{10-}$ Cluster

The values of MO energies and other quantities for $FeO_6.OH^{10-}$ adsorbent-adsorbate cluster (σ-interactions) from molecular orbital studies are given below:

Table 5.3: Results for the FeO_6OH^{10-} System: Orbital Energies and Other Quantities, σ-Interactions

MO energy (eV) etc MOs and other quantities	EHT	SCF-MO EHT -SP
$1a_{1g}\uparrow$	-4.3656	-5.3419
$2a_{1g}\uparrow$	-8.0048	-7.7361
$2a_{1g}\downarrow$	-8.0048	-7.2706
$1b_{1g}\uparrow$	-5.9000	-5.9000
$2t_{2g}\uparrow$	-7.8000	-7.8000
$1\Pi\uparrow$	-2.9050	-2.9050
$1\Pi\downarrow$	-2.9050	-2.9050
$\{^{\alpha}\sigma_{BOND}^{a-b}\}$	NE	-0.0207
$\{^{\beta}\sigma_{BOND}^{a-b}\}$	NE	-0.0138
λ_1^{α}	NE	0.0342
λ_2^{α}	NE	0.0181
λ_1^{β}	NE	-
λ_2^{β}	NE	0.0181
Eigenvectors	0.7942 -0.6076 0.6076 0.7942	0.8387 -0.5423 0.5413 0.8402

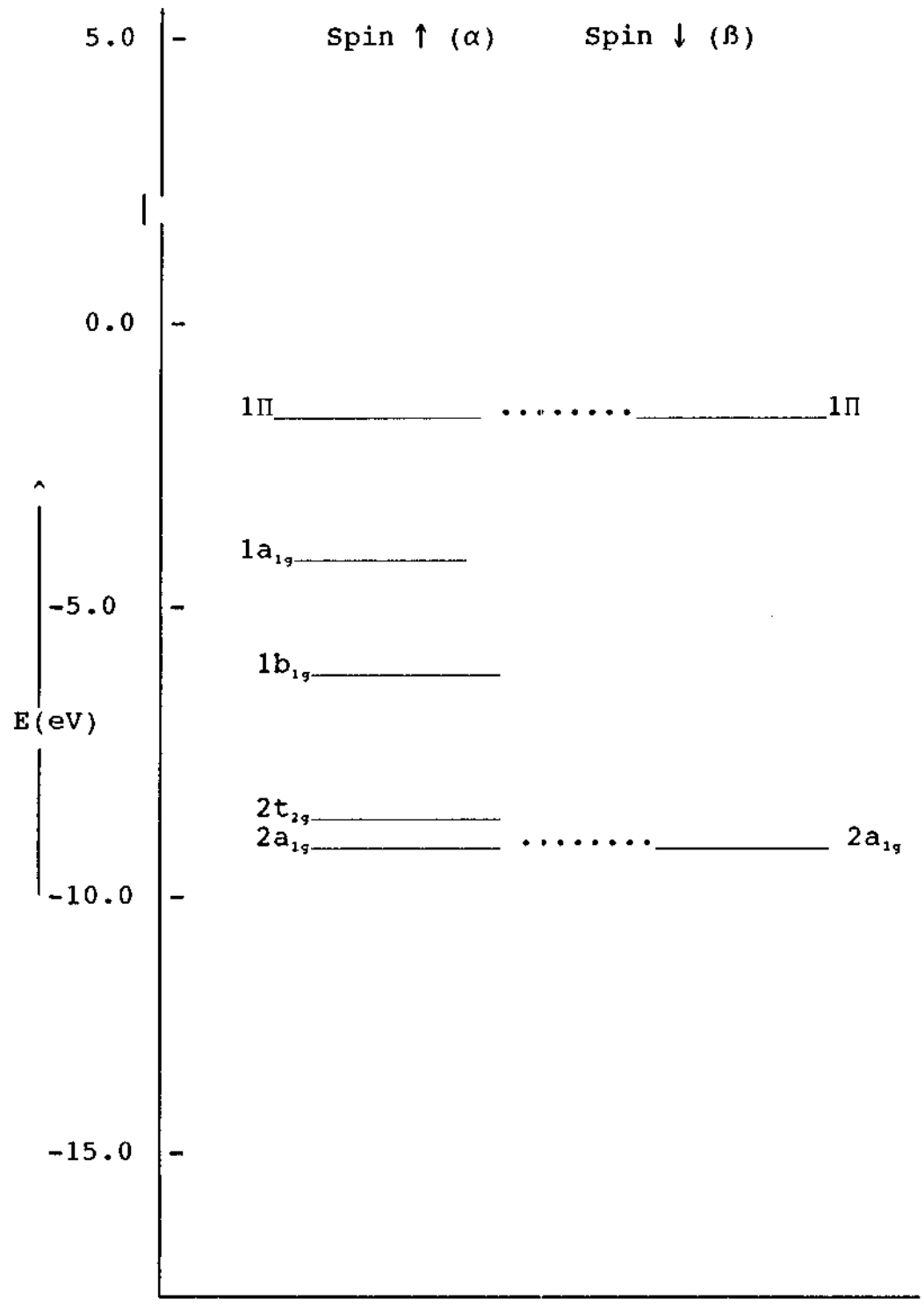


Figure 5.5: **The Energy Levels of the Adsorbent-Adsorbate system of FeO_6OH^{10-} Cluster: (OH^- ion σ-Bonding) Calculated by EHT.**

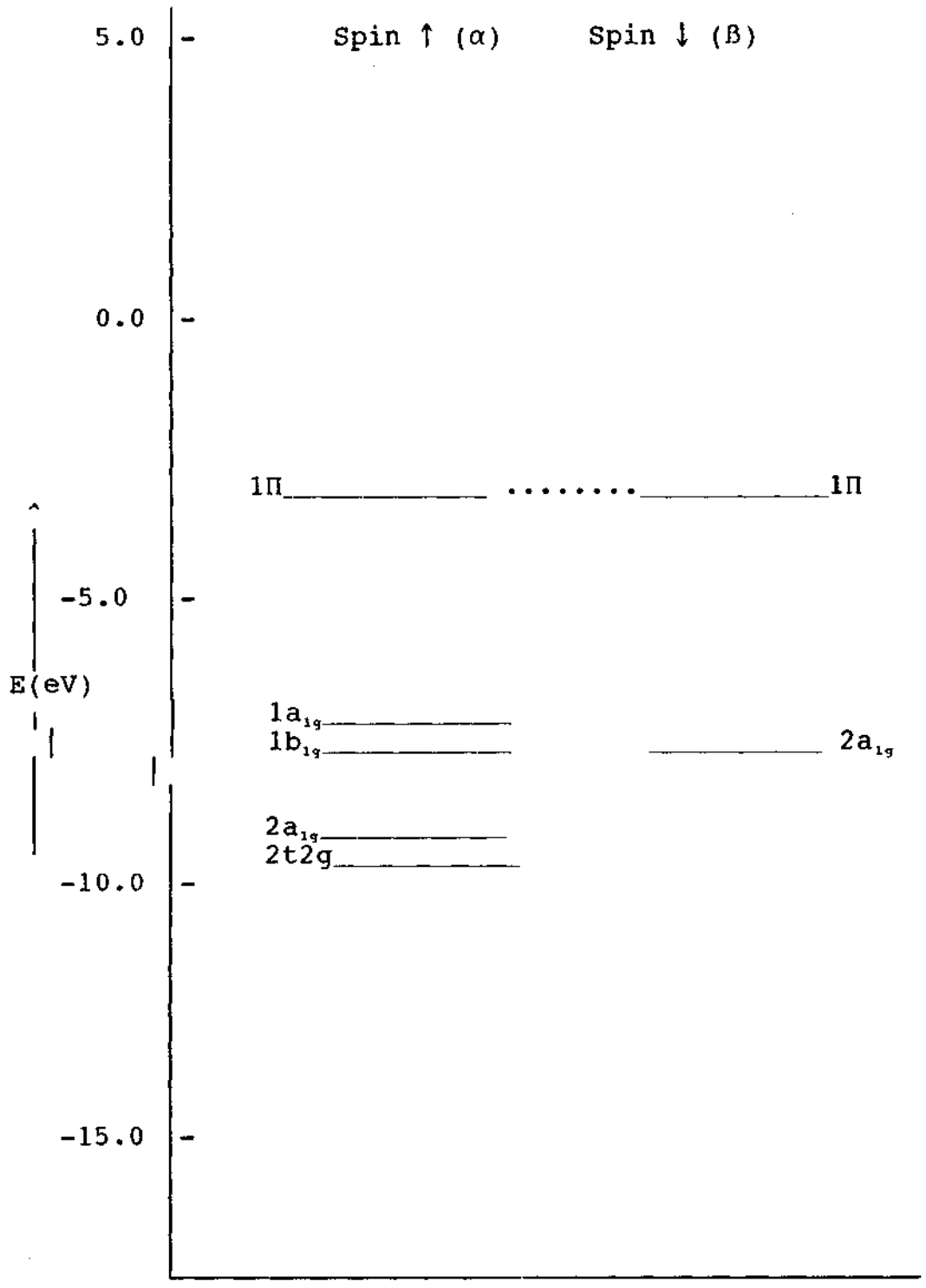


Figure 5.6: **The Energy Levels of the Adsorbent-Adsorbate system of FeO_6OH^{10-} Cluster: (OH^- ion σ-bonding) Calculated by SCF-MO EHT-SP.**

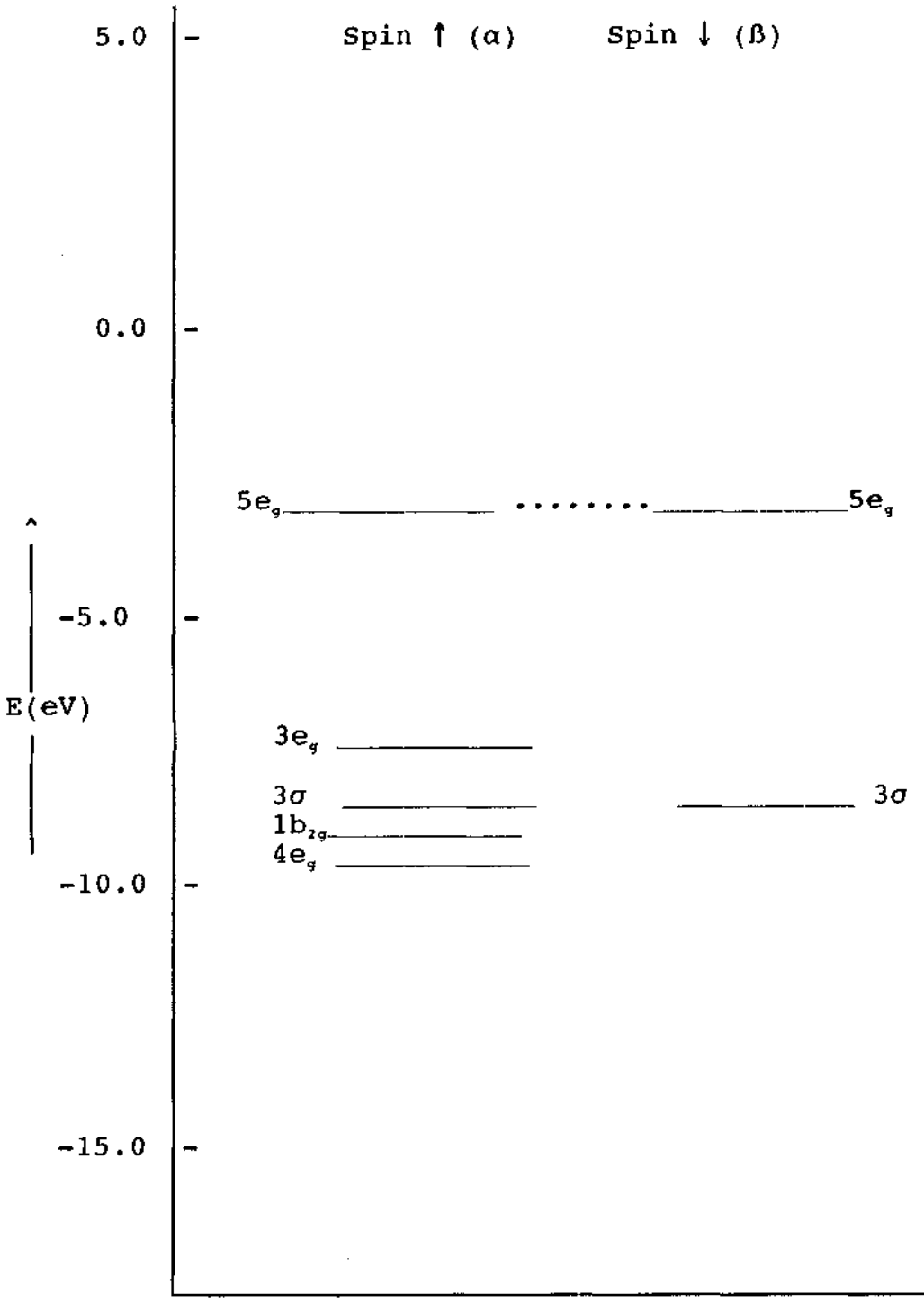


Figure 5.7: **The Energy Levels of the Adsorbent-Adsorbate system of FeO_4OH^{10-} Cluster: (OH^- ion Π-bonding) Calculated by EHT.**

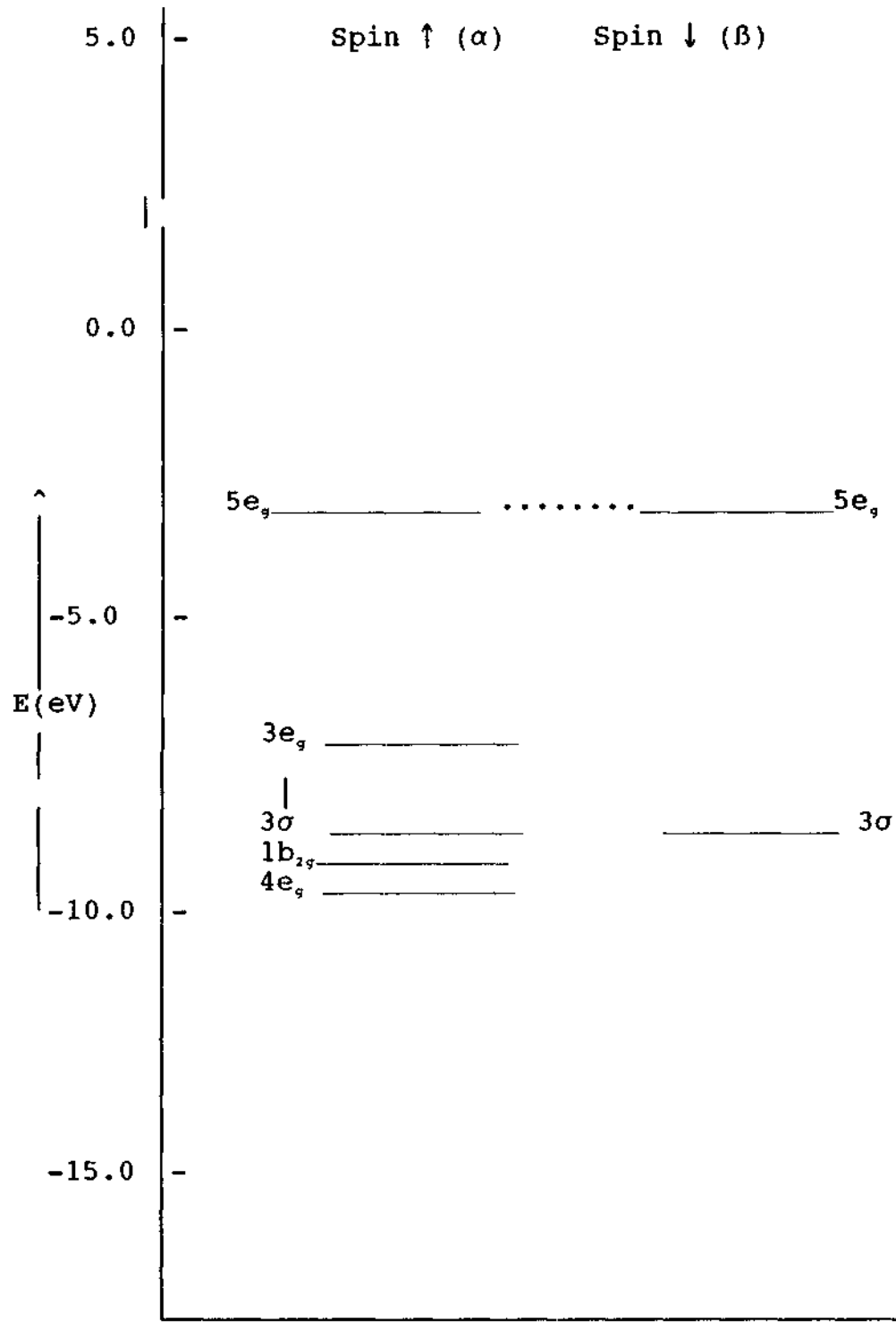


Figure 5.8: **The Energy Levels of the Adsorbent-Adsorbate system of FeO_4OH^{10-} Cluster: (OH^- ion Π-bonding) Calculated by SCF-MO EHT-SP.**

The MO diagrams, for the FeO_6OH^{10-} adsorbent-adsorbent system σ-interactions, are shown in figures 5.5 and 5.6 as calculated by the EHT and SCF-MO EHT-SP methods respectively. Looking at the eigenvectors, it is immediately apparent that there is a very considerable FeO_6^{9-}-------OH- orbitals admixture, and one naturally expects stronger bonding of OH- ion compared to H^+ ions. However, this admixture is slightly more pronounced in the results of EHT slightly than in SCF-MO EHT-SP method.

The $1a_{1g}\uparrow$ is slightly lower in energy by SCF-MO EHT-SP method than by the EHT. The $2a_{1g}\uparrow$ and $2a_{1g}\downarrow$ MOs generally lie lower in energy by the EHT than by the former. However, they (the $2a_{1g}\uparrow$ and $2a_{1g}\downarrow$ MOs) have the same energy in the EHT scheme. In the SCF-MO EHT-SP method they have different energies. The $2a_{1g}\uparrow$ MO is raised by about = 0.5 eV above the $2a_{1g}\uparrow$ MO. This difference in the $2a_{1g}$ spin down-spin up MO energy is brought about by the difference in exchange correlation energy they receive from the electrons located in the $3e_g\uparrow$ orbital of the FeO_6OH^{9-} cluster, resulting in the electron of the $3\sigma\uparrow$ of OH- being attracted more than that in $3\sigma\downarrow$ orbital. The $2t_{2g}$, $1b_{1g}$ and 1Π orbitals are non-bonding.

The difference in attraction experienced by the electrons of $3\sigma\uparrow$ and $3\sigma\downarrow$ orbitals of OH- is also shown from the values of $\{^{\alpha}\sigma_{BOND}^{a-b}\}$ and $\{^{\beta}\sigma_{BOND}^{a-b}\}$ obtained. $\{^{\alpha}\sigma_{BOND}^{a-b}\}$ is greater than $\{^{\beta}\sigma_{BOND}^{a-b}\}$ in magnitude even though $\{1+^{\alpha}\sigma_{BOND}^{a-b}\}$ is smaller than $\{1+^{\beta}\sigma_{BOND}^{a-b}\}$. The

difference between $\{1 + {}^{\alpha}\sigma_{BOND}^{a-b}\}$ and $\{1 + {}^{\beta}\sigma_{BOND}^{a-b}\}$ is small and did not probably have any appreciable effects on the MO energies.

Table 5.4: Results for the $FeO_4.OH^{10-}$ System: Orbital Energies and Other Quantities, Π-Interactions

MO energy (eV) etc --- MOs and other quantities	EHT	SCF-MO EHT -SP
$3e_g\uparrow$	-5.9000	-5.9000
$4e_g\uparrow$	-7.8056	-7.8003
$5e_g\uparrow$	-2.9023	-2.9053
$5e_g\downarrow$	-2.9023	-2.9070
$1b_{2g}\uparrow$	-7.8000	-7.8000
$3\sigma\uparrow$	-6.9006	-6.9006
$3\sigma\downarrow$	-6.9006	-6.9006
$\{{}^{\alpha}\sigma_{BOND}^{a-b}\}$	NE	0.0000
$\{{}^{\beta}\sigma_{BOND}^{a-b}\}$	NE	0.0000
λ_1^{α}	NE	0.0000
λ_2^{α}	NE	0.0007
λ_1^{β}	NE	-
λ_2^{β}	NE	0.0007
Eigenvectors	0.9999 -0.0126 0.0012 0.9999	0.0156 0.9999 0.9999 -0.0156

The table contains values for the $FeO_6.OH^{10-}$ adsorbent-adsorbate system MO energies and other quantities for the Π-interaction mode in the chemisorption of OH- adsorbate. The corresponding MO diagrams are shown in figures 5.7 and 5.8 for both EHT and SCF-MO EHT-SP levels of calculation respectively.

The MOs involved in the Π-interaction, which give rise to the adsorbent-adsorbate Π-MOs, are only slightly lowered or raised in energy. For example, the $4e_g\uparrow$ MO is only lowered by about 6 x 10^{-3} and 10^{-4} eV from the $2t_{2g}\uparrow$ orbital which primarily constitutes it as EHT and SCF-MO EHT-SP methods predicted respectively. The $5e_g$ orbital, essentially OH- 1Π in character, is raised by only about 3 x 10^{-3} eV in EHT scheme where as lowered averagely by about 10^{-3} eV in the SCF-MO EHT-SP prediction. This automatically suggests that the FeO_6^{9-}-------OH- Π-interaction is very weak.

This is further confirmed by the extent of OH- 1Π and FeO_6^{9-} $2t_{2g}$ pie orbitals admixture that could be seen from the values of the eigenvectors for both the EHT and SCF-MO EHT-SP methods. The $4e_g$ and $5e_g$ MOs are thus essentially FeO_6^{9-} and OH- orbitals respectively. The $3e_g$, $1b_{2g}$ and 3σ orbitals are non-binding.

The bond functions, $\{^{\alpha}\sigma_{BOND}^{a-b}\}$ and $\{^{\beta}\sigma_{BOND}^{a-b}\}$, have zero values.

Invoking the physical interpretation of the bond function σ_{BOND}^{a-b},

section 3.4, the SCF-MO EHT-SP results predict that no chemical bond is formed between the OH- adsorbate and the surface through

Π-interactions. The binding is just due to weak electrostatic forces; the FeO_6^{9-} and OH- Π-electrons did not mix appreciably to cause chemical bond to form. The $5e_g\uparrow$----> $5e_g\downarrow$ splitting in the SCF-MO EHT-SP scheme is only about 10^{-3} eV showing insignificant electronic mixing as compared to 0.5eV for the $2a_{1g}\uparrow$------> $2a_{1g}\downarrow$ σ-interactions.

5.3 Results for the $FeO_6.NH^{9-}$ Cluster

The values of MO energies and other quantities for the $FeO_6.NH_3^{9-}$ adsorbent-adsorbate cluster system (σ-interactions) from MO studies are given in the table below.

Table 5.5: Results for the $FeO_6.NH_3^{9-}$ System: Orbital Energies and Other Quantities, σ-Interactions

MO Energy (eV) etc. ---------- MOs and Other Quantities	EHT	SCF-MO EHT-SP
$1a_{1g}\uparrow$	-5.5108	-5.9461
$2a_{1g}\uparrow$	-12.0644	-12.0323
$2a_{1g}\downarrow$	-12.0644	-11.6455
$1b_{1g}\uparrow$	- 5.9000	- 5.9000
$2t_{2g}$	- 7.8000	- 7.8000
$1e\uparrow$	-17.2720	-17.2720
$1e\downarrow$	-17.2720	-17.2720
${}^{\alpha}\sigma_{BOBD}{}^{a-b}$	NE	0.0056
${}^{\beta}\sigma_{BOBD}{}^{a-b}$	NE	0.0023
λ_1^{α}	NE	0.0338
λ_2^{α}	NE	0.0008
λ_1^{β}	NE	-
λ_2^{β}	NE	0.0008
Eigenvectors	0.9657 0.2597 -0.2597 0.9657	0.9850 0.1650 -0.1648 0.9863

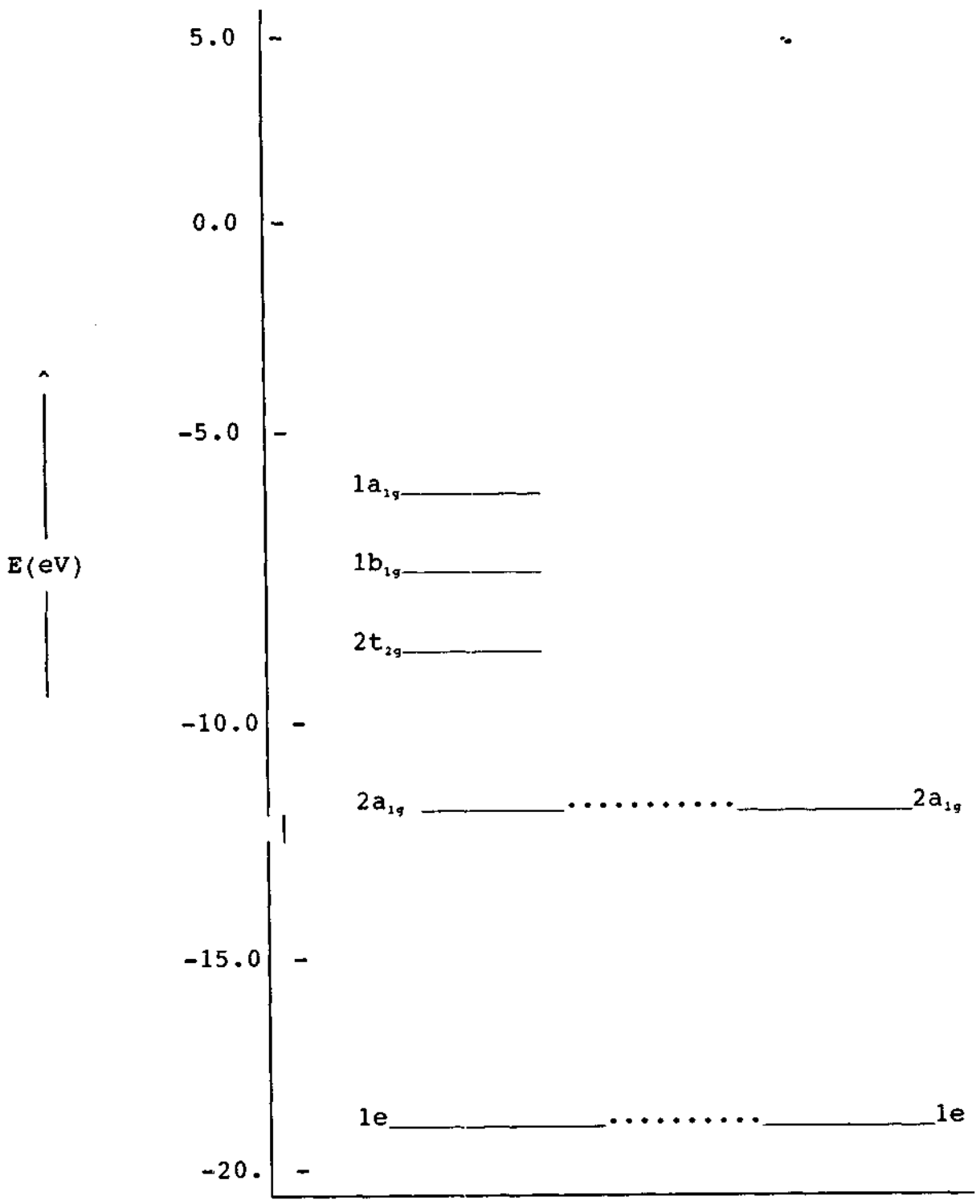


Figure 5.9: The Energy Levels of the Adsorbent - Adsorbate System of $FeO_6.NH_3^{9-}$ Cluster (NH_3 σ-bonding), Calculated by EHT.

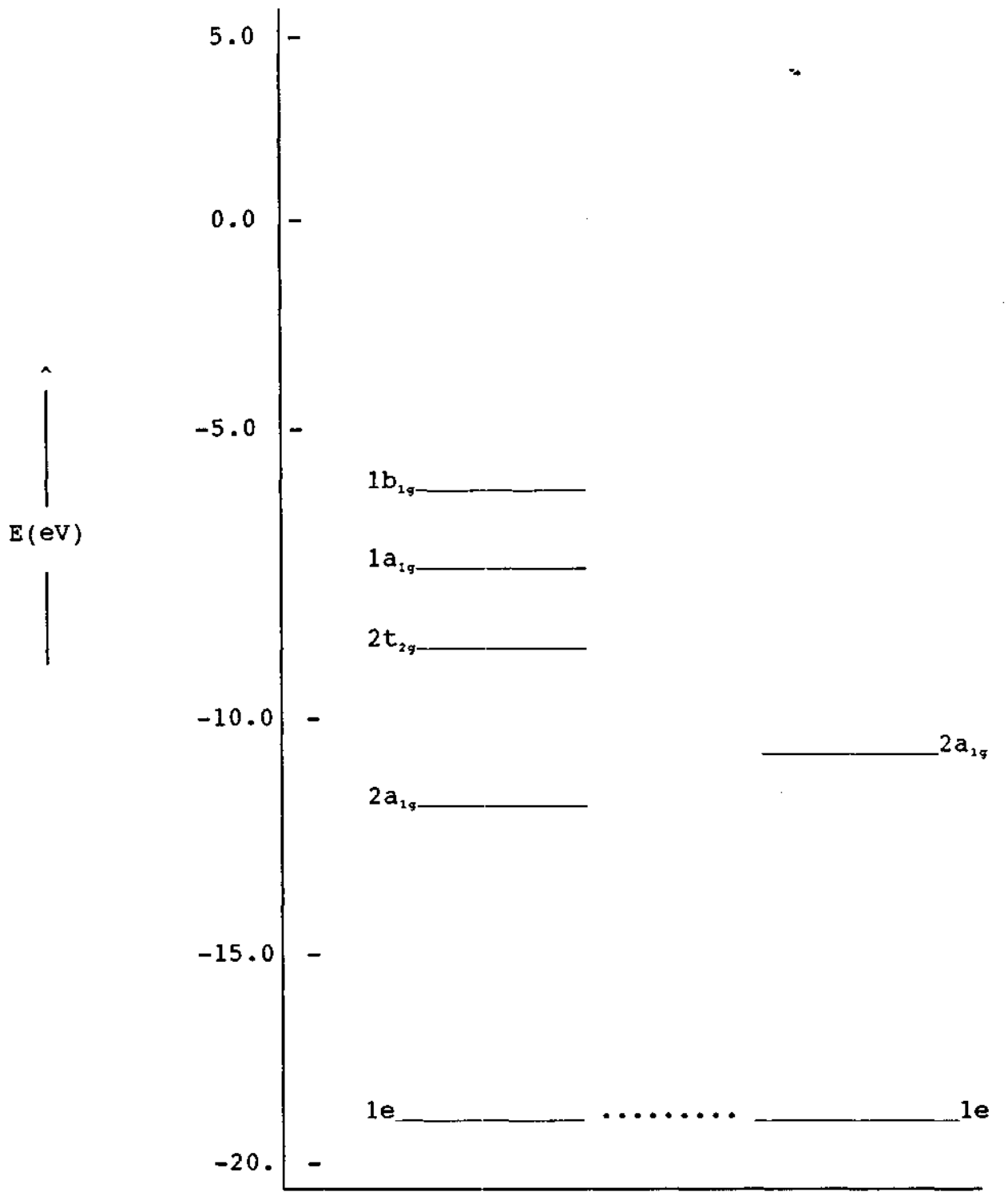


Figure 5.10: The Energy Levels of the Adsorbent - Adsorbate System of $FeO_6.NH_3^{9-}$ Cluster (NH_3 σ-bonding), Calculated by SCF-MO EHT-SP.

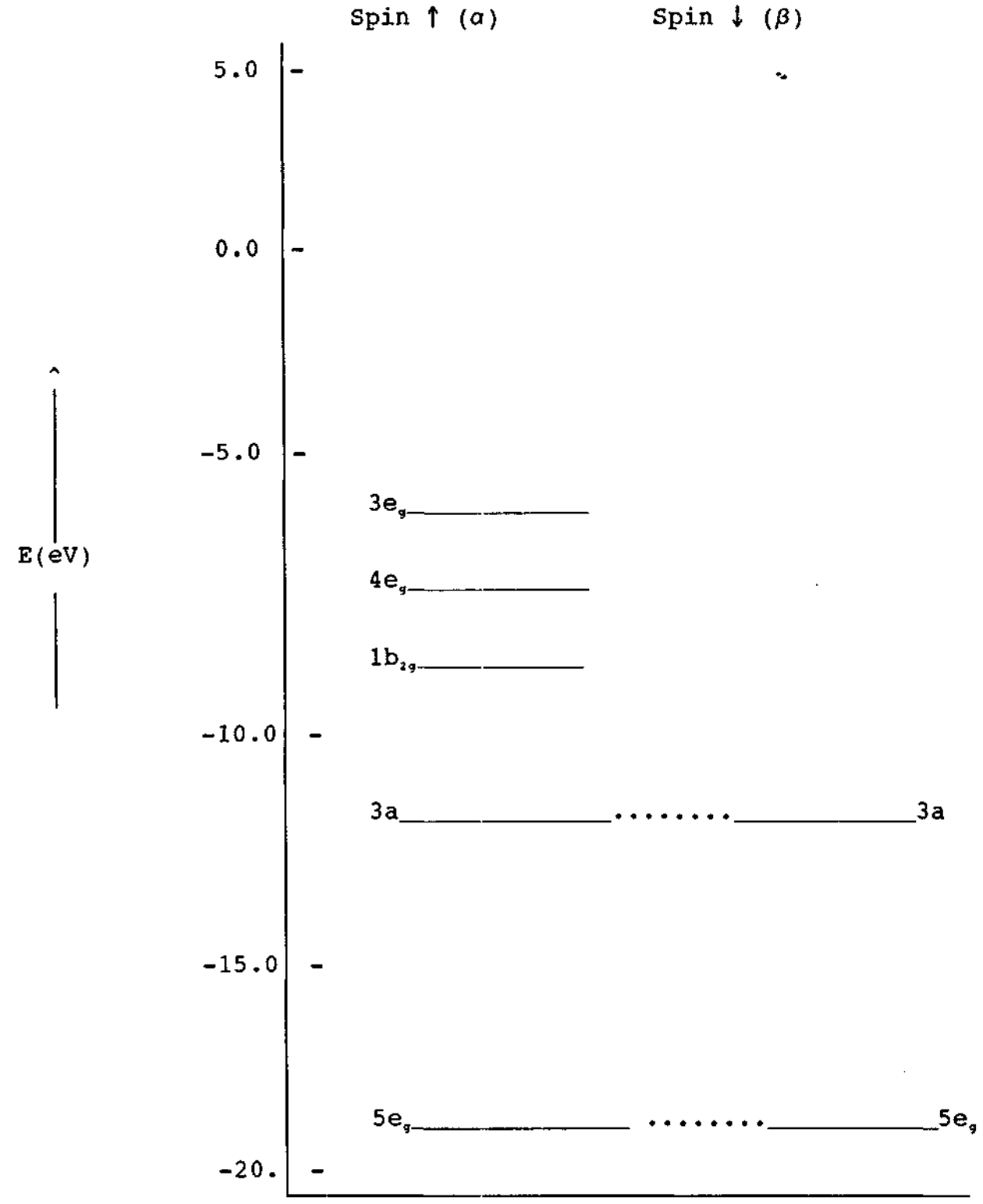


Figure 5.11: The Energy Levels of the Adsorbent - Adsorbate System of $FeO_6.NH_3^{9-}$ Cluster (NH_3 Π-bonding), Calculated by EHT.

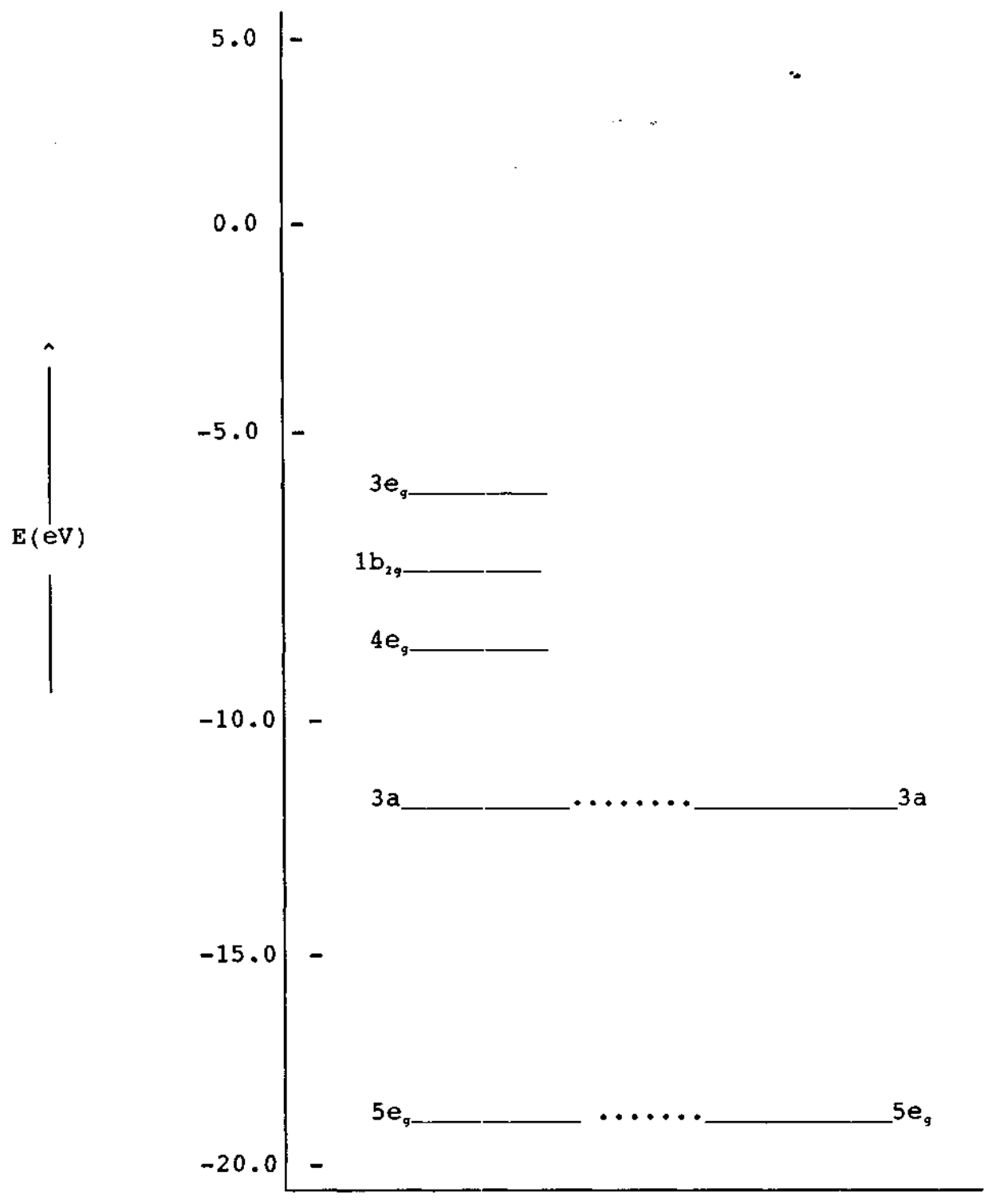


Figure 5.12: The Energy Levels of the Adsorbent -Adsorbate System of $FeO_6.NH_3^{9-}$ Cluster (NH_3 Π-bonding), Calculated by SCF-MO EHT-SP.

while that of $FeO_6.NH_3^{9-}$ Π-interactions are given in table 5.6.

Table 5.6: Results for the $FeO_6.NH_3^{9-}$ System: Orbital Energies and Other Quantities, Π-Interactions

MO Energy (eV) etc. ---------- MOs and Other Quantities	EHT	SCF-MO EHT-SP
$3e_g\uparrow$	-5.9000	-5.9000
$4e_g\uparrow$	-7.6504	- 7.8037
$5e_g\uparrow$	-17.3869	-17.2766
$5e_g\downarrow$	-17.3869	-17.2766
$1b_{2g}\uparrow$	- 7.8000	- 7.8000
$3a\uparrow$	-11.6362	-11.6362
$3a\downarrow$	-11.6362	-11.6362
${}^{a}\sigma_{BOND}{}^{a-b}$	NE	0.0000
${}^{\beta}\sigma_{BOND}{}^{a-b}$	NE	0.0000
$\lambda_1{}^{\alpha}$	NE	0.0007
$\lambda_2{}^{\alpha}$	NE	0.0000
$\lambda_1{}^{\beta}$	NE	-
$\lambda_2{}^{\beta}$	NE	0.0000
Eigenvectors	0.9923 0.1242 -0.1242 0.9923	0.9999 0.0137 -0.0137 0.9999

The MO diagrams for the $FeO_6.NH_3^{9-}$ adsorbent-adsorbate system, for both σ- and Π-interactions, as calculated by EHT and SCF-MO EHT-SP methods are shown in figures 5.9 to 5.12. The MOs of the system follow the general features exhibited by the MOs of the $FeO_6.OH^{10-}$ system. However, the $2a_{1g}\uparrow$----->$2a_{1g}\downarrow$ splitting is about 0.3eV in the $FeO_6.NH_3^{9-}$ SCF-MO EHT-SP prediction as compared to 0.5eV for $2a_{1g}\uparrow$----->$2a_{1g}\downarrow$ separation for the $FeO_6.OH^{10-}$ system.

The $5e_g\uparrow$-------> $5e_g\downarrow$ level splitting of the $FeO_6.NH_3^{9-}$ system is predictd to be zero although the corresponding splitting in $FeO_6.OH^{10-}$ system is about -10^{-3}eV. Though the $FeO_6.NH_3^{9-}$ MO studies revealed sigma interactions to be stronger than Π-interactions, as was the case for the $FeO_6.OH^{10-}$ syste, in general, the results showed that the FeO_6^{9-} - NH_3 interactions are weaker than FeO_6^{9-} - OH- interactions.

The ${}^{\alpha}\sigma_{BOND}^{a-b}$ and ${}^{\beta}\sigma_{BOND}^{a-b}$ values for the $FeO_6.NH_3^{9-}$ adsorbent-adsorbate system σ-interactions are non-zero indicating the evidence of "σ-chemical bond" formation between the NH_3 adsorbate and the surface. The magnitudes of the bond functions for the FeO_6^{9-}-----NH_3 σ-interactions are less than those of FeO_6^{9-}------OH- σ-interactions confirming again that FeO_6^{9-}--OH- interactions are stronger than FeO_6^{9-}--NH_3 interactions. The values for these functions in Π-interactions, as in the case of $FeO_6.OH^{10-}$ system, are zero showing that no "Π-chemical bond" was formed in the $FeO_6.NH_3^{9-}$ system. Also, the charge dependent quantities, λ_k^{α} and λ_k^{β}, have larger values for $FeO_6.OH^{10-}$ system than $FeO_6.NH_3^{9-}$.

1.4 Results for $FeO_5.A^{a-7}$ Type Clusters

In this section, the energy levels or potential energy curves of the $FeO_5.A^{a-7}$ type adsorbent-adsorbate systems are presented. The chemisorption of H^+ and OH^- by the FeO_5H^{6-} and $FeO_6.OH^{8-}$ cluster models were studied with EHT method. In this simulation, H^+ ion (and so does OH^-) was only allowed to mix with the electrons of the central Fe^{3+} ion and the five O^{2-} anions were assumed to provide only a constant crystalline field, as in the original model of cluster physisorption model. Using the simulation, the calculated

molecular orbital diagrams for the FeO_5H^{6-} and $FeO_5.OH^{8-}$ adsorbent-adsorbate systems are presented in figures 5.13 and 5.14 respectively (only the orbitals that are involved in the adsorbent -adsorbate bonding are shown in the diagrams).

The $a_1{}^{\cdot}\uparrow$ MO is the bonding level of the FeO_5H^{6-} system. This MO, primarily Fe^{3+} $3dz^2$ with some partial H^+ 1s character, is located about -78.6 eV in energy. The antibonding MO is $a_2{}^{\cdot\cdot}\uparrow$ and is essentially H^+ 1s orbital with some Fe^{3+} $3dz^2$ character. It is located about -13 eV in energy. There are no corresponding spin $\downarrow$ levels. In the same simulation, OH^- adsorbate was assumed to donate its paired $3\sigma^2$ electrons into the vacant (or empty) 4s orbital of the Fe^{3+} ion. As shown in figure 5.14, the $a_1{}^{\cdot}$ (spin $\uparrow$ and spin $\downarrow$) MO mainly Fe^{3+} 4s with some OH^- 3σ character, is located about -7-6 eV in energy. The $a_2{}^{\cdot\cdot}$ MO, primarily OH-3σ with some Fe^{3+} $3dz^2$ character, comes at about -7.2 eV. The chemisorption of NH_3 by $FeO_5.NH_3{}^{7-}$ model was simulated by an electron pair bond pseudo-diatomic molecule model and the potential energy curve obtained is presented in figure 5.15.

The physisorption of H^+, OH^- and NH_3 adsorbates was studied by the H^+ point charge model FeO_5H^{6-} and the (OH^- and NH_3) dipole $FeO_5.OH^{8-}$ and $FeO_5.NH_3{}^{7-}$ adsorption models. The calculations were performed, as shown in chapter four, by a modified crystal field theory. The potential energy curves for the physisorptions were calculated from equations (4-21) and (4-68). The orientation of the dipoles at β=0 was found to yield the strongest binding of the dipoles. These curves are shown in figure 5.16, to 5.18 for the H^+, OH^- and NH_3 physisorptions respectively.

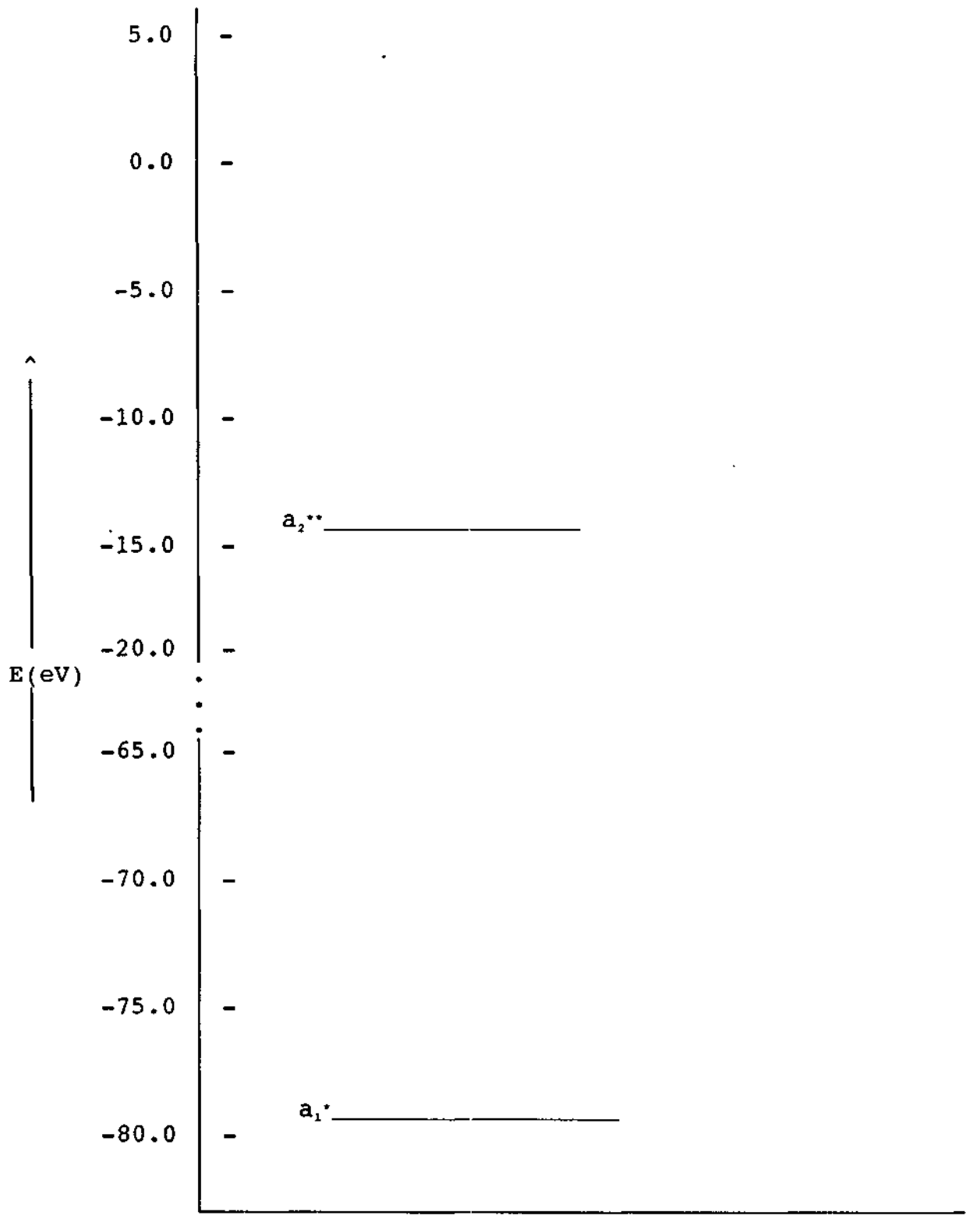


Figure 5.13: The MO Diagram of the FeO_5H^{6-} Adsorbent - Adsorbate Cluster: Calculated by EHT

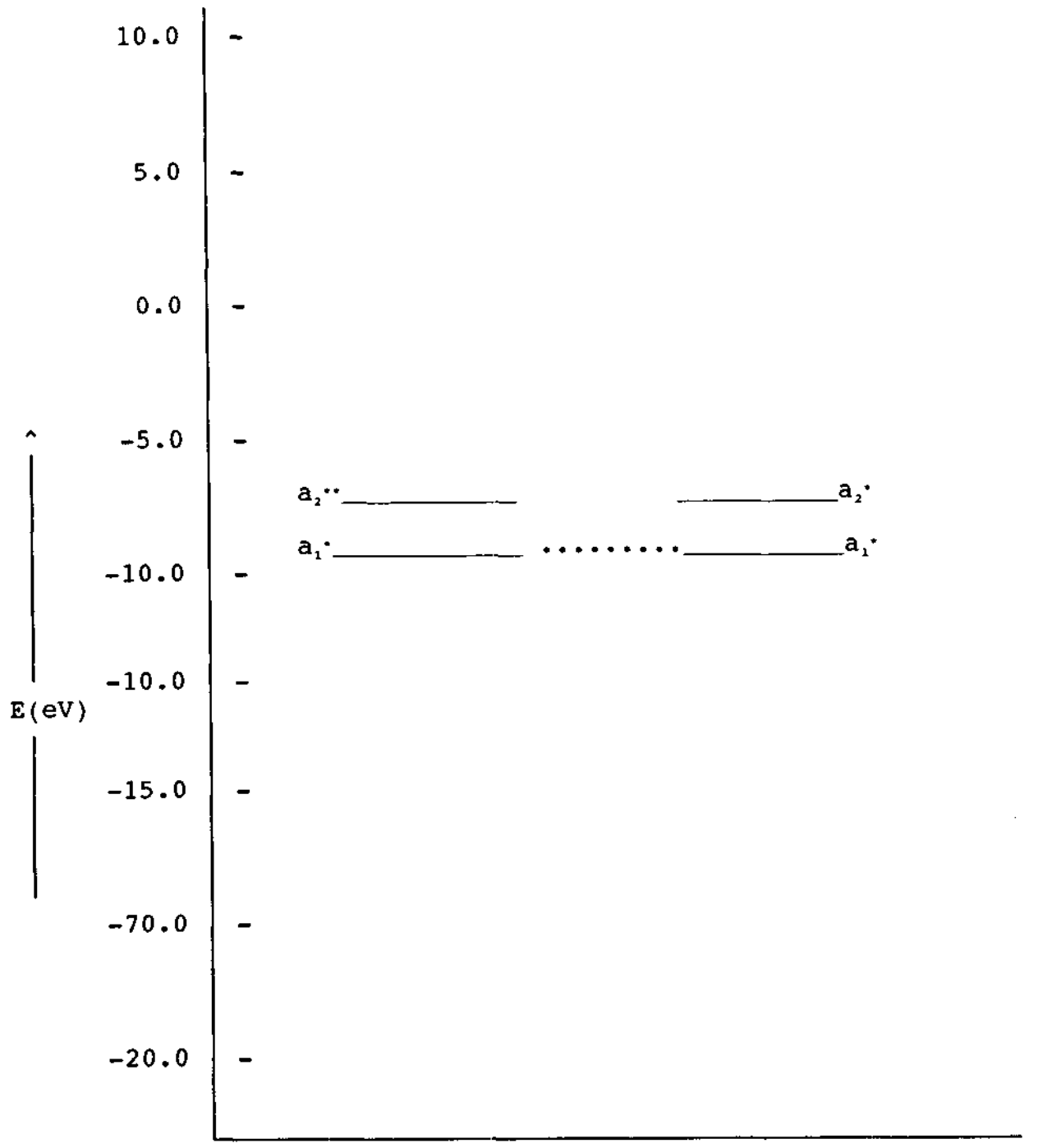


Figure 5.14: The MO Diagram of the FeO_5H^{8-} Adsorbent - Adsorbate Cluster: Calculated by EHT

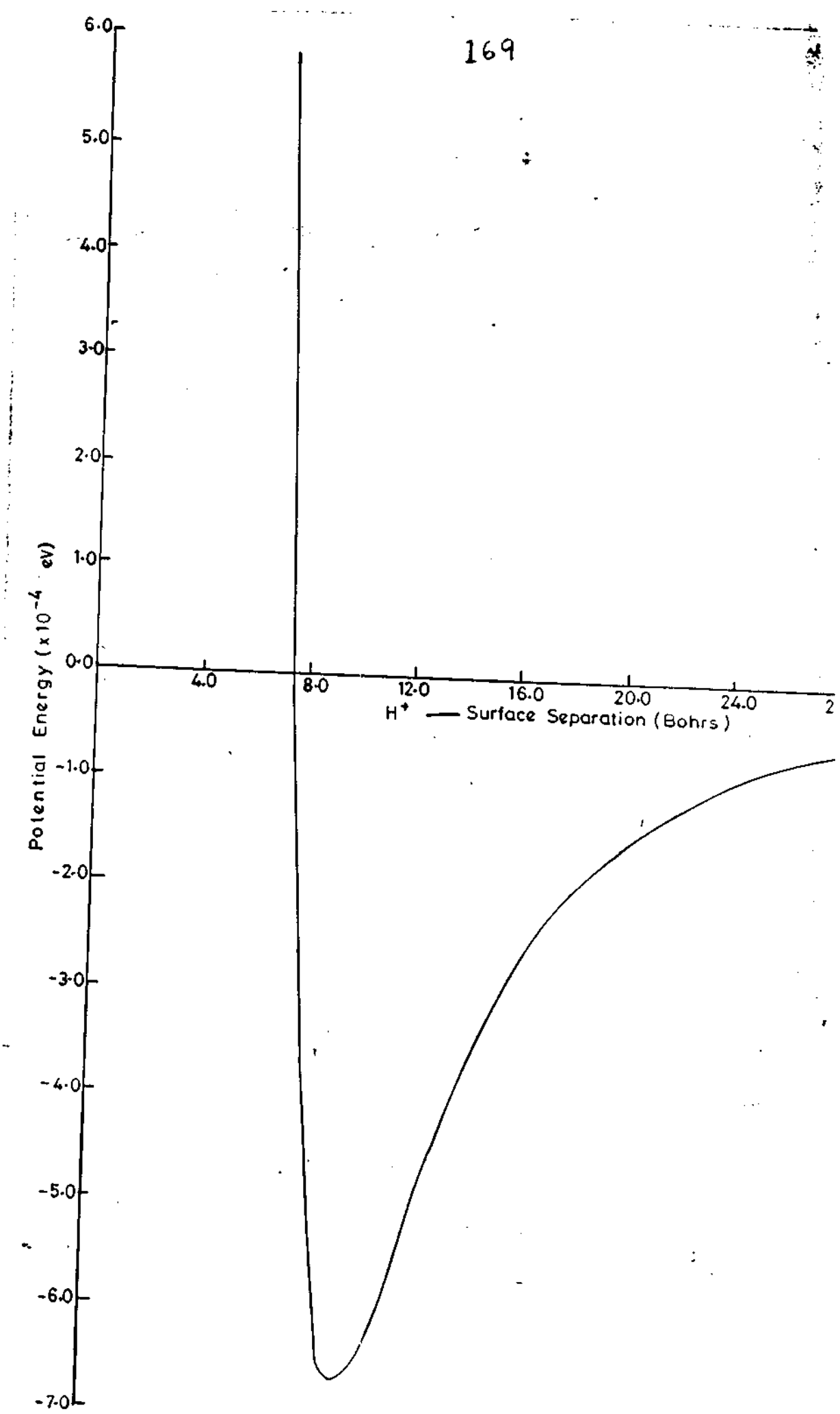


FIG. 5.16 : THE POTENTIAL ENERGY CURVE FOR

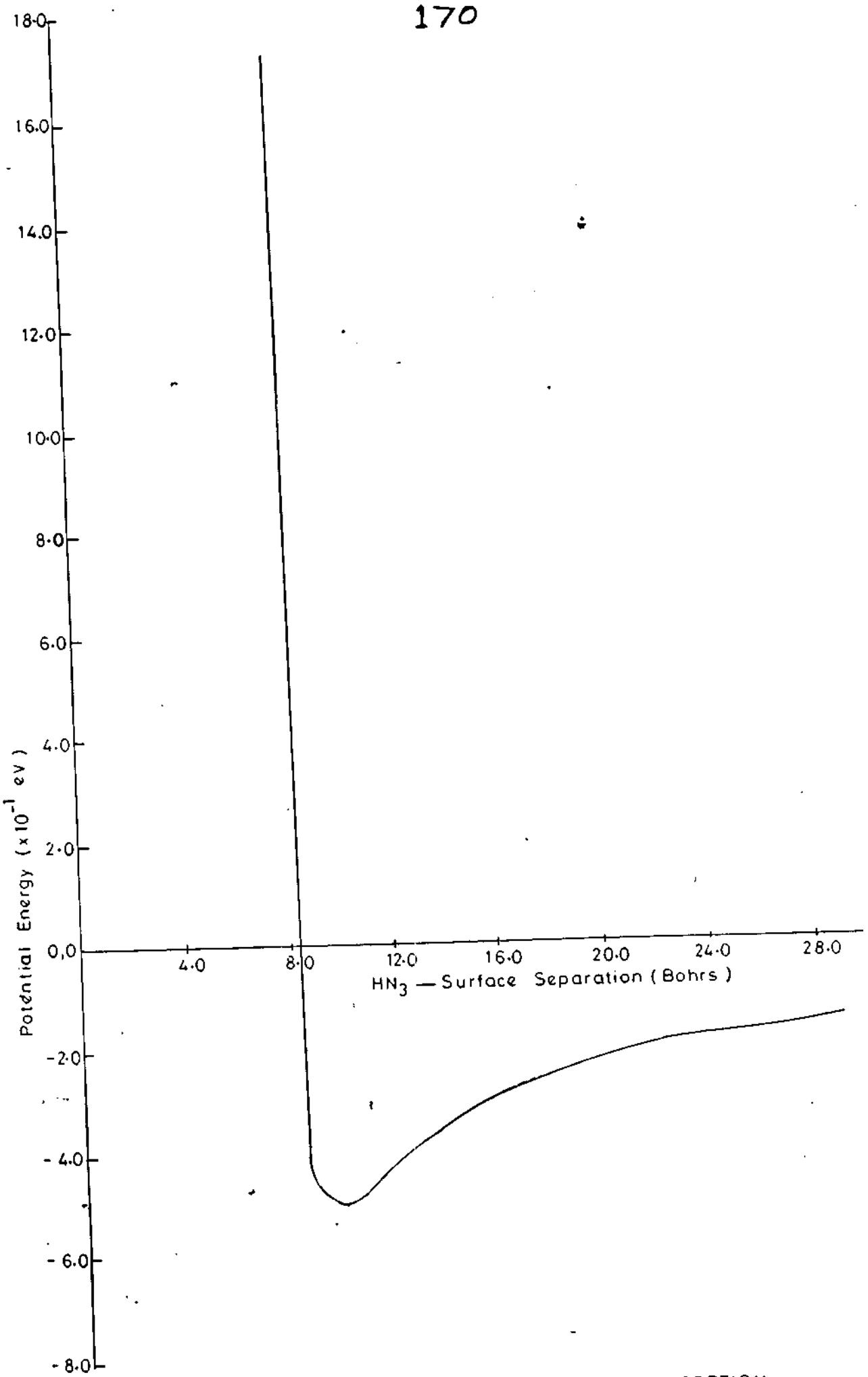


FIG.5.15: THE POTENTIAL ENERGY CURVE FOR NH_3 CHEMISORPTION

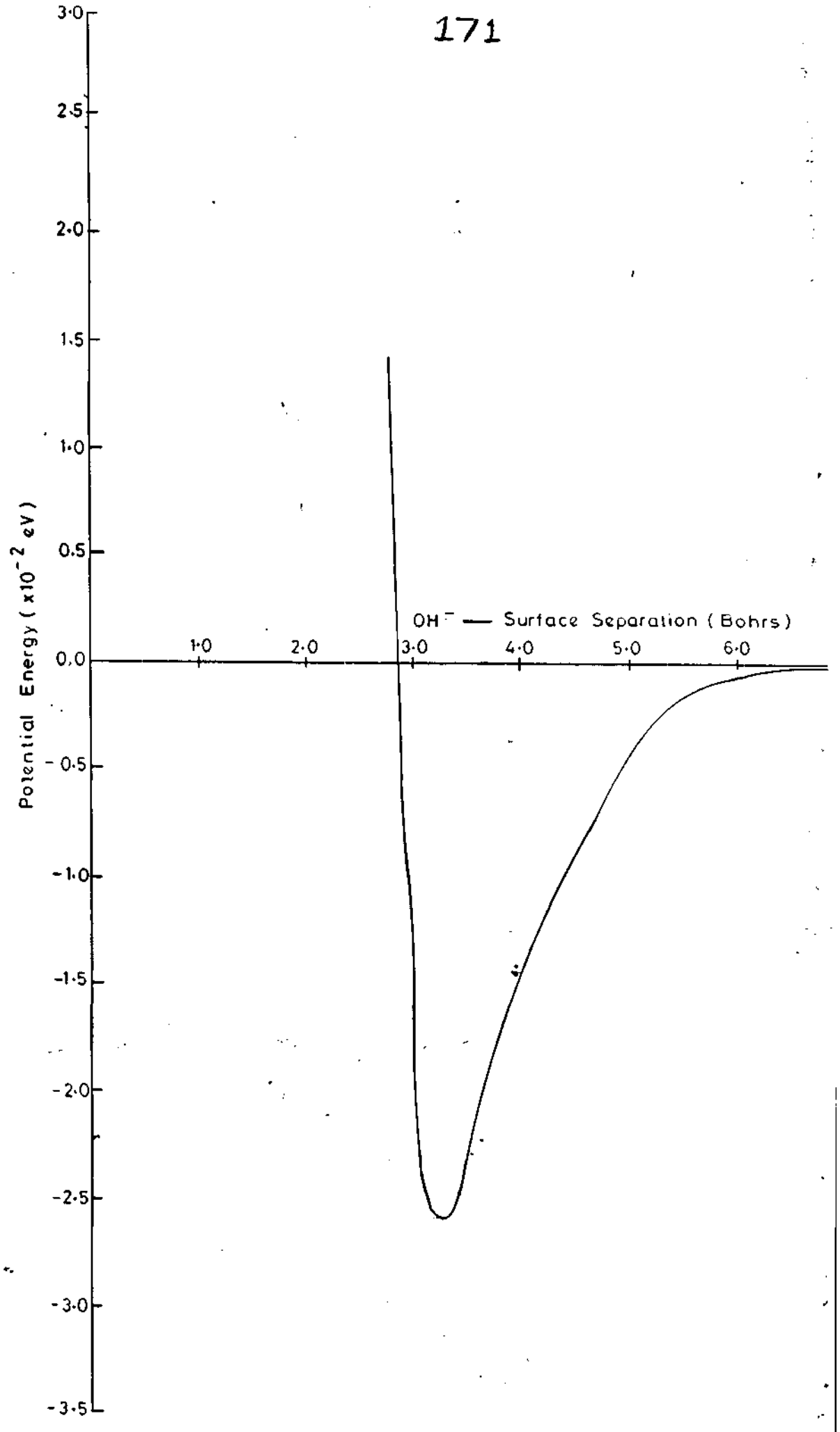


FIG.5.17: THE POTENTIAL ENERGY CURVE FOR OH^- PHYSISORPTION

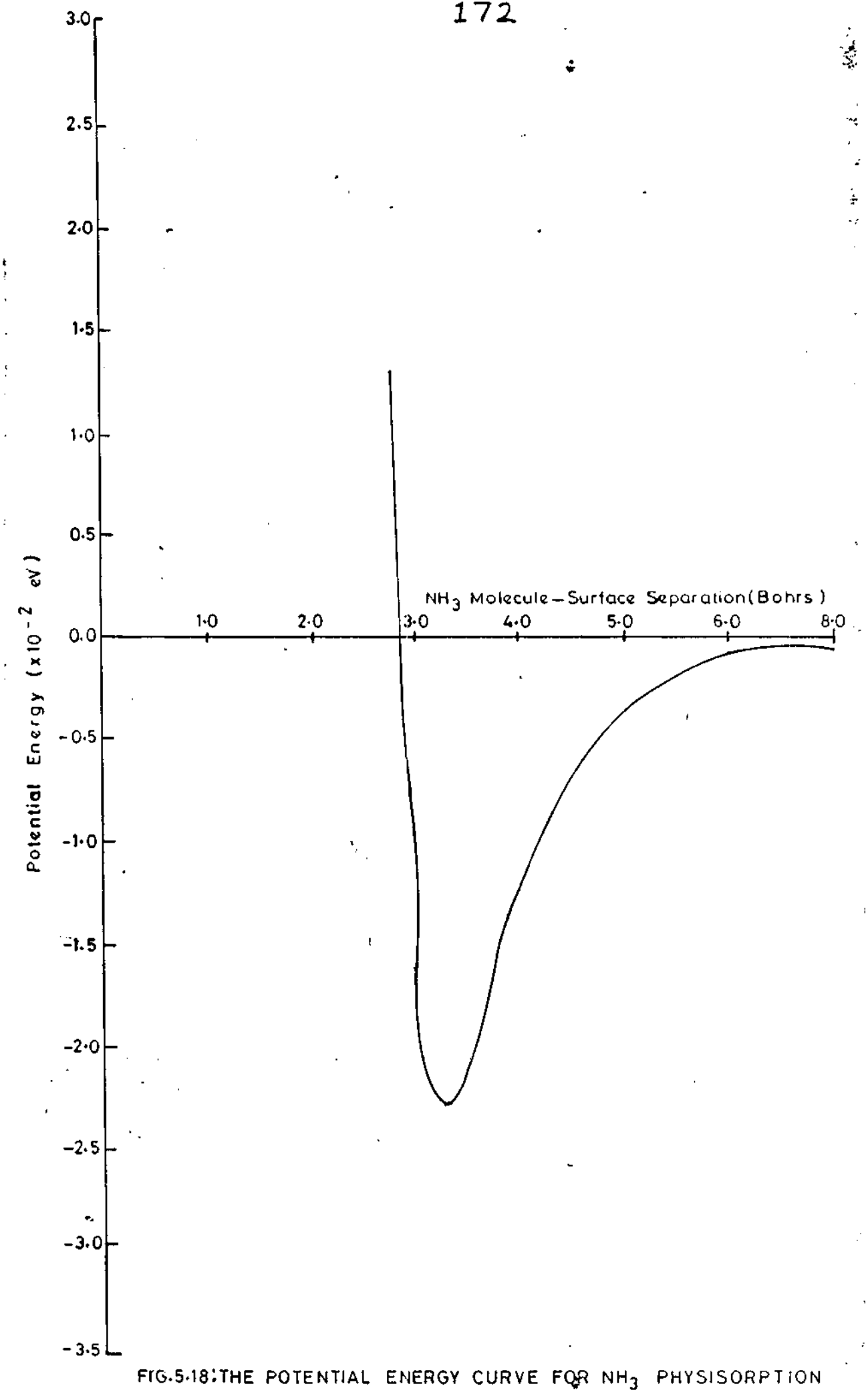


FIG.5.18: THE POTENTIAL ENERGY CURVE FOR NH_3 PHYSISORPTION

CHAPTER SIX

6. RESULTS AND DISCUSSION II: ADSORPTION ENERGIES OF H^+, OH^- AND NH_3 ADSORBATES ON THE (111) FACE OF α-Fe_2O_3

The adsorption energies of the H^+, OH^- and NH_3 adsorbates on the (111) surface of α-Fe_2O_3 simulated by FeO_3A^{n-7} and FeO_6 A^{n-9} adsorbent-adsorbate cluster adsorption models, obtained from modified crystal field theory and MO studies, are presented and discussed in this chapter. The calculated physisorption and chemosorption energy and equilibrium adsorbate-surface distances corresponding to the adsorptions are presented.

6.1 Physisorption Energies of H^+, OH^- and NH_3 on the (111) Surface of α-Fe_2O_3

The physisorption energies of the adsorbates under study, simulated by the FeO_3A^{n-7} cluster physisorption model, are given in the table below:

Adsorbate	Physisorption Energy (kJ/mol)	Equilibrium Bond Distance (Å)
H^+	-6.6173×10^{-2}	5.035-
OH^-	-2.5775	1.749
NH_3	-2.2766	1.749

As can be seen from table 6.1, the adsorbates are H^+, NH_3 and OH^- in order of increasing magnitude of physisorption energy on α-Fe_2O_3 (111) surface. Furthermore, the results predict that dipole attractions in the electric field at the surface are stronger than that of a simple point charge, at least proton charge. Since the physisorption energy of OH^- is larger in magnitude than that of H^+ ion on this oxide, the surface of this oxide can exhibit

interesting properties during hydration or when in contact with an aqueous phase.

When water is adsorbed from the gas phase, the number of H^+ and OH^- ions adsorbed must be equal. In aqueous suspension, however, there is no such restriction and from the results above, it suggests that the (111) surface of the oxide will be seldom neutral. If one introduces a dry powdered α-Fe_2O_3 into neutral water (which initially of course has 10^{-7} mol dm^{-3} each of H^+ and OH^- ions present), since OH^- ions physisorb more strongly than H^+ ions, the suspension may be acidic if only physisorb species were present on the (111) surface (thus causing the water to become acid of pH less than 7). This will happen because the physisorption energy of the H^+ ion is less than, in magnitude than the H_2O molecule proton affinity (69.3889 x 10^{-2} kJ/ml), i.e.

$$S + H^+ = SH^+ + (\Delta H = -6.6173 \; x \; 10^{-2} kJ/mol)$$

$$H_2O + H^+ = H_3O^+ + (\Delta H = -69.3889 \; x \; 10^{-2} kJ/mol)$$

where S represents the (111) surface, and the physisorption energy of OH^- is greater, in magnitude, than its proton affinity

$$S + OH^- = SOH^- + (\Delta H = -2.5775 kJ/mol)$$

$$OH^- + H^+ = H_2O + (\Delta H = -1.5933 kJ/mol).$$

Thus, in the aqueous suspension of α-Fe_2O_3, only the following

reactions are energetically favoured:

$$S + OH^- = SOH^-(s)$$

and $H_2O + H^+ = H_3O^+(l)$

making the suspension slightly acidic (of pH less than 7.)

The physisorption results also show that if other ions (than H^+ and OH^-) are present in the aqueous suspension of α-Fe_2O_3, a process termed "ion exchange" can occur. The protons at the interface can be replaced by other cations, e.g.

$$SH^+ + Na^+ = SNa^+ + H^+ \quad \ldots\ldots\ldots\ldots\ldots\ldots\ldots\ldots \quad (6\text{-}1)$$

and the hydroxyl ions by other anions

$$SOH^- + F^- = SF^- + OH^- \quad \ldots\ldots\ldots\ldots\ldots\ldots\ldots\ldots \quad (6\text{-}2)$$

Such ion exchange are of great technological importance in controlling the surface acidity or basicity in industrial catalysis.

This physisorption study also confirmed what Edwin and Blyholder (1962) observed from NH_3 (aq) adsorption on α-Fe_2O_3: NH_4^+ ion was detected to form when only physically adsorbed NH_3 and H_2O were present and not when chemisorbed NH_3 and OH^- (from water) were present. From table 6.1, NH_4^+ ion can easily form because the physisorption energy of H^+ ion is so small, in magnitude, that the reaction

$$NH_3 + H^+ = NH_4^+(aq) \quad \ldots\ldots\ldots\ldots\ldots\ldots\ldots\ldots \quad (6\text{-}3)$$

is energetically more favourable and that, since both OH^- and NH_3 were present in the suspension, OH^- physisorption is more energetically favoured at the adsorption sites

$$S + OH^- = SOH^- + (\Delta H = -2.5775 kJ/mol)$$

over NH_3 physisorption

$$S + NH_3 = SNH_3 + (\Delta H = -2.2766 kJ/mol)$$

so that NH_3 molecules are free to combine with the protons as in (6-3).

Unfortunately, experimental or theoretical data on energies of H^+,OH^- and NH_3 physisorptions on α-Fe_2O_3 are not yet available, but since heats of vaporisation is the upper limit to physisorption energies, our results must quantitatively be less in magnitude than the (heat) energy of an escaping water molecule in the gas phase at 100°C from the surface:

$$|\Delta H \ physisorption| < RT \ (T = 373K) = 3.1935 kJ/mol \ldots\ldots\ldots\ldots (6\text{-}4)$$

where R is the gas constant. Since the physisorption energies of H^+ and OH^- satisfy equation (6-4), our results have reasonably well predicted the energetics of their physical adsorption on ferric oxide (111) face. As for NH_3 adsorbate, its physisorption energy must also satisfy (6-4) since the magnitude of its experimental dipole moment is less than tht of OH^- ion

$$\mu_{NH_3} < \mu_{OH^-}$$

6.2. The Chemisorption Energies of H^+,OH^- and NH_3 on α-Fe_2O_3 (111) Surface

The chemisorption of the above adsorbates was studied by the FeO_5A^{a-7} and FeO_6A^{a-9} cluster models. The chemisorption energies of

the adsorbates obtained from FeO_3A^{n-7} cluster studies will first be presented. Then, the ones obtained from the FeO_6A^{n-9} cluster simulation. In the case of the latter cluster, there will be two subsections dealing with σ- and Π-chemisorption energies separately.

6.2.1. The Chemisorption Energies of H^+, OH^- and NH_3 from FeO_3A^{n-7} Cluster Model

The chemisorption energies of H^+ and OH^- obtained from EHT studies and that of NH_3 obtained from the electron pair bond pseudo-diatomic molecule model together with equilibrium bond distances are given in the table below:

Table 6.2: Chemisorption Energies and Equilibrium Bond Distances of H^+, OH^- and NH_3 on (111) face of α-Fe_2O_3 simulated by the FeO_3A^{n-7} Cluster Model.

Adsorbate	Chemisorption Energy (kJ/mol)	Equilibrium Bond Distance (Å)
H^+	-42.3742	0.530
OH^-	-61.6045	1.378
NH_3	-49.9630	5.300

From the values of the chemisorption energy (Table 6.2) it is clear that chemisorptive forces are much stronger than physical forces that play a dominant role in physical adsorption. The values are of the order of chemical bond energies. The ferric oxide (111) surface exhibits the same binding affinity towards the adsorbates as in their physisorption: the hydroxyl ion is the most strongly bound to the surface, then NH_3 and H^+ ion last. This is in agreement with the notion that physisorbing a specie may be the first step toward chemisorbing it and the amount chemisorbed may be

determined by the equilibrium amount physisorbed.

6.2.2. The Chemisorption Energies of H^+, OH^- and NH_3 from FeO_6A^{n-9} Cluster Model

The chemisorption energies of H^+, OH^- and NH_3 adsorbates on α-Fe_2O_3 (111) surface calculated by the FeO_6A^{n-9} cluster model, for both σ- and Π-interactions, are presented below:

(a) **σ-Interactions**

Table 6.3: Chemisorption Energies and Equilibrium Bond Distances of H^+, OH^- and NH_3 from FeO_6A^{n-9} Cluster Model

Adsorbate	EHT		SCF-MO EHT-SP	
	E_{CHEMI} (kJ/mol)	R_e(Å)	E_{CHEMI} (kJ/mol)	R_e(Å)
H^+	-5.1369	1.060	-41.0630	1.060
OH^-	-66.9484	2.120	-66.5062	2.120
NH_3	-46.4070	3.445	-44.8475	3.445

NB: E_{CHEMI} = Chemisorption Energy; R_e = equilibrium Bond Distance.

Table 6.4: The Chemisorption Energy of H^+ ion Bonding by the Surface Oxygens Only Simulated by FeO_6H^{n-} O2p Nonbonding Orbital

Adsorbate	EHT		SCF-MO EHT-SP	
	E_{CHEMI} (kJ/mol)	R_e(Å)	E_{CHEMI} (kJ/mol)	R_e(Å)
H^+	-1860.6796	1.855	-2300.3239	1.855

(b) **Π-Interactions**

Table 6.5: Chemisorption Energies and Equilibrium Bond Distances of OH^- and NH_3 Adsorbates from FeO_6A^{n-9} Cluster Model

Adsorbate	EHT		SCF-MO EHT-SP	
	E_{CHEMI} (kJ/mol)	R_e(Å)	E_{CHEMI} (kJ/mol)	R_e(Å)
OH-	-39.7320×10^{-2}	1.060	-51.6516×10^{-2}	1.060
NH_3	-15.9300	1.060	-2.5627	1.060

The chemisorption energy values of the adsorbates on the ferric oxide (111) surface from σ-interactions are of the order of chemical bond energies, and they agree with the values obtained from the FeO_3A^{n-7} cluster studies. However, the value obtained for H^+ ion bonding by the α-Fe_2O_3 (111) surface oxygens, table 6.4, is rather too large in magnitude for a covalent bond.

As could be seen from table 6.5, both EHT and SCF-MO EHT-SP methods did not predict OH- ion and NH_3 molecule to chemisorb on α-Fe_2O_3 (111) surface through Π-interactions. The Π-bond binding energies obtained, by both the two methods, fall in the range of physisorption energies. Furthermore, the SCF-MO EHT-SP method gives the Π-bond functions ${}^{a}\sigma_{BOND}^{a-b}$ and ${}^{b}\sigma_{BOND}^{a-b}$ (Tables 5.4 and 5.6) to be zero, implying physically that no chemical bond was formed. This is quite a remarkable achievement in molecular quantum mechanics that a theory having predicted molecular binding, it further reveals, through some bond function σ_{BOND}^{a-b}, whether the binding is due to a chemical bond or just physical forces.

The chemisorption energies of the three adsorbates calculated by EHT agree well with those obtained from SCF-MO EHT-SP methods for σ-interactions, energies in kJ/mol,

Table 6.6: Comparison of Chemisorption Energies of the Adsorbates on α-Fe_2O_3 (111) Surface as Obtained by EHT and SCF-MO EHT-SP Methods

Adsorbate / Method	H^+	OH^-	NH_3
EHT	-5.1369	-66.9484	-46.4070
SCF-MO EHT-SP	-41.0630	-66.5062	-44.8475

except that EHT does not predict H^+ adsorbate to chemisorb on α-Fe_2O_3 (111) surface. The adsorption energy -5.1369 kJ/mol falls in the range of physisorption energies. However, the agreement is not so good quantitatively in the case of Π-interactions, but qualitatively agree as both predicted that no Π-chemical bond was formed.

Because of the energetics of H^+, OH^- and NH_3 chemisorption, NH_4^+ will not form in the α-Fe_2O_3/NH_3(aq) (111) interface when only chemisorbed NH_3 and OH (from water) are present (Edwin and Blyholder, 1962) because, then our results predict that NH_3 molecule forms a chemical bond with the (111) surface and is not as such free to combine with H^+ ion, even if the latter were to be available. Thus, NH_4^+ ion cannot occur in that case.

An oxide, such as α-Fe_2O_3, was shown to have a pH value termed the I.E.P., "isoelectronic pont", at which there is no net surface charge in aqueous solution, i.e., oxide's surface electrically

neutral (because chemisorption of H^+ coverage equals that of OH^- ions). The IEP was shown to vary in a systematic manner with the properties of the cations for a series of oxides. It varies according to the following empirical formula (Morrison, 1978).

$$IEP = 18.6 - 11.5\ (Z/R) \quad \ldots\ldots\ldots\ldots\ldots\ldots\ldots \quad (6\text{-}5)$$

where Z is the oxidation state of the cation (in this case Fe^{3+}) and R is the separation distance in Ångströns of an adsorbed proton from the cation. Our calculated value for the IEP of α-Fe_2O_3 (111) surface is found to be

$$IEP\ (\alpha\text{-}Fe_2O_3) = 8.5439 \quad \ldots\ldots\ldots\ldots\ldots\ldots\ldots \quad (6\text{-}6)$$

This pH value, IEP(α-Fe_2O_3), determines the condition of H^+ and OH^- adsorption by α-Fe_2O_3 (111) surface in aqueous solution, and the occupation of the (111) surface by OH^- ions will then be dependent on the pH of solution. If the solution has a pH less than IEP (α-Fe_2O_3), OH^- ions on the (111) surface will be replaced by water, thus favouring H^+ ions adsorption (i.e. H^+ ions remain the only adsorbed species on the surface).

$$SOH^- + H^+\ (soln) \quad \underline{pH<8.5439}\ SH_2O \quad \ldots\ldots\ldots\ldots\ldots\ldots \quad (6\text{-}7)$$

On other hand, however, if the pH of solution is more basic than IEP (α-Fe_2O_3), H^+ ions on the (111) surface will be replaced by water, favouring OH^- ions adsorption on the surface.

$$SH^+ + OH^-\ (soln) \quad \underline{pH>8.5439}\ SH_2O \quad \ldots\ldots\ldots\ldots\ldots\ldots \quad (6\text{-}8)$$

This pH dependence of H^+ and OH^- ions adsorption on α-Fe_2O_3 was first observed by Elwira and Proszynska (1963) and later by Berube et al (1967) in their studies of H^+ and OH^- adsorption on ferric oxide. They observed that at low pH of solution, adsorption of H^+ ions is the greatest and decreases as pH increases until at last adsorption ceases. At still high pH, adsorption of OH^- ions begins and increases with an increasing pH. Thus this work has predicted the IEP of α-Fe_2O_3 at the (111) surface to be 8.5439 and its selective adsorption of the H^+ and OH^- ions below or above this point in aqueous solution.

Agreement between our chemisorption energies with experimental chemisorption energies is good:

Table 6.7: Comparison of Chemisorption Energies from FeO_6A^{n-7} Chemisorption Model with Experiment

Adsorbate	Theoretical Value (kJ/mol)	Experimental Value (kJ/mol)
H^+	-42.3742	-
OH^-	-61.6045	-
NH_3	-49.9630	-49.5359(Edwin and Blyholder, 1962)

Table 6.8: Chemisorption Energies by SCF-MO EHT-SP Method from FeO_6A^{n-9} Chemisorption Model Compared with Experiment

Adsorbate	SCF-MO EHT-SP Value (kJ/mol)	Experimental Value (kJ/mol)
H^+	-41.0630	-
OH^-	-66.5062	-
NH_3	-44.8475	-49.5359 (Edwin and Blyholder, 1962)

Table 6.9: Chemisorption Energies by EHT Method from FeO_6A^{n-} Chemisorption Model Compared with Experiment

Adsorbate	EHT Value (kJ/mol)	Experimental Value (kJ/mol)
H^+	-5.1369	-
OH^-	-66.9484	-
NH_3	-46.4070	-49.5359 (Edwin and Blyholder, 1962)

Only the experimental chemisorption energy of NH_3 on α-Fe_2O_3 was found in the literature(Edwin and Blyholder, 1962). The predictions of both the two chemisorption model agree with the NH_3 experimental chemisorption energy, though the FeO_3A^{n-} chemisorption model agreed better. As for H^+ and OH^- adsorbates, one may compare their theoretical chemisorption energies with their experimental or theoretical values on other systems that are similar to α-Fe_2O_3. Unfortunately, even for other transition metal oxides, theoretical or experimental H^+ and OH^- adsorption energies are scarce. Only the adsorption energies of CO, CO_2, O_2, CO/O_2 and CO_2/O_2 etc. adsorbates, which do not have similarities chemically with H^+ or OH^- ions, are readily available on the iron-group transition metal oxides. Even then, adsorption energies of the CO group adsorbates on the α-Fe_2O_3 are not available.

We can say that while experimental results, for H^+ and OH^- chemisorption energies on α-Fe_2O_3, are eargerly awaited we hope that our results will be of help to the surface chemist in understanding the mechanisms of α-Fe_2O_3 catalysis and its properties when immersed in aqueous solution. we also hope that the work will serve as a

reference material for future theoretical and experimental research on the surface activities of the oxide.

6.3 Conclusion

The new self-consistent field EHT that was used to calculate the adsorption energies satisfactorily reduces the number of adhoc integral approximations, used in the self-consistent field methods of the CNDO/MINDO etc families, without complicating the calculations further. Furthermore, unlike the other bonding theories, the new self-consistent field EHT, having predicted molecular binding, goes one step further by predicting whether the binding is due to chemical bonding or not (through the bond function σ_{BOND}).

The cluster model for adsorption on the (111) surface of α-Fe_2O_3 reasonably well predicted good values of adsorption energies for the adsorbates considered; agreement with experiment was very good for those adsorbates whose experimental adsorption energy is available. Although the results for the (111) surface satisfactorily agreed with experiment, adsorption studies on other surfaces of the oxide might be worth exploring.

REFERENCES

1. Adler, D. (1968): Insulating and Metallic States in Transition Metal Oxides, Solid State Physics, 21, 1.

2. Appelbaum, J.A. and Hamann, D.R. (1980): Chemisorption on Semiconductor Surfaces, **Topics in Current Physics, 19, 43.**

3. Ballard, S.A., Harry, V.F. and Elbert, A.P. (1956): Unsaturated Alcohols, **U.S. 2,767,221, Oct. 16.**

4. Baullhausen, C.J. (1962): Introduction to Ligand Field Theory (McGraw-Hill, New York).

5. Baullhausen, C.J. and Gray, H.B. (1962): The Electronic Structure of Vanadyl ion, **Inorg. Chem. 1, 111.**

6. Bel'Chev, F.V. (1958): Catalytic Amination of Aliphatic Alcohols with Mixed Oxide Catalysts, **Trudy Beloness. Sel,Skokhoz. Akad. 27 No 2, 87.**

7. Berube, Y.G., Onoda, B.Y. (Jr.) and de Bryn, P.L. (1967): Proton Adsorption at Ferric Oxide - Aqueous Solution Interface, **Surface Sci. 7(3), 448.**

8. Bielanski, A., Deren, J., Haber, J. and Nedona, J. (1956): Study of the Electrical Conductivity of Catalysts Used in the Production of Acetone from EtOH, **Przemylsl Chem. 12, 642.**

9. Bikerman, J.J. (1958): Surface Chemistry (Academic Press Inc. New York).

10. Bragg, L., Claringbull, G.F. and Taylor, W.H. (1965): Crystal Structures of Minerals (G. Bell and Sons Ltd. London).

11. Cotton, F.A. (1972): Advanced Inorganic Chemistry (Third Edition, Interscience New York).

12. Cremer, E. and Grunner, R. (1951): Measurements of the Adsorption of Ammonia on Ferric Oxide from the Thinnest Coating to a Multilayer, **Z. Physik. Chem. 196, 319.**

13. Dewar, M.J.S. and Baird, N.C. (1963): Ground States of σ - Bonded Molecules. IV. **J. Chem. Phys. 50, 262.**

14. Diaconescu, S.A. and Pantea, N. (1957): Catalysts for the Dehydrogenation of Butanes and Butenes to Butadiene, **Rev. Chim. (Bucharest) 8, 657.**

15. Doggett, G. and McKendrick, A. (1968): Use of Integral Approximations in Non-Empirical LCAO MO SCF Calculations on XCN Systems, Symposia of the Faraday Society No. 2 (Butterworth & Co. Ltd., London, WC2).

16. Edwin, A.R. (1962): Solid-Gas Phase Interactions: An Infrared Study of the Adsorption of Ammonia and Other Polar Gasses on Activated Iron (111) Oxide, **Univ. Microfilms (Ann. Arbo, Mich.), Order No 62-2281, 146pp.**

17. Edwin, A.R. and Blyholder, G. (1962): Infrared and Volumetric Data on the Adsorption of Ammonia, Water and Other Gases on Activated Iron (III) Oxide, **J. Phys. Chem. 66, 2597.**

18. Elwira, H. and Proszynska, K. (1963): Adsorption of H^+ and OH^- ions on various Metallic and Oxide Surfaces, **Naturwissenschaften 50, 351.**

19. Evans, L.T. and Russel, E.W. (1959): Adsorption of Humic and Fulvic Acids by Clays, **J. Soil Sci. 10, 119.**

20. Gerald, A.S. (1977): Semi-Empirical Methods of Electronic Structure Calculation Part A (Plenum Press, New York).

21. Gerloch, M. and Slade, R.C. (1973): Ligand Field Parameters (Cambridge University Press).

22. Gregg, S.J. (1961): Surface Chemistry of Solids (Champman & Hall Ltd. London).

23. Grzelczyk, S., Jarowska, I, Kohman, Z., Sznajder, J. and Treszcanowicz, E. (1955): A Long-life Catalyst for the Synthesis of Acetone from EtOH, **Przemysl Chem. 34, 28.**

24. Hands, C.H.G. and Walker, B.Y. (1948): The Preparation of Ethylene Cynohydrin and Acrylonitrile on a laboratory and semi-technical scale, **J.Soc. Chem. Ind. (London) 67, 458.**

25. Haskel, W.C. and Charles, A.R. (1953): Dehydration of Alcohols to Olefins, **U.S. 2,636,057, April 21.**

26. Hirochi, U., Michio, K., Kurita, M. and Hosoyo, T. (1953): Product Distribution in a Synthetic Ammonia Converter, **Repts. Govt. Chem. Ind. Research Inst. Tokyo 48, 12.**

27. Hirokawa, K. and Masaoku, O. (1979): Application of (X-ray Photoelectron - XPS and X-ray - excited Auger - electron spectroscopy - XAES) ESCA to Semiquantitative Surface and State Analysis of Iron Oxides, **Talanta, 26, 855.**

28. Hoffmann, R. (1963): An Extended Hückel Theory. I. Hydrocarbons, **J. Chem. Phys. 39, 1397.**

29. Jaromir, J. (1960): Catalytic Dealkylation and Isomerization of Alkylphenols, **Czech. 95,413, May 15.**

30. Jean, T. and Bernard, C. (1962): Hydrofining Catalysts, **Fr.,1, 287, 439, Mar. 16.**

31. Jiri, P. and Jaros, S. (1963): Catalyst for the Oxidation of Ammodia in the Manufacture of Nitric Acid, **Czech. 107, 755, July 15.**

32. Johnson, K.H. (1973): Scattered Wave Theory of the Chemical Bond, **Adv. Quant. Chem. 1, 143.**

33. Joseph, C. (1991): Quantum Theory of Solid State (Academic Press, Inc. 2nd Edition London).

34. Kagan, I.M. and Ya,M. (1933): Successive Reactions on the Surface of a Single Catalyst, **J. Gen. Chem. (USSR) 3, 337.**

35. Kamarov, V.A. and Chernikova, E.A. (1962): Influence of Additives to Al_2O_3 and Fe_2O_3 on the catalytic Decomposition of Formic Acid, **Mezhvuz. Soveshch. PO Katalizu 1958(1), pt. 2, 281.**

36. Kirillov, I.P. (1956): The Kinetics of Catalytic Conversion of Carbon Monoxide on Ferric Oxide Catalysts, **Trudy Ivanovsk. Khim. Technol. Inst. No 5, 45.**

37. Klopman, G. (1964): A Semi-Empirical Treatment of Molecular Structure II. Molecular Terms and Application to Diatomic Molecules, **J. Am. Chem. Soc. 86, 4550.**

38. Komori, S. (1941): Preparation of Unsaturated Higher Alcohols by Catalytic Reduction, **J. Soc. Chem. Ind. Japan 44, 740.**

39. Koshcheev, S.V. and Cherkashin, A.E. (1980): Study of the Energy Spectrum of Hematite by the Methods of External Photoeffect, Optical Spectra, and Electrical Conductivity, **IZV. Akad. Nauk SSSR, Neorg. Mater. 16(7), 1239 (Rus).**

40. Koshurrikov, G.S. (1948): Adsorbed Layers as a Passivating Factor, **Zhur. Obshchei Khim. (J. Gen. Chem) 18, 388.**

41. Kunz, A.B. (1980): Cluster Chemisorption, **Topics in Current Physics, 19, 115.**

42. Maidanovskaya, L.G., Panfilov, I.A. and Zakharova, R.D. (1955): Adsorption of Hydrogen and Some Electrolytes on Iron (111) Oxide, **Uchenye Zapiski Tomsk. Gosudarst, Univ. No 26, 43.**

43. Moley, J.D. (1979): O-Benzyltoluene and Alkylderivatives, **Ger. Offen. 2,840, 272, (Cl. CO7C15/16), 05 Apr.**

44. Morrison, R.S. (1978): The Chemical Physics of Surfaces (Plenum Press).

45. Mulliken, R.S. (1955): Electronic Population Analysis on LCAO MO Molecular Wavefunctions. II Overlap Populations, Bond Orders, and Covalent Bond Energies, **J. Chem. Phys. 23, 1841.**

46. Pauling, L. (1929): The Principles Determining the Structure of Complex Ionic Complex, **J. Am. Chem. Soc. 51, 1010.**

47. Pauling, L. and Hendricks, S.B. (1925): The Crystal Structure of Hematite and Corundum, **J. Am. Chem. Soc. 47, 781.**

48. Per-Olov Löwdin (1953): Approximate Formula for Many Centre Integrals in the Theory of Molecules and Crystals, **J. Chem. Phys. 21, 374.**

49. Phillips, C.S.G. and Williams, R.J.P. (1965): Inorganic Chemistry Vol.1 (Oxford University Press, New York and Oxford).

50. Pople, J.A. and Nesbet, R.K. (1954): Self-Consistent Orbitals for Radicals, **J. Chem. Phys. 22, 571.**

51. Pople, J.A. and Segal, G.A. (1966): Approximate Self -Consistent Molecular Obrital Theory. III. CNDO Results for AB_2 and AB_3 Systems, **J. Chem. Phys. 44, 3289.**

52. Pople, J.A., Beveridge, B.L. and Dobosh, P.A. (1967): Approximate Self-Consistent Molecular Orbital Theory V. Intermediate Neglect of Differential Overlap, **J. Chem. Phys. 47, 2026.**

53. Pralus, C., Francois, F. and De Mourgues, L. (1970): Examples of Bifunctional Catalysis: Production of Acetone from Propene on Iron Molybdate, **C.R. Acad. Sci. Ser. C 271(1), 20.**

54. Remy, H. (1956): Treatise on Inorganic Chemistry Vol2 (Elsevier, Amsterdam).

55. Ruedenberg, K. (1951): On the Three - and Four - Centre Integrals in Molecular Quantum Mechanics, **J. Chem. Phys. 19, 1433.**

56. Ryonosuke, A. (1931): The Influence of Catalyst on the Liquefaction of Fushun Coal in the Bergius Process, **J. Soc. Chem. Ind., Japan, 34, 500.**

57. Salem, L. (1966): The Molecular Orbital Theory of Conjugated Systems (W.A. Benjamin, INC. New York Amsterdam).

58. Salmoiraghi, E. (1931): The Action of Ferric Oxide and Ferric Chloride in the Cracking and Hydrogenation of Oil from Ragusa **Ann. Chim. applicata 21, 27.**

59. Slater, J.C. (1974): Quantum Theory of Molecules and Solids, Volume 4 (McGraw Hill New York).

60. Slater, J. C. (1975): Quantum Theory of Molecules and Solids (McGraw-Hill Book Company, New York).

61. Slater, J.C. and Johnson, K.H. (1972): SCF-Xα Cluster Method for Polyatomic Molecules and Solids. **Phys. Rev. B5, 844.**

62. Thomas, J.M. and Thomas, W.J. (1967): Introduction to the Principles of Heterogenous Catalysis. (Academic Press London, New York).

63. Tomassi, W. and Bulawa, J. (1959): Evaluation of Feric Oxide Preparations as Catalysts in Dehydrogenation of iso-propyl-alcohol by Potentiometric, Kinetic, and Conductometric Methods, **Ukrain. Khim. Zhur. 25, 699.**

64. Tossel, J.A. and Vaughan, D.J. (1973): Electronic Structure of Ferric Iron Octahedrally Coordinated to Oxygens, **Nature 244, 42.**

65. Tossel, J.A. and Vaughan, D.J. (1974): The Electronic Structure of Rutite, Wustite and Hematite from Molecular Orbital Calculations, **American Mineral. 59, 319.**

66. Usines de Mille (1949): Aldehydes and Ketones, **Britain 615,543, January 7.**

67. Van-Catledge, F.A. (1971): A Semi-Empirical Investigation of σ-π Excitations in Nonplanar Hydrocarbons, **J. Am. Chem. Soc. 93, 4365.**

68. Virginia, L.C. and Charles, E. (1952): Hydrocarbon Synthesis, **U.S. 2,589,925, March 18.**

69. Warren, E.A. and Wilson, N.J. (1960): Catalyst for Dehydrogexation of Olefins, **U.S., 2,940,940, June 14.**

70. Wolfberg, M. and Helmholz, L (1952): Spectra and Electronic Structure of the Tetrahetral Ions MnO_4^-, CrO_4^{2-} and ClO_4^-, **J. Chem. Phys. 20, 837.**

71. Yoshiro, T. and Ishikura, A. (1971): Catalyst Containing Antimony Trioxide, **Japan 71 03,457 (C1 B 01j,C o7c,C o16) January 28.**

72. Yukel'son, I.I. and Raevskaya, V.I. (1970): Alkyloxybenzenes, **Otkrytiya, Izobret., Prom. Obrastsy, Tovarm Znaki 47(23), 29.**

73. Zoltan, C., Makadi, J and Tibor, C. (1948): Catalytic Decarboxylation of Organic Acids, **Magyan Chem. Folyoirat 54, 9.**